SERIES TAPPING OF HIGH VOLTAGE DIRECT CURRENT TRANSMISSION

by

Saeed Arabi

A thesis
presented to the University of Manitoba
in partial fulfillment of the
requirements for the degree of
Doctor of Philosophy
in
Department of Electrical Engineering

Winnipeg, Manitoba

SERIES TAPPING OF HIGH VOLTAGE DIRECT CURRENT TRANSMISSION

BY

SAEED ARABI

A thesis submitted to the Faculty of Graduate Studies of
the University of Manitoba in partial fulfillment of the requirements
of the degree of

DOCTOR OF PHILOSOPHY

I hereby declare that I am the sole author of this thesis.

I authorize the University of Manitoba to lend this thesis to other institutions or individuals for the purpose of scholarly research.

Saeed Arabi

I further authorize the University of Manitoba to reproduce this thesis by photocopying or by other means, in total or in part, at the request of other institutions or individuals for the purpose of scholarly research.

Saeed Arabi

ABSTRACT

For a small tap, series arrangement of converter stations is more suitable and more economical, as compared with parallel arrangement. However, two inherent drawbacks of an HVDC converter, namely, the consumption of reactive power and the production of characteristic harmonics (especially on the ac side), will become more intense if the converter operates as a series tap. The concept of "differential firing" of two (or more) bridge sets in series is shown to be capable of mitigating these problems. The theoretical studies are supported by digital simulation studies of a prototype so-called "quasi 24-pulse series tap" incorporated in the Bipole II of Nelson River HVDC system, using the electromagnetic transients-direct current (EMTDC) program of Manitoba Hydro. The results show the feasibility of the idea with no side effects. For a series tap operating as a rectifier only, a "diode rectifier series tap" is proposed, which results in a less complex, more reliable and more economical system, with no need for any dc circuit breakers. Digital simulation studies of a prototype diode rectifier series tap incorporated in the Bipole II of Nelson River HVDC system, using the electromagnetic transients program (EMTP) of Bonneville Power Administration, are performed as well.

ACKNOWLEDGEMENT

The author wishes to express his gratitude to professor M. Z. Tarnawecky, for his invaluable guidance, support and encouragement.

SYMBOLS

Symbol	Symbol Description	Subscript	Subscript Description
α	1. Firing Angle	e	Effective
		N	At Rated Conditions
		n	Of the nth Bridge Set
		margin	Margin (Normal)
		max	Maximum
		min	Minimum
		0	At Initial Conditions
	2. Attenuation Constant	(n)	At the nth Harmonic Frequency
β	1. Advance Firing Angle		
	2. Phase Constant	(n)	At the nth Harmonic Frequency
γ	1. Margin Angle	n	Of the nth Bridge Set
		min	Minimum
	2. Propagation Constant	(n)	At the nth Harmonic Frequency
Δ	1. Difference		
	2. Small Change		
δ	1. Power Angle	0	At Initial Conditions
	2. Per Unit Frequency Deviation	m	Maximum

δV	Commutation Voltage Loss	N	At Rated Conditions
ϕ	1. Power Factor Angle	i	Of Inverter Tap
		ℓ	Of Load
	2. System Impedance Angle	m	Maximum
λ	Wave Length	(n)	At the nth Harmonic Frequency
μ	Overlap Angle	n	Of the nth Bridge Set
		0	At Initial Conditions
ω	Angular Frequency	s	At Synchronous Speed
		0	At Initial Conditions
ρ	Damping Factor		
σ	Real Part of s		
θ	1. Phase Angle	n	Of the nth Bridge Set
		(n)	At the nth Harmonic Frequency
	2. Angle of Damping Factor		
A	1. System Matrix		
	2. Constant		
a	Constant	n	Index
B	1. Susceptance	C	1. Capacitive
			2. At Converter Bus
		F	Of Filters
		L	Inductive
		t	Of the Line
	2. Constant		

C	Capacitance	(H.P.)	Of High-Pass Filter
		(n)	Of the nth Harmonic Filter
		C	At Converter Bus
c	1. Capacitance Per Unit Length	ℓ	Of the Line
	2. Cost per Year		
D	Absolute-Speed Self-Damping Coefficient		
e'	Internal Voltage	q	Of Quadrature Axis
f	1. Frequency	s	At Synchronous Speed
	2. A Function of		
G	1. Conductance	R	Of Load (Resistive)
	2. Forward Transfer Function		
g	1. Conductance Per Unit Length	ℓ	Of the Line
	2. A Function of		
H	1. Inertia Constant		
	2. Feedback Transfer Function		
I	Current Magnitude	d	Direct (dc)
		F	Through Filter
		g	Of Generator
		i	Of Inverter
		ℓ	Of Load
		m	Of Main (Converter)
		margin	Margin

		N	At Rated Conditions
		n	1. Of nth Bridge Set
			2. Of nth Line Section
		(n)	Of the nth Harmonic
		O	Ordered
		P	Active Component
		Q	Reactive Component
		R	Real Component
		r	Of Rectifier
		t	Of Tap
		X	Imaginary Component
		0	At Initial Conditions
i	1. Instantaneous Current		
	2. Current in d-q Axes (pu)		Of Machine
		d	Of Direct Axis
		q	Of Quadrature Axis
		i	Of Inverter Tap
		ℓ	Of Load
		0	At Initial Conditions
	3. Annual Rate of Interest		
ID	Direct Current		
IV	Valve Current		
j	Square Root of(-1)		
K	Cost of Filter	min	Minimum
k	Controller Gain	e	Of Exciter

KI1	Inverter Current Controller Gain		
KI2	Inverter Current Controller Proportional Gain		
KR1	Rectifier Current Controller Gain		
KR2	Rectifier Current Controller Proportional Gain		
L	Inductance	(H.P.)	Of High-Pass Filter
		n	At nth Line Section
		(n)	Of the nth Harmonic Filter
		t	1. Total (At the Tap)
			2. Of the Line
		c	Of Commutation
ℓ	1. Inductance Per Unit Length	ℓ	Of the Line
	2. Line Length	n	Of the nth Section
Loss	Filter Loss at Fundamental Frequency	(n)	Of the nth Harmonic Filter
M	Moment of Inertia		
n	Order of Harmonic		
NB	Number of Bridge Sets in Series		

P	Power	d	Direct (dc)
		N	At Rated Conditions
		O	Ordered
p	1. Power (pu)	e	Electrical
		m	Mechanical
	2. Number of Pulses		
Q	1. Reactive Power	c	Of Capacitor
		N	At Rated Conditions
		NB	For NB Bridge Sets
		0	At No Load
	2. Quality Factor	o	Optimum
R	Resistance	eq	Equivalent
		(H.P.)	Of High-Pass Filter
		(n)	Of the nth Harmonic Filter
		t,ℓ	Of the line
r	1. Resistance (pu)	a	Of Armature
	2. Resistance Per Unit Length	ℓ	Of the Line
	3. Annual Fixed Charged Rate		
S	Size of Filter	(H.P.)	Of High-Pass Filter
		min	Minimum
		(n)	Of the nth Harmonic Filter
s	Laplace Transform Variable		

T	Time Constant	ω	Of Speed Transducer
		e	Of Exciter
		i	Of Current Transducer
		n	Of nth PI controller
		v	Of Voltage Transducer
t	Time		
T'_{do}	Open-Circuit Field Time Constant		
T"	Damper Time Constant	d	Direct Axis
		o	Open-Circuit
		q	Quadrature Axis
U	Unit Cost	C	Of Capacitor
		L	Of Inductor
V	Voltage Magnitude	d	Direct (dc)
		f	Of Field
		i	Of Inverter
		m	Of Main (Converter)
		N	At Rated Conditions
		n	1. Of nth Bridge Set
			2. Of nth Line Section
		(n)	Of the nth Harmonic
		R	Real Component
		r	Of Rectifier
		s	Of the (ac) System
		t	1. Of the Tap
			2. Of Machine Terminal
		X	Imaginary Component
		0	At No Load

v	1. Instantaneous Voltage		
	2. Voltage (pu)	d	Of Direct Axis
		f	Of Field
		q	Of Quadrature Axis
		t	Of Machine Terminal
		0	At Initial Conditions
VA	Voltage of Phase A		
VV	Valve Voltage		
X	1. Reactance	c	Of Commutation
		g	Of Generator
		t	1. Of the Line
			2. Of Transformer
	2. Variables Vector		
x	Synchronous Reactance (pu)	d	Of Direct Axis
		ℓ	Of Armature Leakage
		q	Of Quadrature Axis
		t	Of Transformer
		0	Of Zero Sequence
x'	Transient Reactance (pu)	d	Of Direct Axis
		q	Of Quadrature Axis
x"	Subtransient Reactance (pu)	d	Of Direct Axis
		q	Of Quadrature Axis
Y	Admittance	n	Of nth Line Section
		(n)	At the nth Harmonic Frequency
		π	Of π-Circuit (Shunt)

y	Admittance Per Unit Length	(n)	At the nth Harmonic Frequency
Z	Impedance	c	Characteristic
		F	Of Filter
		n	Of nth Line Section
		π	Of π-Circuit (Series)
z	Impedance Per Unit Length	(n)	At the nth Harmonic Frequency

ABBREVIATIONS

AC / ac	Alternating Current
BPA	Bonneville Power Administration
BPS	By-Pass Switch
B1Y	First Bridge Connected to a Star Winding
B2Y	Second Bridge Connected to a Star Winding
C.B.	Circuit Breaker
Comm'd	Commutated
Cont'd	Controlled
Conv.	Converter
DC / dc	Direct Current
Diff.	Differential
d-q	Direct and Quadrature (Axes)
e.g.	For Example
EMTDC	Electromagnetic Transients-Direct current (Program)
EMTP	Electromagnetic Transients Program
ESCR	Effective Short Circuit Ratio
etc.	Etcetera
FL	Full Load
G	Synchronous Generator
H.P.	High-Pass (Filter)
HVDC	High Voltage Direct Current (Transmission)
i.e.	That Is
Inv.	Inverter / Inversion

IS	Isolation Switch
L-G	Line to Ground
L-L	Line to Line
Max	Maximum
mes.	Measured
Min	Minimum
Min VAr	Minimum Reactive Power (Operation)
NL	No Load
P.F.	Power Factor
PI	Proportional-Integral (Controller)
Pos.	Positive
pu	Per Unit
Q 24-P	Quasi Twenty Four-Pulse (Operation)
Rect.	Rectifier / Rectification
ref.	Reference
r.m.s.	Root Mean Squared
S.C.	Surge Capacitor
S.R.	Smoothing Reactor
Syn. C	Synchronous Condenser
VAr	Reactive Volt-Amper
12-P	Twelve-Pulse (Operation)

CONTENTS

ABSTRACT iv

ACKNOWLEDGEMENT v

SYMBOLS vi

ABBREVIATIONS xv

Chapter page

I. INTRODUCTION 1

General Review 1
Motivations And Objectives 5
Outline Of The Thesis 7

II. THEORETICAL BACKGROUND 9

General 9
Comparison of Parallel and Series Arrangements 9
Transmission Losses 11
Insulation Aspects 12
Reactive Power Requirements 12
Differential Firing 16
Harmonics 17
AC Current Harmonics 19
DC Voltage Harmonics 24
Harmonics Entering the DC Line 26
Differential Firing 28
Diode Rectifier Technique 30

III. DIODE RECTIFIER SERIES TAPPING 33

General 33
Operation Modes of the System 33
Normal Operation Mode 34
Abnormal Operation Mode 34
Tapping Station 35
Typical Arrangements 35
Blocking and Deblocking 37
Simulation Modelling 39
Simulation Results 42
Waveforms and Harmonics of the Tap 42
Blocking and Deblocking of the Tap 45
Faults in the AC System of the Tap 49

Major Disturbances in the Main DC System . . 52
Comparison with other Schemes 58
Conclusions 62

IV. DIFFERENTIAL FIRING IN SERIES TAPPING 63

General 63
VAR Control 63
Harmonics Control 67
Control System Modifications 67
Behavior of Overall Harmonic Magnitudes . . . 69
Typical Functions for a Quasi 24-Pulse Operation 71
Overall Harmonic Magnitudes and Other Effects 74
Simulation Network and Controls 76
Controls of the Tapping Station 78
Simulation Results 90
Steady-State Studies 90
Disturbances in the Tapping Station 97
Disturbances of the Main DC System 106
Economic Aspects and Other Applications . . . 109
Cost Comparison 110
Other Applications 114
Conclusions 117

V. CONCLUSIONS AND SUGGESTIONS FOR FURTHER STUDIES . 119

Conclusions 119
Major Contributions 121
Suggestions for Further Studies 122

REFERENCES 124

Appendix page

A. SIMULATION DATA OF DIODE RECTIFIER SERIES TAPPING 127

The Main Rectifier 127
The Inverter 128
DC Transmission Lines 128
Tapping Station 129

B. AC FILTERS WITH DIFFERENTIAL FIRING 130

Quasi Twenty Four-Pulse Operation 130
Comparison with Twelve-Pulse Operation 133
Minimum VAr operation 134

C. SIMULATION DATA OF DIFFERENTIAL FIRING 135

The Rectifier 135
The Main Inverter 136
DC Transmission Lines 137
Tapping Station 137

LIST OF TABLES

Table		page
2.1.	Comparison of Parallel and Series Arrangements	10
3.1.	Diode Rectifier Schemes Versus Controlled Rectifier Schemes	60
4.1.	Overall Harmonic Magnitudes (Simulation)	93
4.2.	Cost Comparison of Equal and Differential Firing Operations	113
4.3.	Comparison of Various Possibitities	115

LIST OF FIGURES

Figure		page
1.1.	Series and Parallel Arrangements of a Three-Terminal HVDC System.	2
1.2.	Basic Classification of HVDC Systems.	6
2.1.	Reactive Power Characteristics of a Series Tap.	15
2.2.	Voltage and Current Waveforms of a Controlled Bridge.	18
2.3.	11th Harmonic Current of a Series Tap.	21
2.4.	13th Harmonic Current of a Series Tap.	21
2.5.	Square and Trapesoidal Current Waveforms.	23
2.6.	12th Harmonic Voltage of a Series Tap.	25
2.7.	Equivalent Circuit for nth DC Harmonic of a Series Tap.	27
2.8.	Phasor Diagrams for $\Delta\alpha \cong 15^{o}$ and Small $\Delta\mu$.	30
2.9.	A Diode rectifier Bridge and its Output Voltage.	31
3.1.	Typical Diode Rectifier Series Tapping Station Arrangements.	36
3.2.	Simplified Circuit and its Phasor Diagram for Zero Tap Output.	37
3.3.	Simulation Network and Controls.	40
3.4.	Steady-State Waveforms of the Tap.	43
3.5.	Voltage across the Tap Including its Smoothing Reactors.	44
3.6.	Deblocking of the Tap.	46
3.7.	Blocking of the Tap.	47

3.8. Emergency Blocking of the Tap. 48

3.9. Three-Phase Fault in the Tapping Station. 50

3.10. Single Phase-To-Ground Fault in the Tapping Station. 51

3.11. DC Line Fault at the Inverter End. 53

3.12. Single Commutation Failure at the Inverter. . . . 55

3.13. Partial Blocking in the Main System. 57

4.1. Voltage Regulation Versus Number of Bridge Sets at V_d = -0.8 pu. 66

4.2. Control Block Diagram for Predetermined Differential Firing. 68

4.3. Overall Harmonics Versus Difference Angle. 70

4.4. Typical Difference Angle for a Quasi 24-Pulse Operation. 72

4.5. Maximum and Minimum Limits of the Effective Firing Angle. 74

4.6. Overall 11th, 13th and 12th Harmonics (Theoretical). 75

4.7. Simulation Network. 76

4.8. AC Voltage Regulator of the Tap. 79

4.9. Simplified Tap and dc (d-q) Quantities. 83

4.10. Root Locus Plot of the Closed Loop System for $k \geq 0$. 88

4.11. Speed Regulator of the Tap. 89

4.12. Current and Voltage Waveforms of a Quasi 24-Pulse Tap. 91

4.13. Current and Voltage Waveforms of a 12-Pulse Tap. 92

4.14. Valve Voltages and Currents of a Quasi 24-Pulse Tap (FL). 94

4.15. Valve Voltages and Currents of a Quasi 24-Pulse Tap (NL). 95

4.16. Valve Voltages and Currents of a 12-Pulse Tap. . . 96

4.17. 10% Load Reduction (Initial Load 0.83 pu). 98

4.18. 50% Load Reduction (Initial Load 0.83 pu). 99

4.19. Load Disconnection with No Overvoltage Reduction by the Tap. 101

4.20. Load Disconnection with Some Overvoltage Reduction by the Tap. 102

4.21. 6-Cycle 3-Phase Fault at the Tap's Bus. 104

4.22. 6-Cycle Single Phase-to-Ground Fault at the Tap's Bus. 105

4.23. 20% Reduction in the Ordered Current. 107

4.24. DC line Fault at the Inverter End. 108

Chapter I

INTRODUCTION

1.1 GENERAL REVIEW

Since the outset of application of high voltage direct current (HVDC) transmission, consideration has been given to interconnecting more than two terminal stations with some form of dc network. The introduction of thyristor valves increased the interest in multiterminal HVDC systems, since the required extra tasks can be assumed by thyristor valves, more reliably than by mercury arc valves. Another obstacle, namely, the unavailability of dc circuit breakers has, more or less, been overcome. Dc circuit breakers [1,2], which basically consist of breaking switches and energy dissipating devices, have proved feasible, although less flexible and more expensive than their ac counterparts.

Multiterminal HVDC systems can, basically, be divided into two categories, namely, parallel and series arrangements. Series and parallel arrangements of a three-terminal system are schematically shown in Figure 1.1.

Realistic strategies for achieving parallel multiterminal operation were published in 1963 [3], at a time when two-terminal applications were still in their infancy. Two

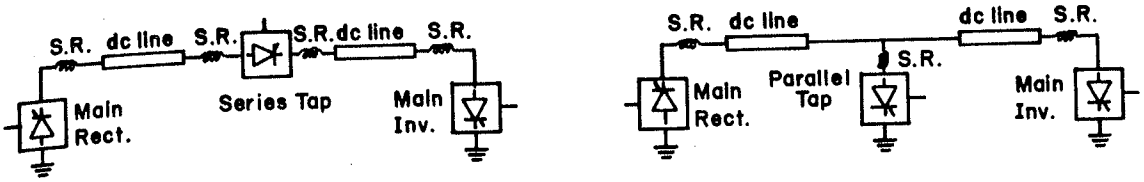

Figure 1.1: Series and Parallel Arrangements of a Three-Terminal HVDC System.

years later, the alternative arrangement, namely, series connection of converters [4], emerged. A comprehensive review of the papers dealing with multiterminal HVDC systems, until 1979, is available in [1]. These papers dealt with multiterminals using line commutated controlled converters, while, in the present decade, diode rectifiers [5] and forced commutated inverters [6] have been introduced to parallel and series multiterminals, respectively.

Kingsnorth HVDC scheme in England, which consists of three terminals, was commissioned in 1976. In 1982 the parallel operation of Bipoles I & II of Nelson River HVDC system for emergency cases [7] became a reality. Since then, a few other multiterminal operations have come into existence around the world. Small series taps, which have recently gained more attention [8-10], can be considered to be among the potential candidates for future multiterminal operations.

A comparison between parallel and series arrangements [8,11] reveals that the series arrangement is more suitable for small taps, up to, say 20% of the main system rating.

Nevertheless, a series tap may suffer from a number of drawbacks, such as higher reactive power consumption and higher filtering requirement on the ac side of the tap.

Production of harmonics and consumption of reactive power are two inherent drawbacks of HVDC converters. Two conventional methods, namely, application of filters and increasing the number of pulses, exist for reducing harmonics. Twelve-pulse operation, effected by providing two bridges with wye- and delta-connected transformer secondary windings, has frequently been used. Nevertheless, increasing the number of pulses beyond twelve, e.g., twenty four, using phase-shifting transformer windings, is considered to be uneconomical [12,13] and has not been practiced in HVDC converter stations.

The required reactive power has been conventionally provided by synchronous condensers, capacitor banks and partially by filter banks. Static VAr systems [14] are more recent sources of production and control of reactive power at HVDC terminals. Forced commutated inverters [15] have also been suggested as alternatives to line commutated inverters, although they are more complex. They are proved to be capable of providing their own reactive power requirement, as well as producing and controlling the reactive power required by their ac systems. Line commutated converters, too, can, to some extent, control their reactive power consumption, in addition to fully controlling their real power.

Such a control can be achieved with a back-to-back HVDC system (where, transmission loss is not a concern) by properly controlling both the inverter voltage and the system current [16].

A similar, but more limited control of reactive power (or ac voltage) can be exercised by an independent operation of individual bridge sets [17], provided that, at least two bridge sets are available. This idea has been suggested for series taps [18], as well. Alternatively, the aim can be the reduction of certain characteristic harmonic magnitudes [15], rather than the reduction and control of reactive power, or even a combination of both. The term "differential firing", as opposed to "equal firing" of all bridges, will be used to indicate such ideas in general. It may be noted that in both cases the individual valves of each bridge will be fired by equidistant pulses at every 60 degrees.

If a converter station is to operate in rectification mode only, the application of diode rectifier bridges may be a favorable option [2,5,19]. A diode rectifier station is attractive from economic and reliability points of view.

1.2 MOTIVATIONS AND OBJECTIVES

As was pointed out in the previous section, two inherent drawbacks of an HVDC converter, namely, reactive power consumption and harmonic production, become more intense when the converter operates as a series tap (i.e., operating at constant dc line current, rather than constant dc voltage). There are indications, in the literature [15,18], that the concept of differential firing is potentially capable of diminishing these drawbacks, although to a limited extent. A special situation may also be recognized, where the tap is to operate as a rectifier only, i.e., transferring power to an HVDC line by a relatively small series tap. In this case, a diode rectifier series tap is potentially an advantageous option [2,5,19].

The objectives of this thesis are the followings:

1. Identification and clarification of the major drawbacks of a series tap as compared with a parallel tap or other HVDC converters.
2. Development of the idea of diode rectifier series tapping, its comparison with other possibilities and the demonstration of its technical feasibility using digital simulation studies of a prototype system.
3. Examination and comparison of various possibilities of the concept of differential firing as used for reactive power reduction and voltage control of a (line commutated) series tap.

4. Development of the concept of differential firing as used for harmonic reduction in the context of a classical application with an appropriate control method, the demonstration of technical feasibility of the idea by digital simulation, and examination of the economic implications.

5. Examination and comparison of various possibilities of harmonic reduction and its combination with reactive power reduction using differential firing.

This study will, thus, be concentrated in the areas indicated by broken lines in Figure 1.2, in conjunction with small series taps.

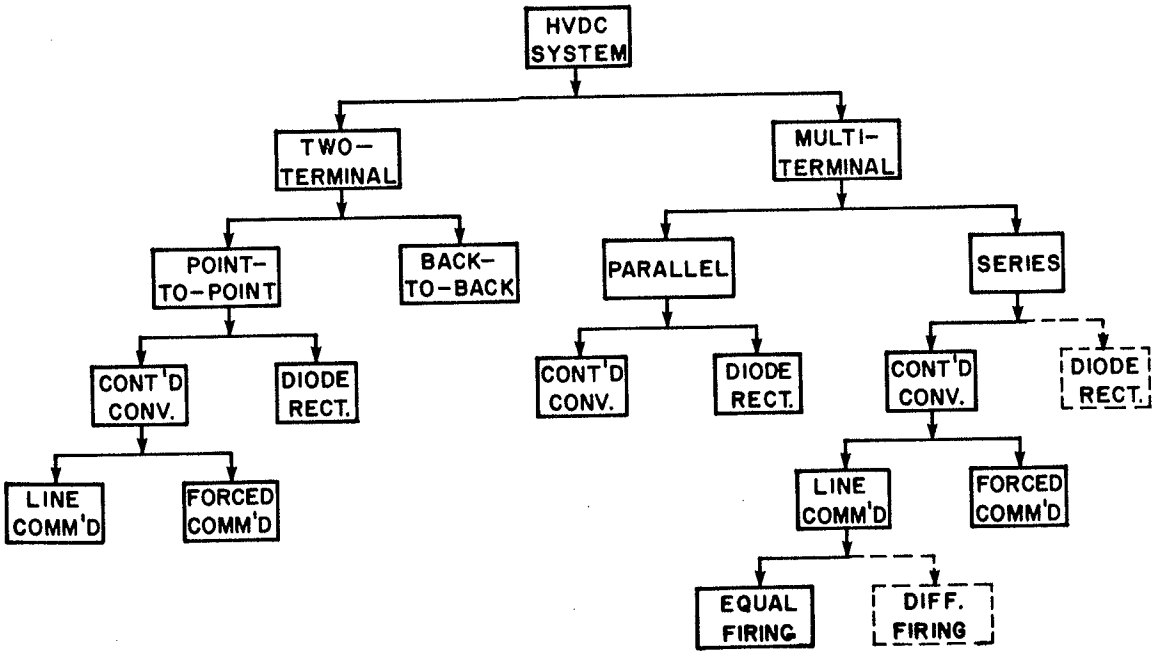

Figure 1.2: Basic Classification of HVDC Systems.

1.3 OUTLINE OF THE THESIS

Parallel and series multiterminal HVDC systems are compared in Chapter II. The drawbacks of series tapping, as well as the methods of their mitigation are pointed out. The reactive power requirements of a series tap for both equal firing and differential firing are formulated and plotted. The harmonics of a series tap are appropriately represented. The concept of differential firing for harmonic reduction is briefly explained. The effect of the location of a series tap on its dc harmonics entering the dc line is analyzed. Some characteristics of diode rectifiers are pointed out and diode rectifier series tapping is introduced.

In Chapter III, diode rectifier series tapping is described. The results of digital simulation studies, carried out for a 10% diode rectifier series tap incorporated in the Bipole II [20] of Nelson River HVDC system, using the electromagnetic transients program (EMTP) of Bonneville Power Administration (BPA) [21], are presented. A comparison with other schemes is presented and economic implications are pointed out.

In Chapter IV, the voltage regulation capability of a series tap, using differential firing, is calculated and plotted versus the number of bridge sets. Various possibilities are discussed. A control method, termed as "predetermined

differential firing" method, is developed. Typical functions for effecting a kind of operation, termed as "quasi twenty four-pulse" operation, are determined. A small disturbance analysis of a prototype tap is presented. The results of digital simulation studies of the prototype system, namely, a 10% quasi twenty four-pulse series tap incorporated in the Bipole II of Nelson River HVDC system, using the electromagnetic transients-direct current (EMTDC) program of Manitoba Hydro [22], are presented and compared with the theoretical results. The economic implications, other options and other applications are discussed.

Finally, conclusions, major contributions and suggestions for further research are stated in Chapter V .

Chapter II

THEORETICAL BACKGROUND

2.1 GENERAL

In this chapter, parallel and series arrangements of multiterminal HVDC systems are compared. The drawbacks of series tapping and their mitigation techniques are discussed. The necessary theoretical background for differential firing and diode rectifier techniques are established.

2.2 COMPARISON OF PARALLEL AND SERIES ARRANGEMENTS

The pros and cons of parallel and series arrangements are given in Table 2.1 [1,8,11,18]. Depending upon the application, each arrangement offers some advantages over the other. For a small tap, in particular, the series arrangement appears more suitable as well as more economical. The reasons are as follows.

1. A small tap is susceptible to system faults, espetially to disturbances on its own ac bus. This might cause commutation failure, recovery from which may be difficult and may even require a momentary shutdown of the whole system in case of parallel tapping. A series tap, however, is less subject to commutation

TABLE 2.1

Comparison of Parallel and Series Arrangements

	DESCRIPTION	PARALLEL ARRANGEMENT	SERIES ARRANGEMENT
1	Tap's Voltage Rating	At System Voltage	Less Than System Voltage
2	Tap's Current Rating	Less Than System Current	At System Current
3	Insulation Level: Line	The Same Along the Line	Different at Each Section
	Insulation Level: Tap Equipment	At Low Voltage	At High Voltage
4	Commutation Failure in One Inverter Station	May Draw Excessive Current from Other Stations (Needs Other Provisions)	Is Handled by Main Rectifier α -Control (Similar to Point-to-Point Systems)
5	Blocking of a Single Bridge (in Series Connection) Requires	Either All Stations Work at Reduced Voltage or That Station Be Disconnected	No Reduction in Other Stations' Voltages
6	DC Circuit Breaker	More Flexible if Used	Not Needed
7	Reversal of Power at any Station Requires	Mechanical Switch Operation	No Mechanical Switch Operation
8	Transmission Losses	Minimized by Keeping the System Voltage at Rated Value	Minimized by Letting the Inverter with the Highest P_{dO}/P_{dN} Set the Current
9	VAr Requirement of the Tap	Somewhat Higher Than Comparable Converter in a Point-to-Point System	Much Higher Than Comparable Converter in a Point-to-Point System
10	Harmonic AC Magnitudes (pu) in the Range of Operation	Slightly Higher Than Those of Point-to-Point Converters	Higher Than Those of Point-to-Point Converters
	Harmonic DC Magnitudes (pu) in the Range of Operation	Slightly Higher Than Those of Point-to-Point Converters	Much Higher Than Those of Point-to-Point Converters But Usually Less on Line Base
11	Probability of Commutation Failure	High (Specially for Small Taps)	Low (with Easy Recovery)
12	Central Control	More Flexible if Used	May or May Not Be Used
13	Dependence on Fast Communication	Higher Than Point-to-Point Systems	More or Less Similar to Point-to-Point Systems

failure and, if a commutation failure happens, it can recover without shutting the main system down [8,18].

2. A parallel tap has to be rated at system voltage (with current rating less than system current). A series tap need not be rated at system voltage (it has to be rated at system current). For a small tap the lower voltage rating lowers the cost considerablly [8,18].
3. Other general advantages of series arrangements (see Table 2.1, rows 4, 5, 6, 7, 12 & 13) may also be exploited.

On the other hand, a series tap may have some drawbacks of its own (see Table 2.1, rows 3, 8, 9 & 10). The techniques for diminishing these drawbacks will be discussed in the following sections.

2.3 TRANSMISSION LOSSES

Incorporation of a series tap in an HVDC system may cause the transmission losses to be increased. However, minimum transmission current and, thus, minimum transmission loss can be achieved by allowing the station with the larger ratio of instantaneous power to rated power to set the reference value for the current controller at the rectifier station. This is termed as "comparison of power ratios" concept [18,23]. The extra losses due to the tap will, then, depend on the daily load curves of the tap as compared with those of the main inverter.

Whether or not the tap should be allowed to set the current at all, depends on the importance of the load at the tap (i.e., a compromise between the minimum loss and the firm supply of the load at the tap). Therefore, it is considered as an optional operation strategy, which does not concern (or interfere) with the objectives of this thesis.

2.4 INSULATION ASPECTS

The idea of using a station in series with the line permits the use of low voltage elements, where the insulation levels are proportional to the energy tapped and the station floats at line voltage. The isolation between the station and the ground is achieved by the dc insulation between the windings of the output transformer and also by the insulated support structure. It has been suggested [8] that it is more economical to collect the energy in a low voltage, relatively complex, but low cost transformer, prior to transfer through an isolation transformer. The application of isolation transformer will be illustrated later in this thesis (see Figure 3.1(a)).

2.5 REACTIVE POWER REQUIREMENTS

The reactive power characteristics (i.e., P-Q characteristics) of a series tap can be derived [16,18] as follows.

The reactive power demand of a bridge is:

$$Q = P_d \tan \phi = V_d I_d \tan \phi, \qquad (2.1)$$

with,

$$\cos \phi \cong [\cos \alpha + \cos(\alpha+\mu)]/2 = V_d/V_o, \qquad (2.2)$$

where,

Q = reactive power,

P_d = dc power,

V_d = dc voltage,

I_d = dc current,

ϕ = power factor angle,

α = firing angle,

μ = overlap angle,

and V_o = no load dc voltage of the bridge.

After some simple manipulations,

$$Q \cong [(V_o I_d)^2 - P_d^2]^{1/2}. \qquad (2.3)$$

It should be noted that the exact reactive power consumption of a bridge [13] is given by,

$$Q = I_d V_0^2 \{2\mu + \sin 2\alpha - \sin(2\alpha + 2\mu)\}/(8\delta V), \qquad (2.4)$$

where,

$$\delta V = 3\omega L_c I_d/\pi, \qquad (2.5)$$

and ωL_c = commutation reactance.

However, Equation 2.3 is more appropriate for representation of the reactive power characteristics and the approximation introduces negligible error, indeed. For convenience, the following per unit (pu) bases are defined:

P_{dN} = rated dc power in inversion mode = MVA base on both ac and dc sides of the tap,

I_{dN} = rated dc line current = kA base on the dc side,

V_{sN} = rated ac system voltage= kV base on the ac side,

and ω_s = synchronous angular frequency = rad/s base.

Also, for convenience and simplicity, the following assumptions are made:

α_{min} = minimum firing angle = 2.0 degrees,

γ_{min} = minimum margin angle = 18.0 degrees,

and δV_N = rated commutation voltage loss = 0.06 pu.

From the above definitions and assumptions the following values are implied:

V_{dN} = rated dc voltage in inversion mode = 1.0 pu,

V_{ON} = rated no load dc voltage = 1.1146 pu,

α_N = firing angle at rated condition = 147.5 degrees,

and X_t = transformer reactance = 10.77% on its own base.

At 1.0 pu ac voltage (on the converter side of the transformer), the P-Q characteristics (for constant dc line currents) are, thus, given by,

$$Q \cong [(1.1146\ I_d)^2 - P_d^2]^{1/2} \text{ pu}, \qquad (2.6)$$

with,

$$Q_N = Q \Big|_{\substack{I_d = 1.0 \text{ pu} \\ V_d = 1.0 \text{ pu}}} = 0.492 \text{ pu},$$

and,

$$Q_O = Q \Big|_{\substack{I_d = 1.0 \text{ pu} \\ V_d = 0.0}} = 1.1146 \text{ pu}.$$

For dc line currents of 1.0 and 0.5 pu, the characteristics (in inversion mode) are plotted in Figure 2.1. Obviously, for any number of bridges in series, having equal firing angles, the characteristics will be the same, if the per unit bases are interpreted as overall values.

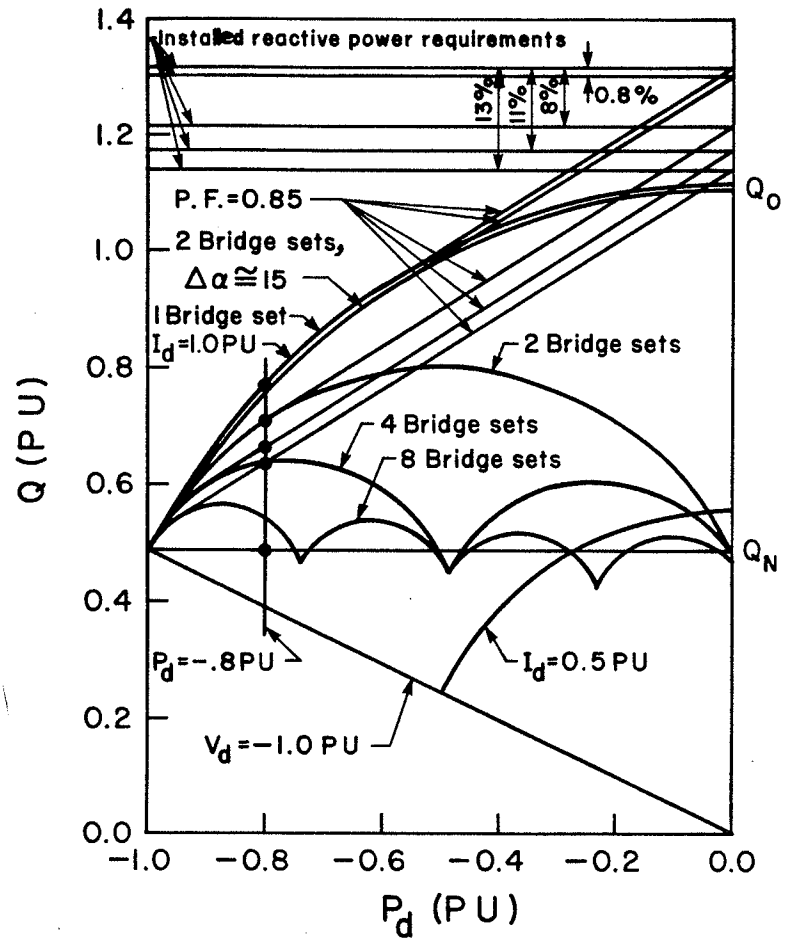

Figure 2.1: Reactive Power Characteristics of a Series Tap.

Assuming a load power factor of 0.85 lagging, the required installed reactive power will be 1.315 pu, as is shown in Figure 2.1. For simplicity, the variable range of the reactive power supply, required for the variations in the load power factor, is not considered here. For the same converter, if it were operated at minimum margin angle only, the required installed reactive power would be 1.112 pu (i.e., a series tap demands 18.26% more).

2.5.1 Differential Firing

If two bridge sets (preferably twelve-pulse bridge sets) are available and one operates at minimum margin angle, the reactive power consumption of the tap [18] will be,

$$Q=\{0.492+[(1.1146\ I_d)^2-(1+2\ P_d)^2]^{1/2}\}/2 \text{ pu}, \qquad (2.7)$$

The characteristic for 1.0 pu dc line current is shown in Figure 2.1, as well. This characteristic will be referred to as minimum VAr characteristic for two bridge sets (for 1.0 pu dc line current). The corresponding characteristic with equal firing will then be called maximum VAr characteristic.

Operation on the minimum VAr characteristic means 8% less installed reactive power and less reactive power consumption, especially at light loads, as can be seen from Figure 2.1. It also means higher frequency of commutation failure, as one bridge set operates at minimum margin angle all the time.

By properly adjusting the firing angles of both bridge sets (i.e., using a differential firing method), any operating point between the maximum and the minimum VAr characteristics can (theoretically) be obtained. This means, if the tap is operating on the minimum VAr characteristic, it is possible to increase the VAr consumption of the converter (i.e., VAr absorption capability) which can be used to reduce the overvoltages in the tap's own ac system. Alternatively, one can create both absorption and production capa-

bilities by simply setting an operation characteristic (e.g., a constant power factor line) between the maximum and the minimum VAr characteristics. In any case, the voltage regulations on the tap's ac bus will be very small at large loads.

Larger voltage regulations can be obtained by using more bridge sets in series. The minimum VAr characteristics of four and eight bridge sets are shown in Figure 2.1, as well. The pros and cons of this idea will be discussed in Chapter IV, after the calculation of the voltage regulation as a function of the number of bridge sets in series.

2.6 HARMONICS

The magnitudes of characteristic harmonics of HVDC converters are conventionally plotted versus the overlap angle, using the firing angle as a parameter [12,13,24]. However, to clarify the behavior of harmonics in a series tap, the higher desirability for their reduction and the way they are to be reduced, a change of variables is desirable to adapt the representations to the way a series tap operates; the real power of a series tap is regulated by controlling the tap's dc voltage rather than the dc line current.

The voltage and the current waveforms of a controlled bridge for a firing angle of 30 degrees, are shown in Figure 2.2 [13]. They can be defined at any firing angle as,

$$i(t)=\begin{cases} I_d \dfrac{\cos\alpha-\cos\omega t}{\cos\alpha-\cos(\alpha+\mu)} \text{ , for } \dfrac{\alpha}{\omega} \leqslant t \leqslant \dfrac{\alpha+\mu}{\omega} \text{ ,} \\ I_d \text{ , for } \dfrac{\alpha+\mu}{\omega} \leqslant t \leqslant \dfrac{2\pi/3+\alpha}{\omega} \text{ ,} \\ I_d \left\{1-\dfrac{\cos\alpha-\cos(\omega t-2\pi/3)}{\cos\alpha-\cos(\alpha+\mu)}\right\} \text{, for } \dfrac{2\pi/3+\alpha}{\omega} \leqslant t \leqslant \dfrac{2\pi/3+\alpha+\mu}{\omega} \text{ ,} \\ 0 \text{ , for } \dfrac{2\pi/3+\alpha+\mu}{\omega} \leqslant t \leqslant \dfrac{\alpha+\pi}{\omega} \text{ ,} \\ -i(t-\pi/\omega) \text{ ,} \end{cases} \tag{2.8}$$

and,

$$v(t)=\begin{cases} \sqrt{2}\, V_s \cos(\omega t+\pi/6) \text{ , for } 0 \leqslant t \leqslant \dfrac{\alpha}{\omega} \text{ ,} \\ \sqrt{2}\, V_s \cos\omega t \text{ , for } \dfrac{\alpha}{\omega} \leqslant t \leqslant \dfrac{\alpha+\mu}{\omega} \text{ ,} \\ \sqrt{2}\, V_s \cos(\omega t-\pi/6) \text{ , for } \dfrac{\alpha+\mu}{\omega} \leqslant t \leqslant \dfrac{\pi}{3\omega} \text{ ,} \\ \text{Repetition of above every } \dfrac{\pi}{3\omega} \text{ ,} \end{cases} \tag{2.9}$$

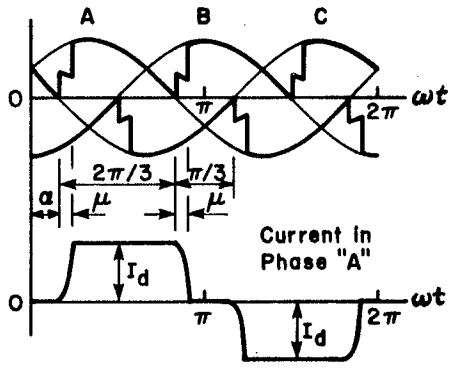

Figure 2.2: Voltage and Current Waveforms of a Controlled Bridge.

where, the firing angle is measurred with reference to the zero axis of Figure 2.2.

The firing and the overlap angles are related to other variables of a bridge by,

$$V_d = V_o[\cos \alpha + \cos(\alpha+\mu)]/2, \tag{2.10}$$

and,

$$V_d = V_0 \cos \alpha - 3\omega L_c I_d/\pi \text{ pu}, \tag{2.11}$$

with,

$$V_0 = V_{ON} \cdot V_s \text{ pu}, \tag{2.12}$$

where, the symbols and per unit bases are as defined in the previous section and the voltage drops on the valves and transformer resistance are neglected. Substituting from Equation 2.12 in Equations 2.10 and 2.11, the firing and the overlap angles can be derived as,

$$\alpha = \arccos \{(V_d/V_s + 3 L_c/\pi \cdot \omega I_d/V_s)/V_{ON}\} , \tag{2.13}$$

and,

$$\mu = \arccos \{(V_d/V_s + 3 L_c/\pi \cdot \omega I_d/V_s)/V_{ON}\} - \alpha , \tag{2.14}$$

Thus, the new variables are V_d/V_s and $\omega I_d/ V_s$, which, at rated ac voltage and synchronous frequency, simply reduce to V_d and I_d, respectively.

2.6.1 AC Current Harmonics

Fourier analysis of i(t) (i.e., Equation 2.8) results in the real (denoted by subscript R) and imaginary (denoted by subscript X) components of the fundamental and the nth characteristic harmonic currents of a line commutated converter as,

$$I_{(1)R}=\frac{\sqrt{3}\,V_0}{4\pi X_c}\{\cos(\pi/3+2\alpha)-\cos(\pi/3+2\alpha+2\mu)-\sqrt{3}\mu\}, \quad (2.15)$$

$$I_{(1)X}=\frac{\sqrt{3}\,V_0}{4\pi X_c}\{\sin(\pi/3+2\alpha)-\sin(\pi/3+2\alpha+2\mu)+\mu\}, \quad (2.16)$$

$$I_{(n)R}=\frac{2\,V_0}{n\pi X_c}\sin\frac{n\pi}{3}\{\frac{1}{n+1}\sin((n+1)\mu/2).\sin((n+1)(\alpha+\mu/2)+n\pi/3)$$
$$-\frac{1}{n-1}\sin((n-1)\mu/2).\sin((n-1)(\alpha+\mu/2)+n\pi/3)\}, \quad (2.17)$$

$$I_{(n)X}=\frac{2\,V_0}{n\pi X_c}\sin\frac{n\pi}{3}\{-\frac{1}{n+1}\sin((n+1)\mu/2).\cos((n+1)(\alpha+\mu/2)+n\pi/3)$$
$$+\frac{1}{n-1}\sin((n-1)\mu/2).\cos((n-1)(\alpha+\mu/2)+n\pi/3)\}, \quad (2.18)$$

where,

n = mp-1 and mp+1,

p = the number of pulses = 6, 12, ... ,

and m = 1, 2, ...

Then (for n=1 as well),

$$I_{(n)}=\sqrt{(I_{(n)R}^2+I_{(n)X}^2)/2} \quad \text{(i.e., r.m.s. value)}, \quad (2.19)$$

$$\theta_{(n)}=\arctan\,(I_{(n)X}/I_{(n)R}), \quad (2.20)$$

and,

$$\bar{I}_{(n)}=I_{(n)}\angle\theta_{(n)}, \quad (2.21)$$

where, the bar denotes phasor quantity.

According to above the ratio of the nth harmonic current magnitude to the fundamental current magnitude (i.e., $I_{(n)}/I_{(1)}$) is a function of two variables, namely, firing and overlap angles only. By substituting for these variables from Equations 2.13 and 2.14, the ratio in question can be determined in terms of the new variables. 11th and 13th harmonic magnitudes in percentage of fundamental current are plotted versus V_d/V_s, using $\omega I_d/V_s$ as a parameter, in Fig-

ures 2.3 and 2.4, respectively. The numerical assumptions and per unit bases of Section 2.5 are implicit in these figures. For different numerical values, the variables can be easily adjusted by simple correction factors.

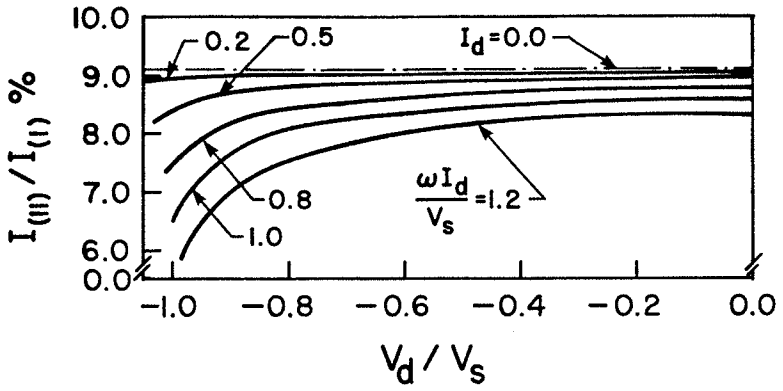

Figure 2.3: 11th Harmonic Current of a Series Tap.

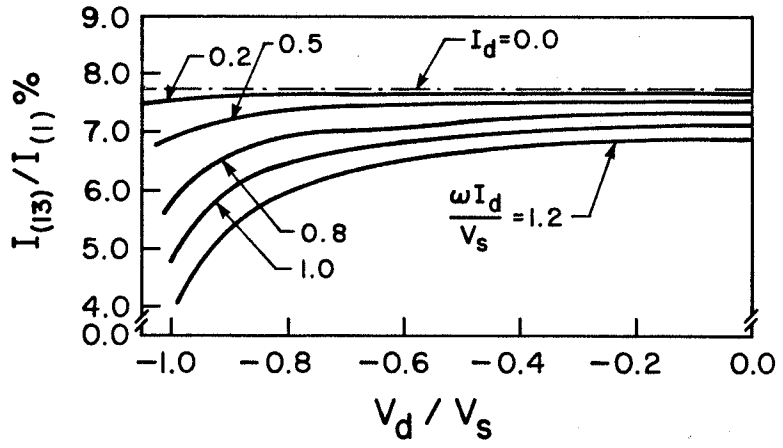

Figure 2.4: 13th Harmonic Current of a Series Tap.

It may be noted that the nth harmonic magnitude in percentage of fundamental current approaches a value of 100/n% as the dc line current (or, in general, as the overlap an-

gle) approaches zero. However, the required level of filtering for nth harmonic does not depend on this value. It depends on the maximum magnitude of the nth harmonic current in Amps or in percentage of the rated fundamental current. Using the latter, the maximum magnitude of 11th harmonic at rated conditions (i.e., synchronous frequency, rated ac voltage and rated dc line current) is 8.57%, as can be found from the curve for $\omega I_d/V_s$ = 1.0 pu in Figure 2.3. The corresponding value at minimum margin angle (i.e., the conventional operating condition of an inverter in a point-to-point HVDC system) is 6.52%, as can be found from the same curve. This means that the 11th harmonic current increases by a ratio of 1.314 due to the operation of the converter as a series tap. Using Figure 2.4, the corresponding ratio for the 13th harmonic current is 7.08/4.76 = 1.478.

The costs of minimum cost tuned filters increase in proportion with the above ratios [12]. Although part of the increase in the cost of tuned filters (i.e., about one half of it) has to be attributed to the increase in the reactive power capability of the filters, the overall cost of the tapping station may increase considerably. It is so, not only because the cost of providing ac tuned filters (and thus its increase) is usually a considerable portion of the overall cost of a converter, but also because the filter losses will be higher as well.

To understand the behavior of the phase angles of the characteristic harmonic currents some approximations are helpful. Approximations of the ac current waveform by a square wave (i.e., for zero overlap angle) and by a trapesoidal wave (i.e., for small overlap angles) are shown in Figure 2.5, with the same zero axis as in Figure 2.2. With the square waveform, if the zero axis is moved to the right by the firing angle plus 60 degrees, the waveform will be symmetrical about the zero axis and, thus, the phase angles of all harmonics will be zero. Therefore, with the zero axis as indicated in Figure 2.5,

$$\theta_{(n)} = n\,(\,\alpha + 60^{\circ}\,)\,. \qquad (2.22)$$

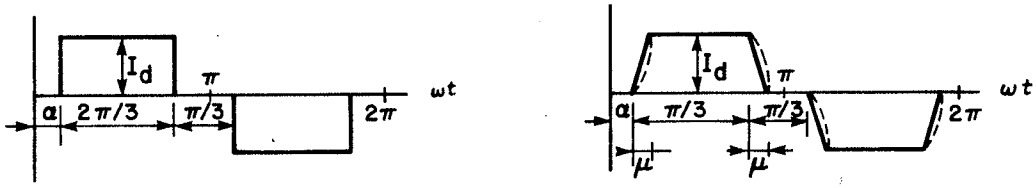

Figure 2.5: Square and Trapesoidal Current Waveforms.

It may be noted that this result is equal to the limit of Equation 2.20 as the overlap angle approaches zero. With the trapesoidal waveform of Figure 2.5, a closer approximation may be achieved. Again, if the zero axis is moved to the right by one half of the overlap angle in excess of the shift for the square wave, the waveform will be symmetrical about the zero axis. Therefore, with the zero axis as indicated in Figure 2.5,

$$\theta_{(n)} = n(\alpha+\mu/2+60^{\circ}). \qquad (2.23)$$

2.6.2 DC Voltage Harmonics

Fourier analysis of v(t) (i.e., Equation 2.9) results in the real and the imaginary components of the nth harmonic voltage as,

$$V_{(n)R}=V_0\{\frac{1}{n+1}\cos((n+1)\mu/2).\cos((n+1)(\alpha+\mu/2)) - \frac{1}{n-1}\cos((n-1)\mu/2).\cos((n-1)(\alpha+\mu/2))\}, \quad (2.24)$$

and,

$$V_{(n)X}=V_0\{\frac{1}{n+1}\cos((n+1)\mu/2).\sin((n+1)(\alpha+\mu/2)) - \frac{1}{n-1}\cos((n-1)\mu/2).\sin((n-1)(\alpha+\mu/2))\}, \quad (2.25)$$

where,

$n = mp$,

p = number of pulses = 6, 12, ...,

and $m = 1, 2, \ldots$.

Then,

$$V_{(n)}=\sqrt{(V_{(n)R}^2+V_{(n)X}^2)/2} \quad \text{(i.e., r.m.s. value)}, \quad (2.26)$$

$$\theta_{(n)}=\arctan(V_{(n)X}/V_{(n)R}), \quad (2.27)$$

and,

$$\bar{V}_{(n)}=V_{(n)}\angle\theta_{(n)} . \quad (2.28)$$

Similar to the ac current harmonics, the ratio of the nth harmonic voltage magnitude to the no load dc voltage can be determined in terms of the new variables, using Equations 2.13 and 2.14. The magnitude of the 12th harmonic voltage in percentage of the no load dc voltage is plotted versus V_d/V_s , using $\omega I_d/V_s$ as a parameter, in Figure 2.6.

As the overlap angle approaches zero,

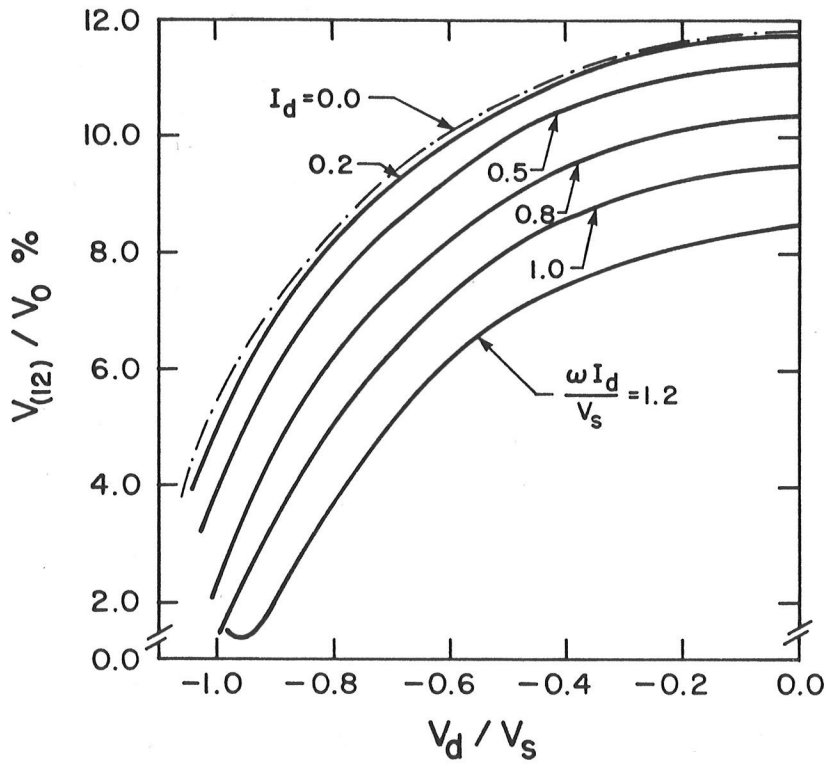

Figure 2.6: 12th Harmonic Voltage of a Series Tap.

$$V_{(n)}/V_{0}^{\%} \xrightarrow[\mu \to 0]{} \frac{100}{n^2-1}\sqrt{(n^2+1)-(n^2-1)\cos 2\alpha} \quad , \tag{2.29}$$

and at a firing angle of 90 degrees, it reaches its maximum,

$$(V_{(n)}/V_{0}^{\%})_{max} = 100\sqrt{2}n/(n^2-1). \tag{2.30}$$

The maximum value for 12th harmonic is then 11.87%, which will, theoretically, be reached at a firing angle of 90 degrees as the dc line current approaches zero. However, assuming that the dc line current can reach as low as 0.2 pu during the operation at light loads (at rated ac voltage and synchronous frequency), this value will be 11.80%, as can be determined from Figure 2.6. The corresponding value at minimum margin angle is 3.90%. This means that the 12th harmonic voltage increases by a ratio of 3.02 due to the operation of

the converter as a series tap. However, the dc harmonics of a small series tap will still be smaller than those of the main converters, if they are based on the dc line voltage.

The phase angle of the nth harmonic voltage can be derived from Equation 2.27 by substituting for the variables from Equations 2.24 and 2.25. After some simple mathematical manipulations,

$$\theta_{(n)}=n(\alpha+\mu/2)-\arctan\{\frac{n+\tan n\mu/2.\tan\mu/2}{1+n\tan n\mu/2.\tan\mu/2}\tan(\alpha+\mu/2)\}, \qquad (2.31)$$

which can be approximated for small overlap angles as,

$$\theta_{(n)} \xrightarrow[\mu \to 0]{} n\alpha - \arctan(n\tan\alpha). \qquad (2.32)$$

2.6.3 Harmonics Entering the DC Line .

To control the magnitudes of harmonics entering a dc line from a series tap, the lengths of the line sections between the tap and the main converters may play important roles. A typical representation of the situation is shown in Figure 2.7 [13], where, each line section is represented by its equivalent pi-circuit at nth harmonic frequency and the tap is represented by its nth harmonic voltage and its smoothing reactors. For nth harmonic frequency, the line sections are virtually short circuited at both main converter ends due to the application of dc harmonic filters at these terminals.

The impedances seen from the tap at sides 1 and 2 are,

$$Z_{1(n)}=\frac{\bar{V}_{1(n)}}{\bar{I}_{1(n)}} = \frac{1}{Y_{\pi 1(n)}/2+1/Z_{\pi 1(n)}} = Z_{c(n)}\tanh(\gamma_{(n)}\ell_1)$$
$$\cong j\, Z_c \tan(2\pi\ell_1 / \lambda_{(n)}), \qquad (2.33)$$

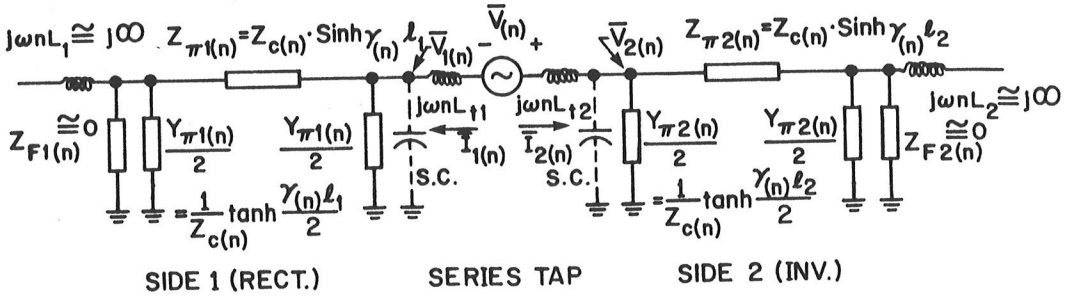

Figure 2.7: Equivalent Circuit for nth DC Harmonic of a Series Tap.

and,

$$Z_{2(n)}=\frac{\bar{V}_{2(n)}}{\bar{I}_{2(n)}}=\frac{1}{Y_{\pi 2(n)}/2+1/Z_{\pi 2(n)}}=Z_{c(n)}\tanh(\gamma_{(n)}\ell_2)$$
$$\cong j\, Z_c \tan(2\pi\ell_2/\lambda_{(n)}), \qquad (2.34)$$

where,

$$Z_{c(n)}=\sqrt{\frac{z_{(n)}}{y_{(n)}}}=\sqrt{\frac{r_\ell+j\omega n\ell_\ell}{g_\ell+j\omega nc_\ell}}\cong\sqrt{\frac{\ell_\ell}{c_\ell}}=Z_c, \qquad (2.35)$$

$$\gamma_{(n)}=\alpha_{(n)}+j\beta_{(n)}=\sqrt{z_{(n)}\cdot y_{(n)}}\cong j\omega n\sqrt{\ell_\ell c_\ell}\cong j\ 2\pi/\lambda_{(n)}, \qquad (2.36)$$

Z_c = characteristic impedance,

γ = propagatin constant,

α = attenuatin constant,

β = phase constant,

and λ = wave length of the line.

Then,

$$\bar{I}_{2(n)}=-\bar{I}_{1(n)}=\bar{V}_{(n)}/(Z_{1(n)}+Z_{2(n)}+j\omega nL_t), \qquad (2.37)$$

where,

$$L_t=L_{t1}+L_{t2}. \qquad (2.38)$$

Therefore, the nth harmonic voltage across the tap including its smoothing reactors is,

$$\bar{V}_{2(n)}-\bar{V}_{1(n)}=\bar{V}_{(n)}-j\omega nL_t\bar{I}_{2(n)}$$

$$=\left[1-\frac{1}{1+\frac{Z_c}{\omega nL_t}\left(\tan\frac{2\pi\ell_1}{\lambda_{(n)}}+\tan\frac{2\pi\ell_2}{\lambda_{(n)}}\right)}\right].\bar{V}_{(n)} \qquad (2.39)$$

or,

$$\bar{V}_{2(n)}-\bar{V}_{1(n)}=\begin{cases}\bar{V}_{(n)}, \text{for } \ell_1 \text{ or } \ell_2=\frac{2k+1}{4}\lambda_{(n)}\\ 0, \text{for } \ell_1=k_1\ell_2=k_2\lambda_{(n)}/2,\ k's=1,2,...\end{cases} \qquad (2.40)$$

This result means that if the line section lengths approach odd multiples of the quarter wave length at nth harmonic frequency, the smoothing reactors will be ineffective. In fact, large harmonic current magnitudes may appear at the current antinodes of the line sections. If this condition is avoided, a proper choice of the smoothing reactors may reduce the harmonic magnitudes to acceptable levels. If surge capacitors (S.C.'s) are used, their proper choice on each side will be helpful as well.

2.6.4 Differential Firing

From Equation 2.22, with two (or two sets of) bridges in series having two different firing angles, the approximate relative phase angle between the nth harmonic currents produced by the two (or the two sets of) bridges is,

$$\Delta\theta_{(n)}=\theta_{2(n)}-\theta_{1(n)}=n(\alpha_2-\alpha_1)=n\Delta\alpha\ , \qquad (2.41)$$

which holds for small dc line currents. A closer approximation can be found from Equation 2.23 as,

$$\Delta\theta_{(n)} = n(\Delta\alpha + \frac{1}{2}\Delta\mu), \qquad (2.42)$$

Equations 2.41 and 2.42 both point to the fact that with a proper difference between the two firing angles a desired phase-shift between the two components of the nth harmonic currents can be effected. This kind of phase-shift can result in drastic reduction in the magnitudes of a family of harmonics with some similarity to the outcome of phase-shifting transformers.

It is well known that an economical twelve-pulse operation can be effected by wye- and delta-connected transformer windings on the valve side, which implies a phase-shift of 30 degrees. A twenty four-pulse operation requires a phase-shift of 15 degrees between each two transformer windings, which, along with other reasons [12,13], makes it uneconomical. To have similar kinds of operation by differential firing, Equation 2.42 shows that $\Delta\alpha + \Delta\mu/2$ should be about 30 and 15 degrees, respectively. A significant difference between the outcomes of the two techniques is that with the differential firing technique no characteristic harmonic can be completely eliminated, since creating the phase-shift means creating a difference between the magnitudes of the individual components of the harmonics as well, which is not the case with phase-shifting transformers. Thus, such operations will be referred to as "quasi n-pulse" operations, where, n = 12, 24, ...

As will be shown later in this thesis, the adoption of a quasi twelve-pulse operation [15] as the normal operation mode of an HVDC converter turns out to be economically unattractive, although it may have other applications. A quasi twenty four-pulse operation of two twelve-pulse bridge sets, however, is potentially economical, if used as the normal operation mode of a series tap. For small $\Delta\mu$, the approximate situation is as shown in Figure 2.8, where, drastic reductions in the overall magnitudes of 11th and 13th harmonic currents and 12th harmonic voltage are achieved due to a difference of about 15 degrees between the two firing angles.

Figure 2.8: Phasor Diagrams for $\Delta\alpha \approx 15°$ and Small $\Delta\mu$.

2.7 DIODE RECTIFIER TECHNIQUE

A converter consisting of simple diode bridges can only operate as a rectifier with no delay angle. A diode rectifier bridge and its output voltage are shown in Figure 2.9. The reactive power consumption and the magnitudes of characteristic harmonics of a diode rectifier bridge are minimum.

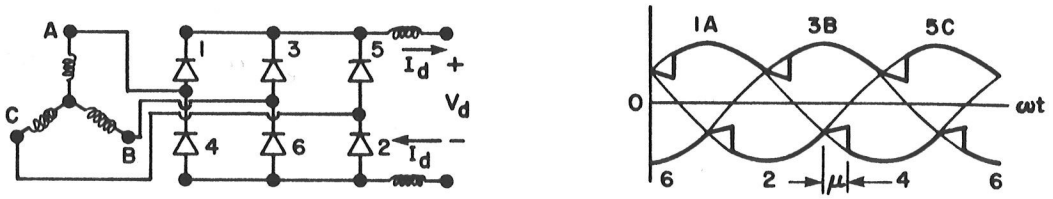

Figure 2.9: A Diode rectifier Bridge and its Output Voltage.

A likely application of a series tapping station is where the electrical energy of a rather small isolated source (e.g., hydraulic generation, wind generation, etc.) is to be transferred to an otherwise point-to-point HVDC system (e.g., a readily existing HVDC line in close proximity). Such a tap will operate in rectification mode only. In fact, it is desirable to run the tap at (or close to) the minimum firing angle limit, to ensure maximum system voltage and thereby minimum transmission losses, as well as minimum reactive power consumption and minimum harmonic magnitudes at the tapping station, pointing to the fact that the valves will virtually act as simple diodes and can be so replaced [25].

Diode Rectifier stations have been proposed in the literature for point-to-point HVDC systems [2,19]. In this case the system voltage is defined by the rectifier while the inverter controls the system current (i.e., contrary to the normal operation mode of a conventional point-to-point HVDC system). This implies higher reactive power requirement and higher voltage rating of the valves at the inverter end. For

comparable security and flexibility a dc circuit breaker (one per pole) is required as well. However, the massive savings at the rectifier end may result in considerable overall savings. Parallel multiterminal HVDC systems incorporating diode rectifier stations have also been suggested [5], with similar implications.

A diode rectifier series tap, however, does not require the control of the current to be normally assigned to the inverter station. Nor does it need any dc circuit breakers. Furthermore, with two diode bridges in series having wye- and delta-connected transformer secondary windings (i.e., a twelve-pulse diode bridge set) there is a great possibility for elimination of all harmonic filters, even on the dc side of a rather small tap.

Chapter III

DIODE RECTIFIER SERIES TAPPING

3.1 GENERAL

In this chapter the incorporation of a diode rectifier series tap in an otherwise point-to-point HVDC system is described. The results of digital simulation studies of a prototype system are presented. Diode rectifier series tapping is compared with other schemes and some conclusions are drawn.

3.2 OPERATION MODES OF THE SYSTEM

The system basically consists of three terminals, namely, a controlled converter station at the main sending end (i.e., main rectifier), another controlled converter station at the receiving end (i.e., inverter) and a diode rectifier station somewhere along the dc line (i.e., tap), all in series. The operation modes of the system are similar to those of a conventional point-to-point HVDC system and the tap simply delivers a constant power for a given dc line current, as described in the subsequent subsections. It may be noted that the imposition of a unidirectional flow of power in the main system is for convenience and is not a must.

3.2.1 Normal Operation Mode

The main rectifier is normally in control of the system current while the inverter, which operates as close to its minimum margin angle as possible, defines the system voltage. This operation mode (also known as alpha-constant control mode) can be described by the following equations:

$$V_{di} = -V_o \cos\gamma_{min} + 3X_c I_d/\pi \ (=-1.0 \text{ pu}), \tag{3.1}$$

$$V_{dt} = V_o - 3X_c I_d/\pi, \tag{3.2}$$

$$V_{dr} = V_o \cos\alpha - 3X_c I_d/\pi, \tag{3.3}$$

$$I_d = (V_{dr} + V_{dt} - V_{di})/R_\ell, \tag{3.4}$$

where,

R_ℓ = total dc line resistance,

and the additional subscripts i, rt and rm indicate inverter, tap rectifier and main rectifier, respectively. These subscripts are implied for each no load dc voltage and each commutation reactance, as well.

3.2.2 Abnormal Operation Mode

If the total rectifier voltage is unable to overcome the inverter voltage (e.g., one rectifier bridge is suddenly blocked), the inverter takes over the control of the system current. The current will be reduced by the current margin (i.e., typically 10%) and the main rectifier will operate at its minimum firing angle. This operation mode (also known as beta-constant control mode) can be described by the following equations:

$$V_{dr} = V_o \cos\alpha_{min} - 3X_c I_d/\pi , \quad (3.5)$$

$$V_{dt} = V_o - 3X_c I_d/\pi , \quad (3.6)$$

$$V_{di} = -V_o \cos\beta - 3X_c I_d/\pi , \quad (3.7)$$

$$I_d = (V_{dr} + V_{dt} - V_{di})/R_\ell , \quad (3.8)$$

where,

β = advance firing angle of the inverter.

3.3 TAPPING STATION

3.3.1 Typical Arrangements

As was mentioned in the previous chapter, it is preferable to use two diode bridges with wye- and delta-connected transformer secondary windings acting as one twelve-pulse set. The bridges have to be isolated from the ground, e.g., placed in a metal housing on a platform at the line voltage. The isolation of the low voltage side from the high voltage side may be provided either by the converter transformer or by an isolation transformer. As was mentioned in Section 2.4, the latter has been suggested to be more economical [8] and is shown in Figure 3.1(a). The former (not shown) can be obtained from Figure 3.1(a) by eliminating the isolation transformer and placing the converter transformer at the ground voltage with the neutral point of its primary winding connected to the ground. Another possibility is to place the generator on the high voltage platform as well, and therefore, eliminate the need for isolation through any transformer. This arrangement is shown in Figure 3.1(b).

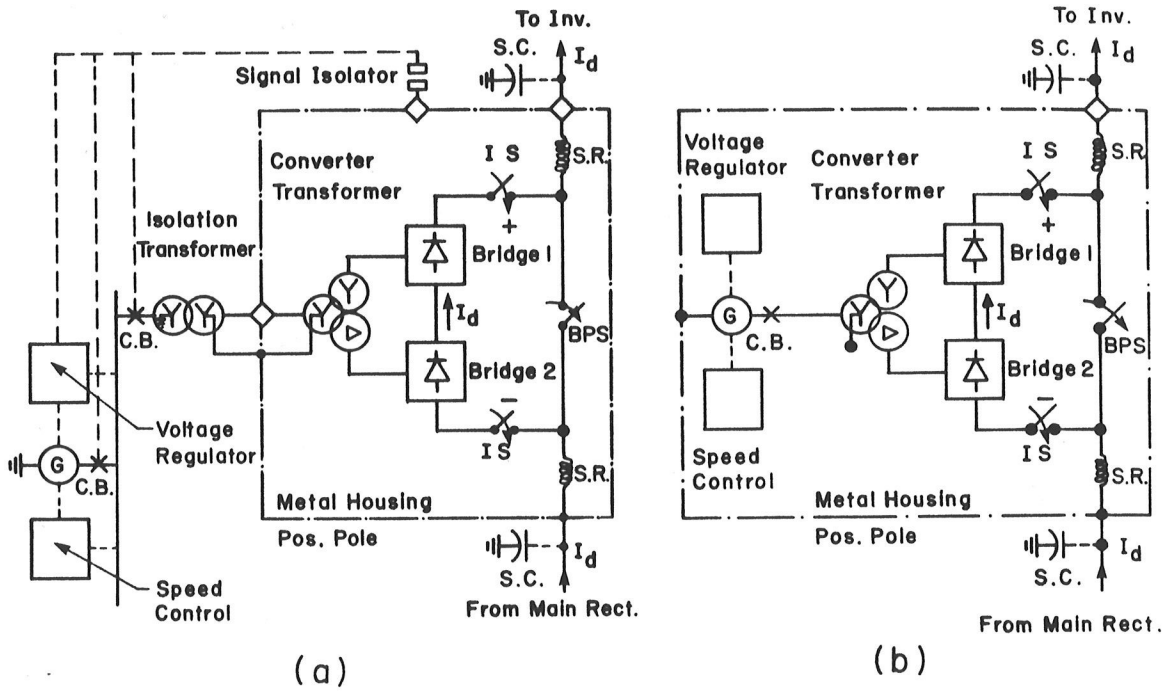

Figure 3.1: Typical Diode Rectifier Series Tapping Station Arrangements.

In each arrangement of Figure 3.1, the basic arrangement of isolation switches (IS's), by-pass switch (BPS) and smoothing reactors (S.R.'s) is shown. To protect the converter station against voltage surges in the dc line (i.e., to reduce dv/dt), surge capacitors (S.C.'s) may be considered on both sides of the tap. Also, as in conventional converters, surge diverters (not shown) are needed for protection purposes [18]. Usually, no harmonic filters is required. The generator is equipped with both voltage and speed regulators. The reactive power of the tap (e.g., 33% of the real power, for 0.06 pu rated commutation voltage loss) can be entirely supplied by the generator. The blocking (or deblocking) of the tap is effected by opening (or

closing) its ac circuit breaker (C.B.), as described in the next subsection. No dc circuit breakers is required. Transformer tap changers, as well as communication between the tapping station and the main stations are not essential.

3.3.2 Blocking and Deblocking

When the tap is out of service, the dc system current passes through the by-pass switch; the by-pass switch is closed and the isolation switches and the tap's ac circuit breaker are open. Closing the isolation switches and then opening the by-pass switch cause the current to be diverted to the diodes; all diodes become forward biased and provide the current with three parallel paths. At this state, closing the tap's ac circuit breaker causes the deblocking of the tap [2]. However, it means a sudden large load (e.g., 1.0 pu for 1.0 pu dc line current) on the generator as well as a significant disturbance in the dc system. This situation can be avoided by reducing the no load terminal voltage of the machine to a predetermined value. The predetermined value may, with sufficient accuracy, be calculated

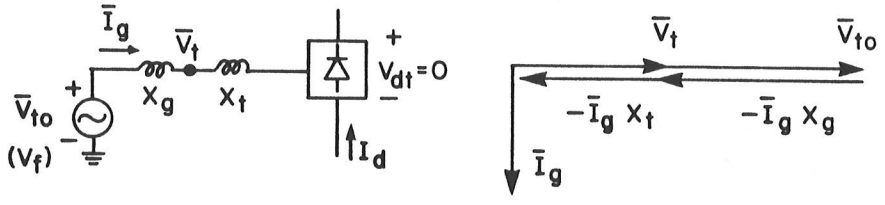

Figure 3.2: Simplified Circuit and its Phasor Diagram for Zero Tap Output.

from a simple phasor diagram, as shown in Figure 3.2, where,

V_{t0} = generator no load terminal voltage,

V_t = generator terminal voltage,

V_f = generator field voltage = V_{t0} in per unit,

I_g = generator current,

X_g = generator reactance,

X_t = transformer leakage reactance(s),

and V_{dt} = dc voltage of the tap.

The generator no load terminal voltage drops entirely on the reactances, resulting in zero voltage on the dc side of the tap (at steady state), i.e., no real power output. The commutation process, however, takes place and the current will lag the terminal voltage by 90 degrees, i.e., only reactive power will be consumed by the tap. Thus, for a smooth start-up of the tap, the procedures will be as follows.

1. Run the generator at synchronous speed (no load).
2. Adjust the generator terminal voltage to a predetermined value which will result in zero (or a small value, say, 0.1 pu) output on the dc side of the tap (see Figure 3.2).
3. At the same time, close the isolation switches and, once all diodes are conducting, open the by-pass switch.
4. Close the tap's ac circuit breaker.
5. Gradually increase the field voltage to reach the desired terminal voltage, while allowing the speed control to maintain the desired speed.

6. Increase the inverter voltage (or deblock the corresponding inverter bridge set).

The procedures for a smooth blocking (shut-off) of the tap can easily be derived from the start-up procedures by a proper rearrangement using the reverse actions and need not be repeated here. It may be noted that it is possible to block the tap without a pre-reduction of the machine terminal voltage. However, such a blocking may cause large stresses on the machine, some overvoltages in the tapping station and a significant disturbance in the dc system and, therefore, should be avoided except in emergency cases. Furthermore, it would be the case with a controlled tap as well.

3.4 SIMULATION MODELLING

For digital simulation studies, basically the Bipole II of Nelson River HVDC system is considered as the main system. Each main converter is modelled by its equivalent circuit seen from its dc side, namely, by an equivalent dc voltage source (i.e., $V_0 \cos \alpha$ for the main rectifier and $V_0 \cos \beta$ for the inverter) and an equivalent resistance (i.e., $R_{eq} = 3\omega L_c/\pi$) at either end, as shown in Figure 3.3(a). The smoothing reactors, the 12th dc harmonic tuned filters and the dc high-pass (H.P.) filters are included at both ends. Furthermore, a thyristor (not shown) is simulated in series with each dc voltage source to ensure that the

current does not flow in reverse direction. Figure 3.3(b) shows the block diagram of the current controller at the main rectifier, which is basically a proportional-integral (PI) controller. Similar current controller is considered at the inverter end, but its ordered current is lowered by a current margin of 10%, as shown in Figure 3.3(c). The minimum margin angle-controller of the inverter is modelled by a simple straight forward block which represents the negative slope of the voltage-current characteristic of the inverter and is shown in Figure 3.3(c) as well.

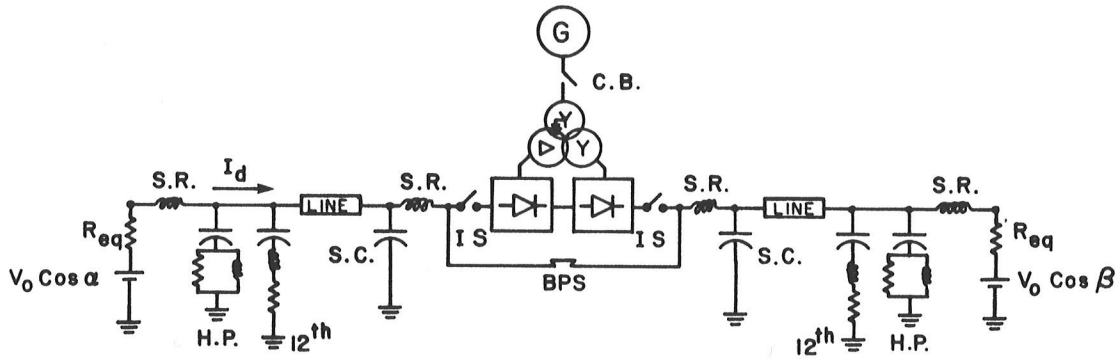

(a) Simulation Network

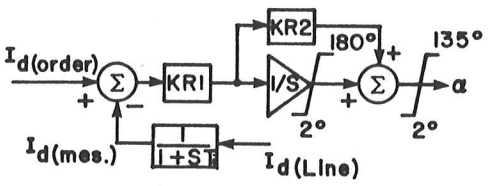

(b) Controls at Rectifier

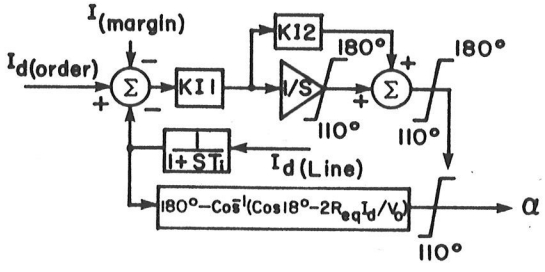

(c) Controls at Inverter

Figure 3.3: Simulation Network and Controls.

The dc transmission line is divided into two sections. One-third of it is considered between the main rectifier and the tapping station and the rest (two-thirds) between the tapping station and the inverter (i.e., Jenpeg would be the approximate location of the tapping station). Distributed parameter line model is used.

The tapping station is modelled in detail, based on Figure 3.1(b). Each bridge consists of six diodes and a snubber circuit (i.e., a resistor in series with a capacitor) across each diode. The field voltage and the mechanical torque of the synchronous generator are kept constant during the study time of the faults and other transients(i.e., at pre-fault values).

To fully utilize the extra power introduced to the system by the tap, the total inverter voltage of the system should be increased correspondingly. This can be achieved by introducing an extra twelve-pulse bridge set at the inverter end (or possibly somewhere else along the line). Alternatively, bridges of higher voltage rating may be considered at the inverter end, which is more appropriate in case of a small rectifier tap. For digital simulation studies presented in the next section the tap is 10% (i.e., its rated dc voltage is 10% of the rated dc voltage of the original inverter station) and the inverter voltage is increased to 110% (e.g., by transformer tap changers, with the implicit assumption that the extra stresses would be tolerable). No extra volt-

age margin at the main rectifier is considered. The simulation data is given in Appendix A. The simulation program is EMTP [20] mode 28. The time step is 0.00004 s except for harmonic analysis, where it is reduced to 0.00002 s for more accuracy. Note that for ac waveforms the maximum (rather than r.m.s.) rated values are used as the per unit bases.

3.5 SIMULATION RESULTS

3.5.1 Waveforms and Harmonics of the Tap

The steady-state waveforms of the tapping station at 1.0 pu dc line current are presented in Figure 3.4. The 11th and the 13th harmonic magnitudes of the ac current and the 12th harmonic magnitude of the dc voltage have been evaluated as 2.24%, 1.35% and 5.6% (or 0.54% on the line voltage base), respectively. Taking the transformer reactance as commutation reactance, the theoretical values are 3.9%, 2.5% and 2.7% [12], respectively. The discripancy between the measured and the theoretical values is mainly due to the fact that the machine causes a significant increase in the commutation reactance (especially so, because no filters is used) which, in turn, increases the commutation (overlap) angle. However, for twelve-pulse operation of the tap, the commutation angle does not increase beyond 30 degrees and, instead, the voltage zero crossings are delayed (say, 5 to 10 degrees). This, in fact, is equivalent to a minimum firing angle limit in a controlled rectifier.

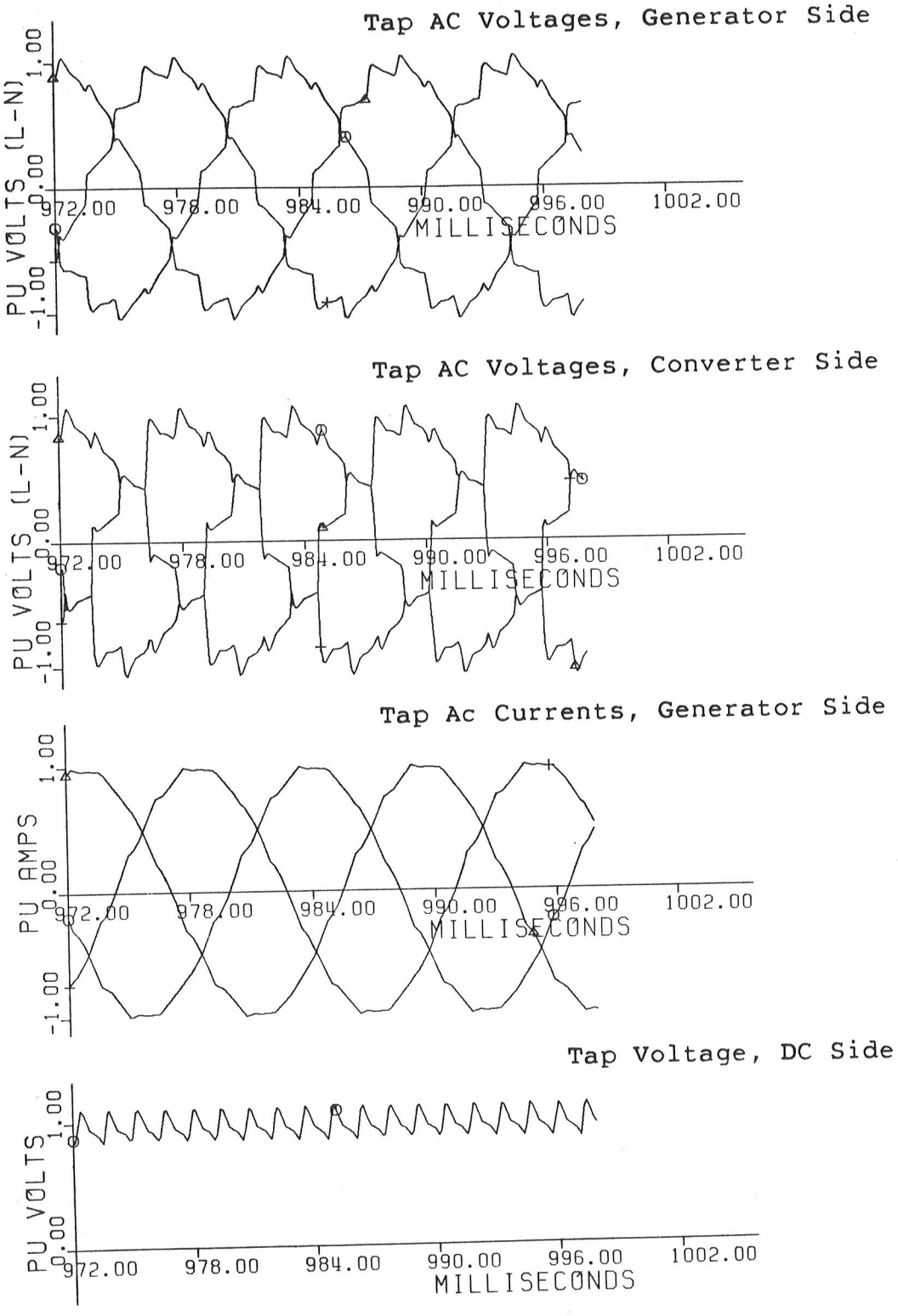

Figure 3.4: Steady-State Waveforms of the Tap.

In Figure 3.5, the voltage across the tap including its smoothing reactors is presented for two different locations of the tapping station. For the first graph, the length of the line sections are nearly even multiples of the quarter wave length at 12th harmonic frequency and the waveform contains negligible amounts of 12th and other harmonics. For the second graph, the lengths of the line sections are nearly odd multiples of the quarter wave length at 12th harmonic frequency and the 12th harmonic magnitude is hardly reduced by the smoothing reactors (compare with the second graph of Figure 3.4). These results are consistent with the theoretical results of Subsection 2.6.3.

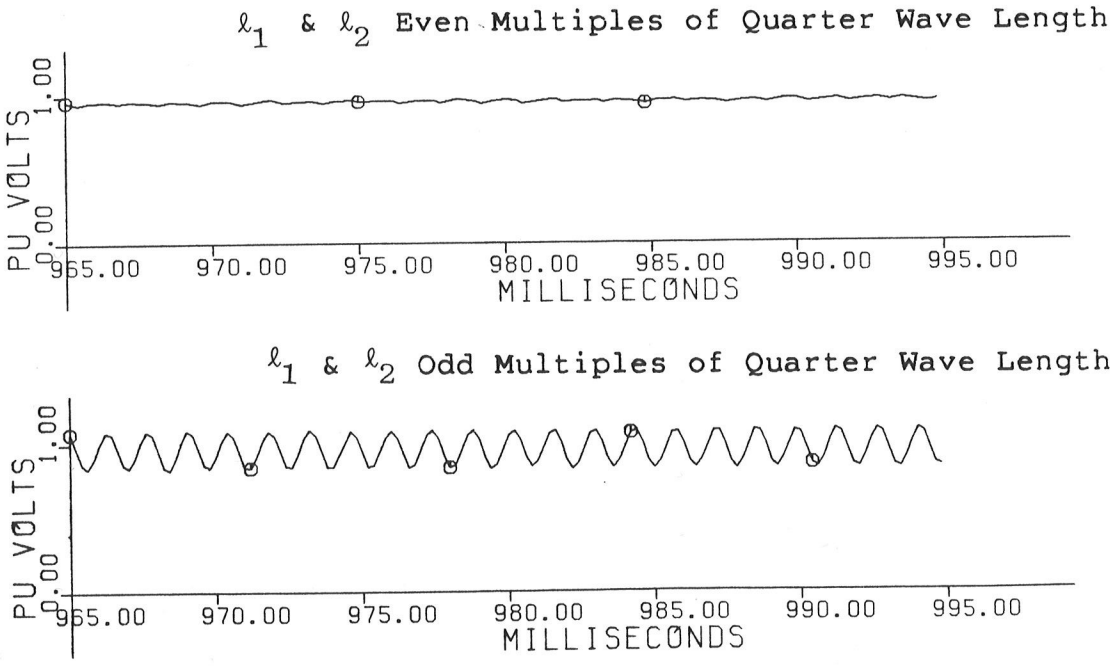

Figure 3.5: Voltage across the Tap Including its Smoothing Reactors.

It may be noted that in another test (not presented) the surge capacitors were disconnected, for both locations of the tap, which resulted in little change in the harmonic content of either waveform. Especially, the change in 12th harmonic magnitude was negligible.

3.5.2 Blocking and Deblocking of the Tap

The results of a deblocking of the tap, carried out according to procedures 1 to 4 of Subsection 3.3.2, are presented in Figure 3.6. Before closing the tap's ac circuit breaker, the dc line current is 1.0 pu and the generator terminal voltage is 0.4 pu. The commutation process starts immediately after closing the tap's circuit breaker at t = 1.025 s. Some voltage appears on the dc side of the tap, which vanishes in less than 0.2 second. The change in the speed of the machine as well as the change in the dc line current were insignificant (not shown).

The results of a blocking of the tap are presented in Figure 3.7. Prior to opening the tap's circuit breaker the field voltage of the machine is 0.4 pu and the dc line current is 1.0 pu. The circuit breaker is opened at first current zero crossings after t = 1.025 s. The current is diverted to the diodes (i.e., all diodes conducting) with virtually no disturbances.

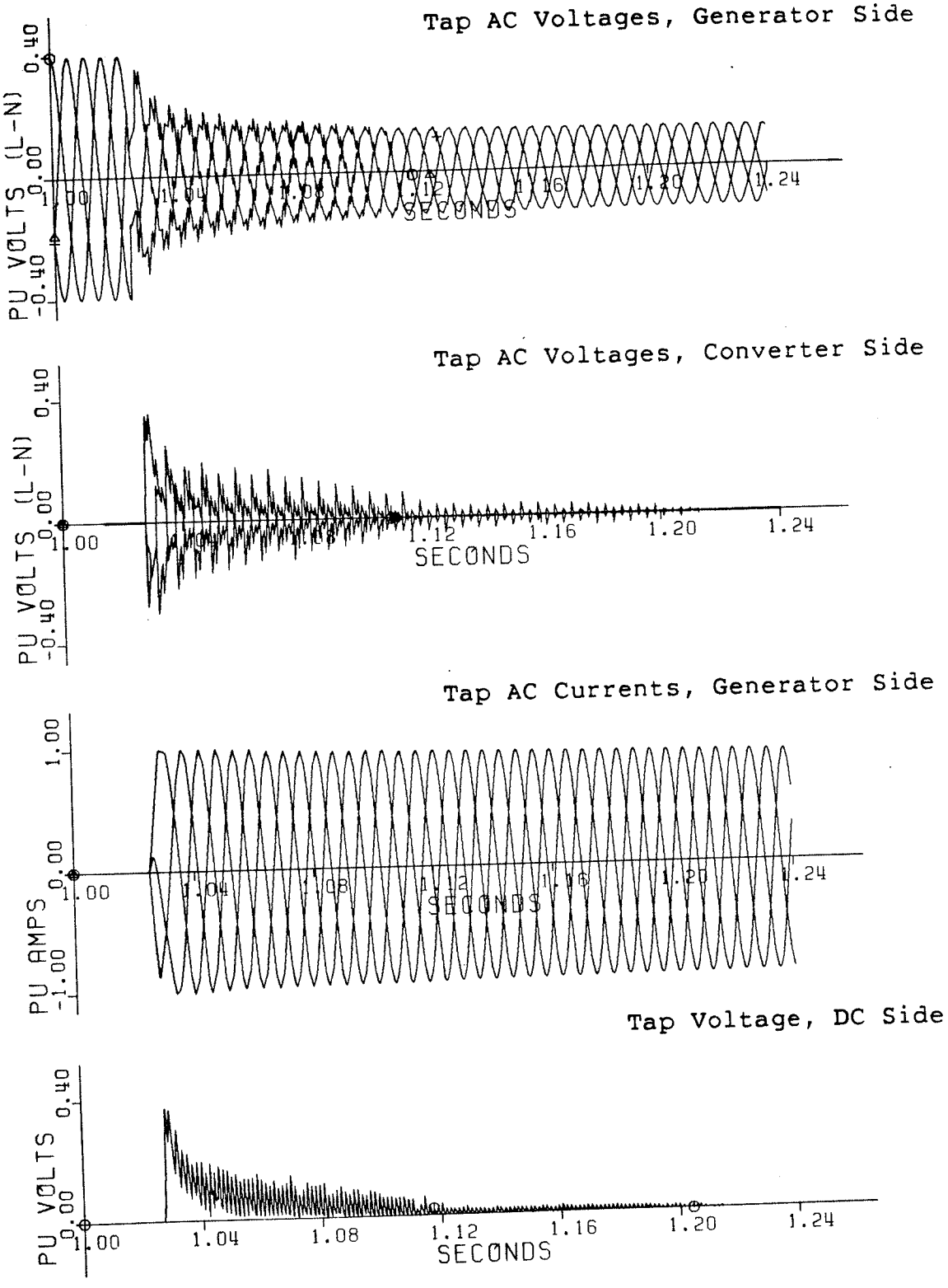

Figure 3.6: Deblocking of the Tap.

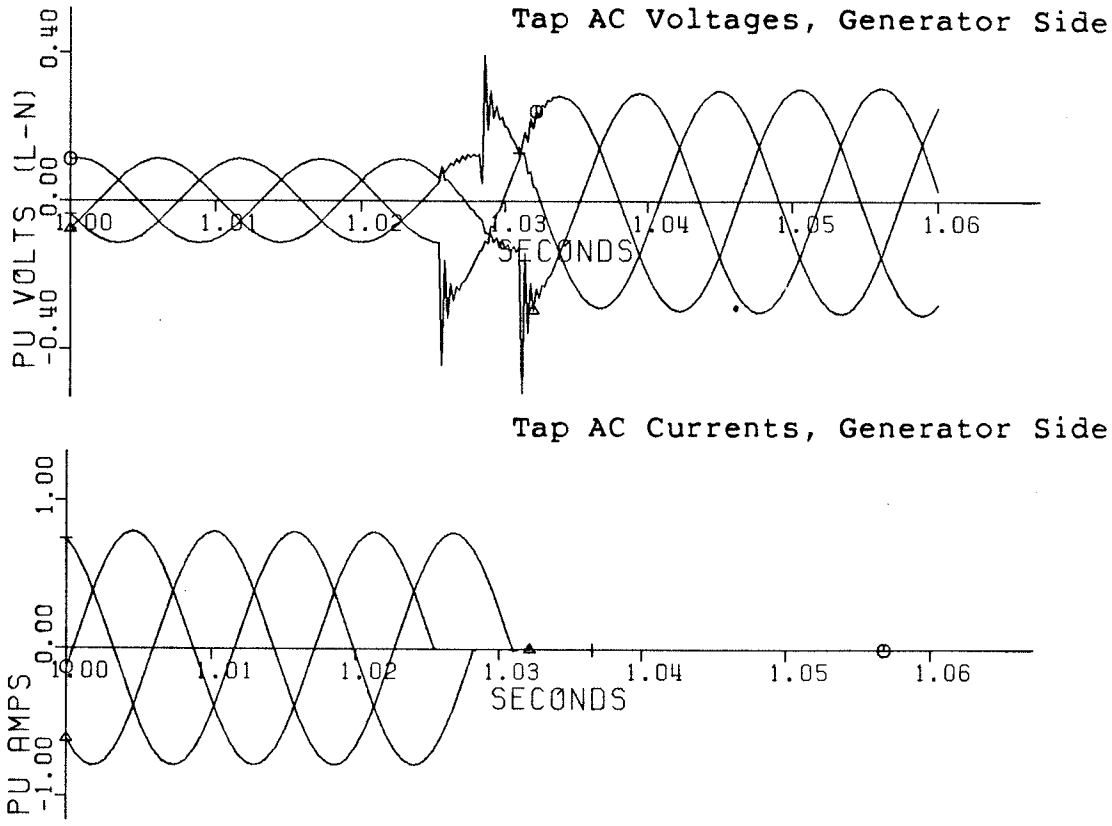

Figure 3.7: Blocking of the Tap.

The results of an emergency blocking of the tap are shown in Figure 3.8. Prior to opening the tap's circuit breaker the terminal voltage of the machine and the dc line current are both 1.0 pu. The circuit breaker is opened at first current zero crossings after t = 0.6 s. The dc line current drops since the main rectifier is unable to maintain it. The inverter's current controller takes over and the current is maintained at 0.9 pu in less than 0.2 second after the blocking of the tap. Now, reducing the dc voltage of the inverter to its original value (i.e., without the tap) would cause the main rectifier's current controller to be in charge again (resulting in 1.0 pu dc line current).

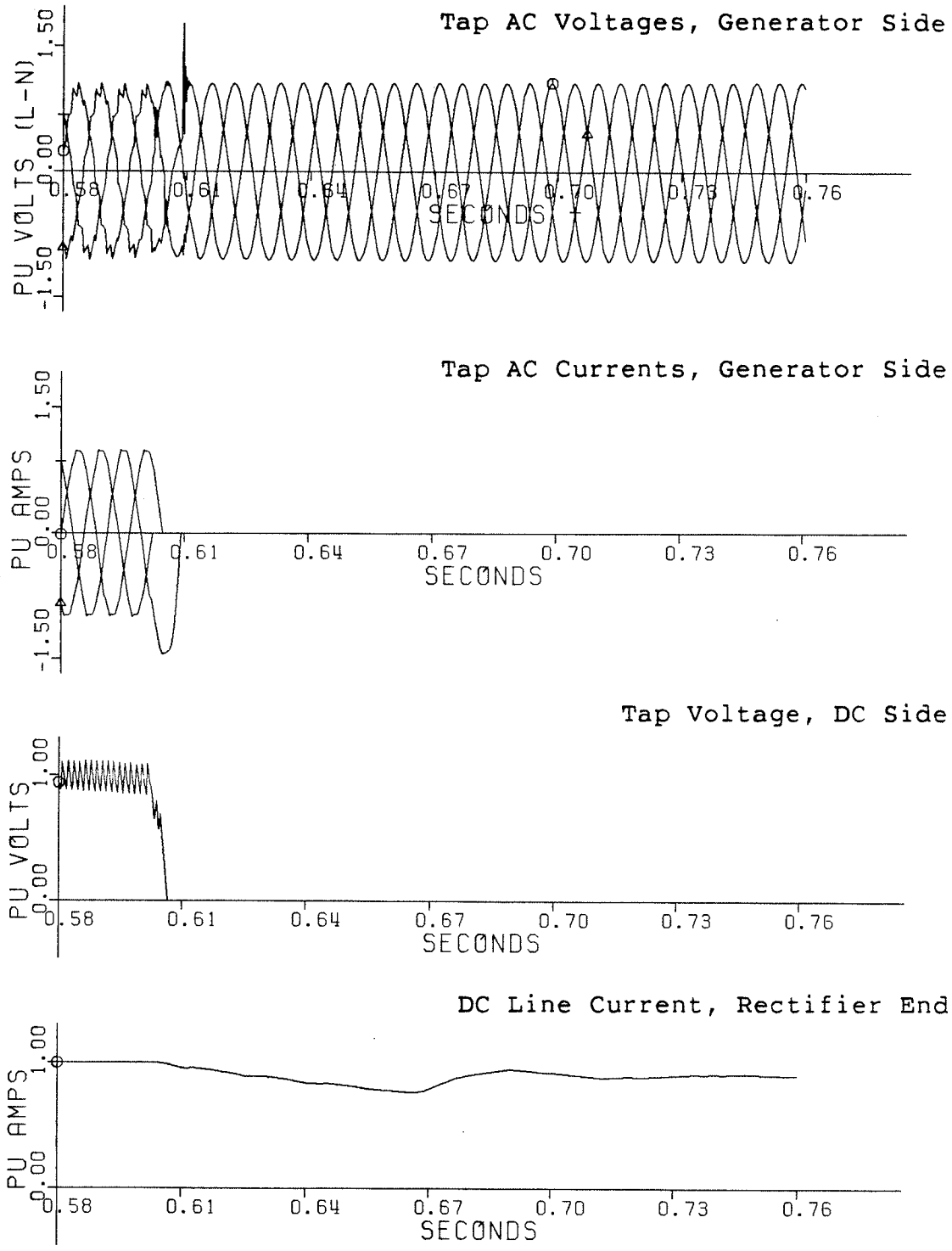

Figure 3.8: Emergency Blocking of the Tap.

3.5.3 Faults in the AC System of the Tap

The results of a three-phase (to ground) short circuit and a single phase-to-ground short circuit at the generator's bus are presented in Figures 3.9 and 3.10, respectively. Both faults start at t = 0.6 s and last for 100 ms (i.e., 6 cycles). Figures 3.9 and 3.10 reveal that these faults cause relatively minor disturbances in the dc system, as is expected to be the case for a small tap.

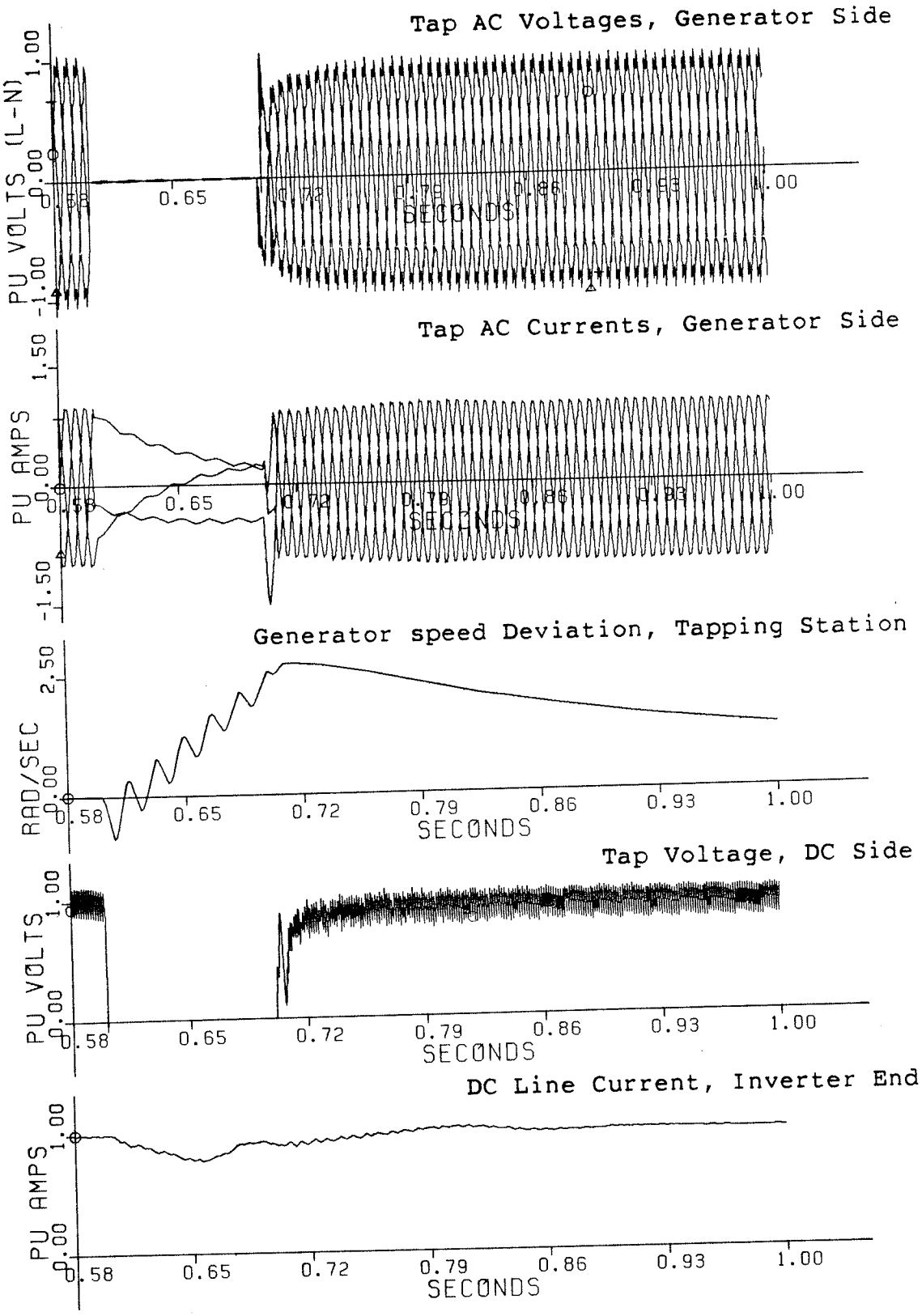

Figure 3.9: Three-Phase Fault in the Tapping Station.

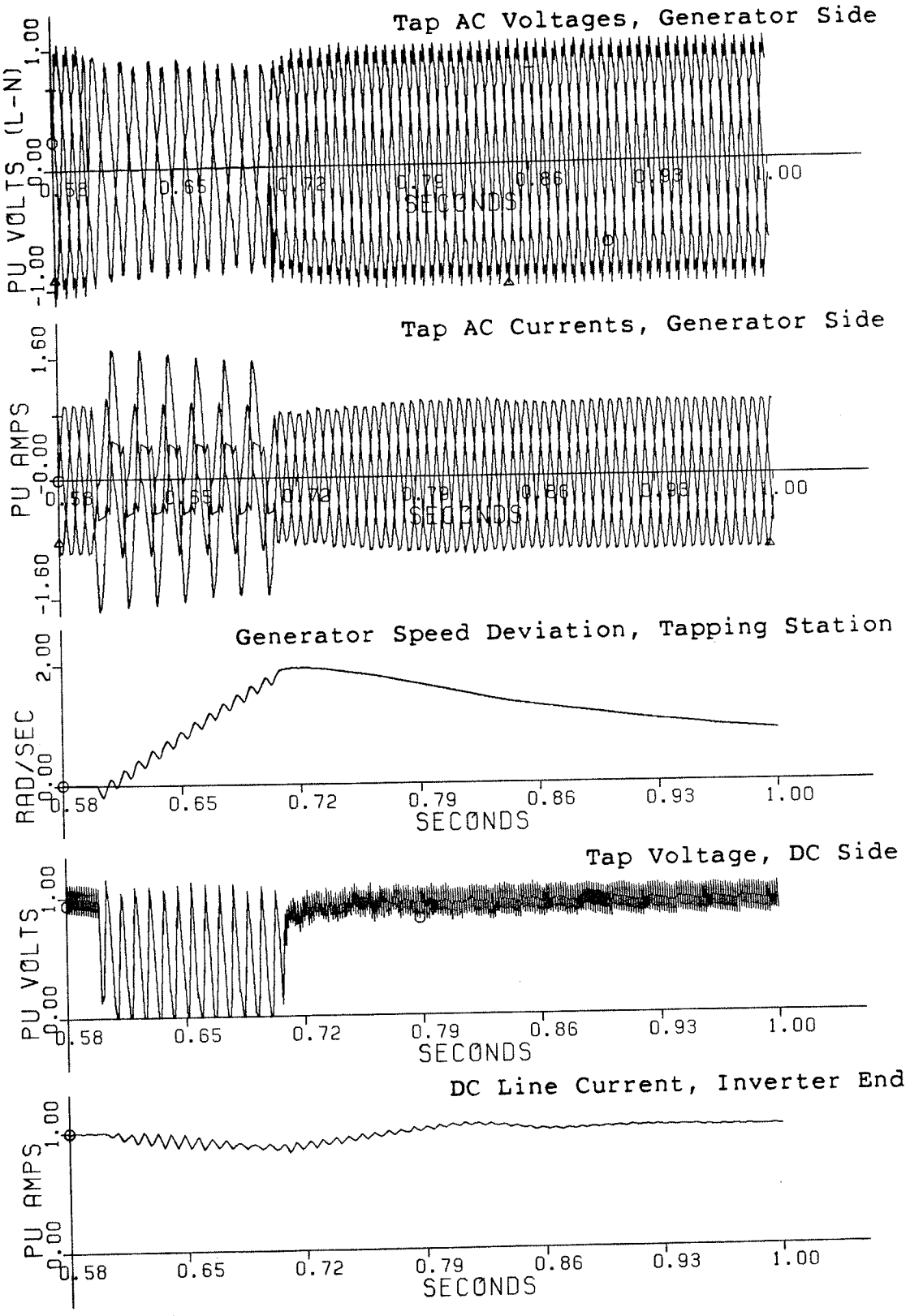

Figure 3.10: Single Phase-To-Ground Fault in the Tapping Station.

3.5.4 Major Disturbances in the Main DC System

A dc line fault is usually the most severe fault in an HVDC system and requires the current to be brought to zero. This is usually accomplished by applying a forced retard at the rectifier end, i.e., forcing the rectifier into inversion mode to quickly absorb the energy stored in the dc system. Similar provision is assumed with the system incorporating a diode rectifier series tap. The results of a dc line (to ground) fault at the inverter end, right before the inverter's smoothing reactor, are presented in Figure 3.11. The first graph represents the fault with the tap out of service and is provided for comparison. The fault initiates at t = 0.63 s. The forced retard is applied by changing the current order to zero, 6.5 ms after the conception of the fault to allow for the line travel time as well as the fault detection time. After 200 ms from the conception of the fault (i.e., to allow for deionization), the fault is removed and the current order is changed to its pre-fault value, namely 1.0 pu.

It may be noted that once the current reaches zero the tap automatically stops and there is no need to block the tap by opening its ac circuit breaker, which would be much slower than the converter action. Nor is any dc circuit breakers needed. Once the fault is removed and the current starts to build up in the dc line, the commutation process will also automatically take place in the tapping station.

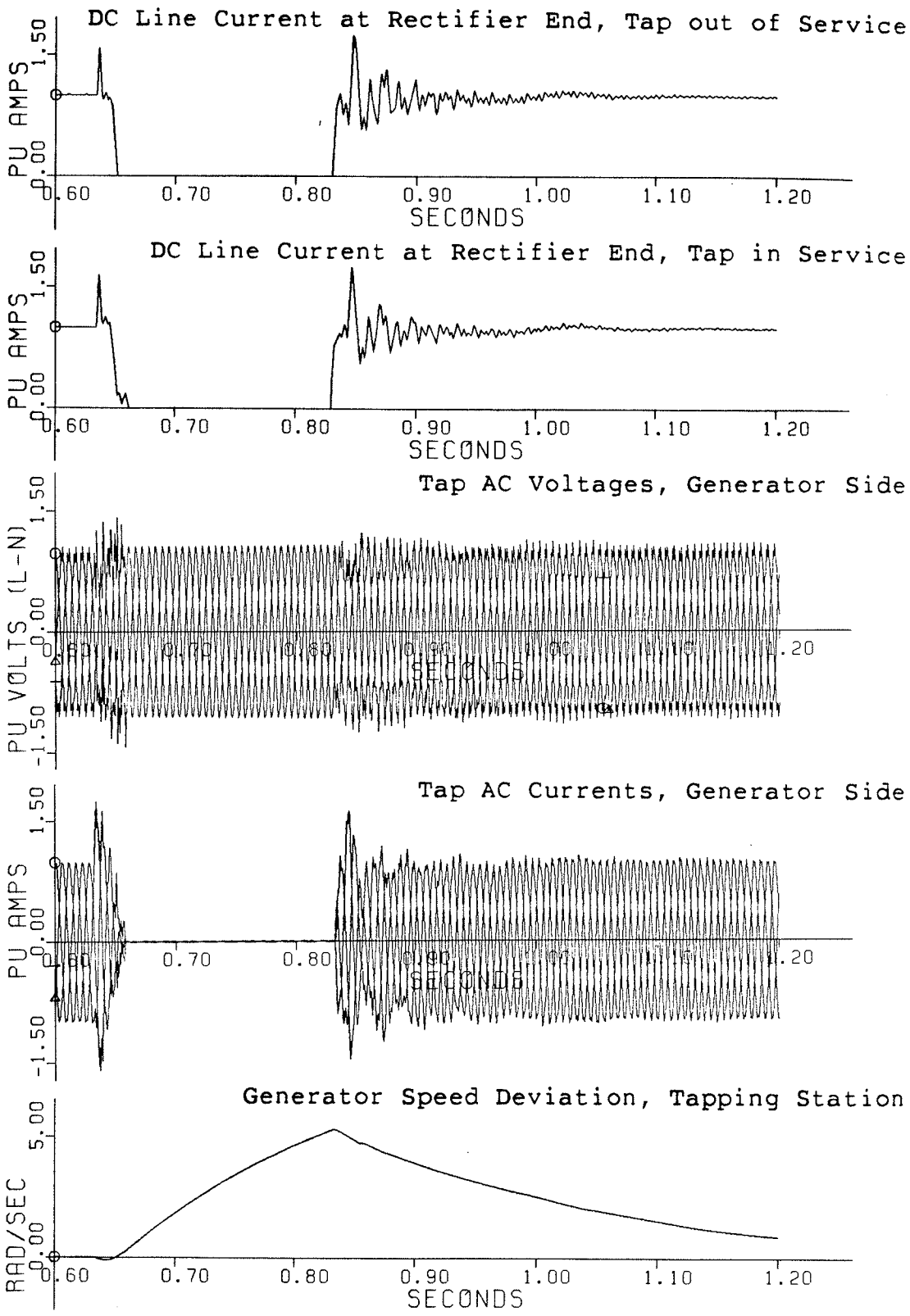

Figure 3.11: DC Line Fault at the Inverter End.

Comparison of the second graph with the first graph in Figure 3.11 indicates that both the current peak and the duration for bringing the current to zero have slightly increased due to the tap. Such increases will set a limit to the relative rating of the tap and may become decisive in this respect.

Dc line faults at both sides of the tap, as well as at the main rectifier end, have been investigated as well. The results (not presented) have shown no extra significance as compared with that of Figure 3.11. Not surprisingly, the faults between the tap and the main rectifier were as significant as the corresponding faults with the tap removed.

A single commutation Failure in an inverter station virtually results in a simple short circuit on its dc side for somewhat less than one half of a cycle. The results of such a short circuit at the inverter end, starting at t = 0.6 s and lasting for 8 ms, are presented in Figure 3.12. The first graph represents the fault with the tap out of service. It may be noted that the tap has caused a slight increase in the current peak. In an HVDC incorporating a diode rectifier station as a main rectifier station, such a current peak may be relieved by a negative ceiling demand of the excitation system of the generator at the diode rectifier station [2]. Such provision in the tapping station has been neither needed nor significantly helpful. However, it may become desirable, as well as more helpful, for larger tapping stations.

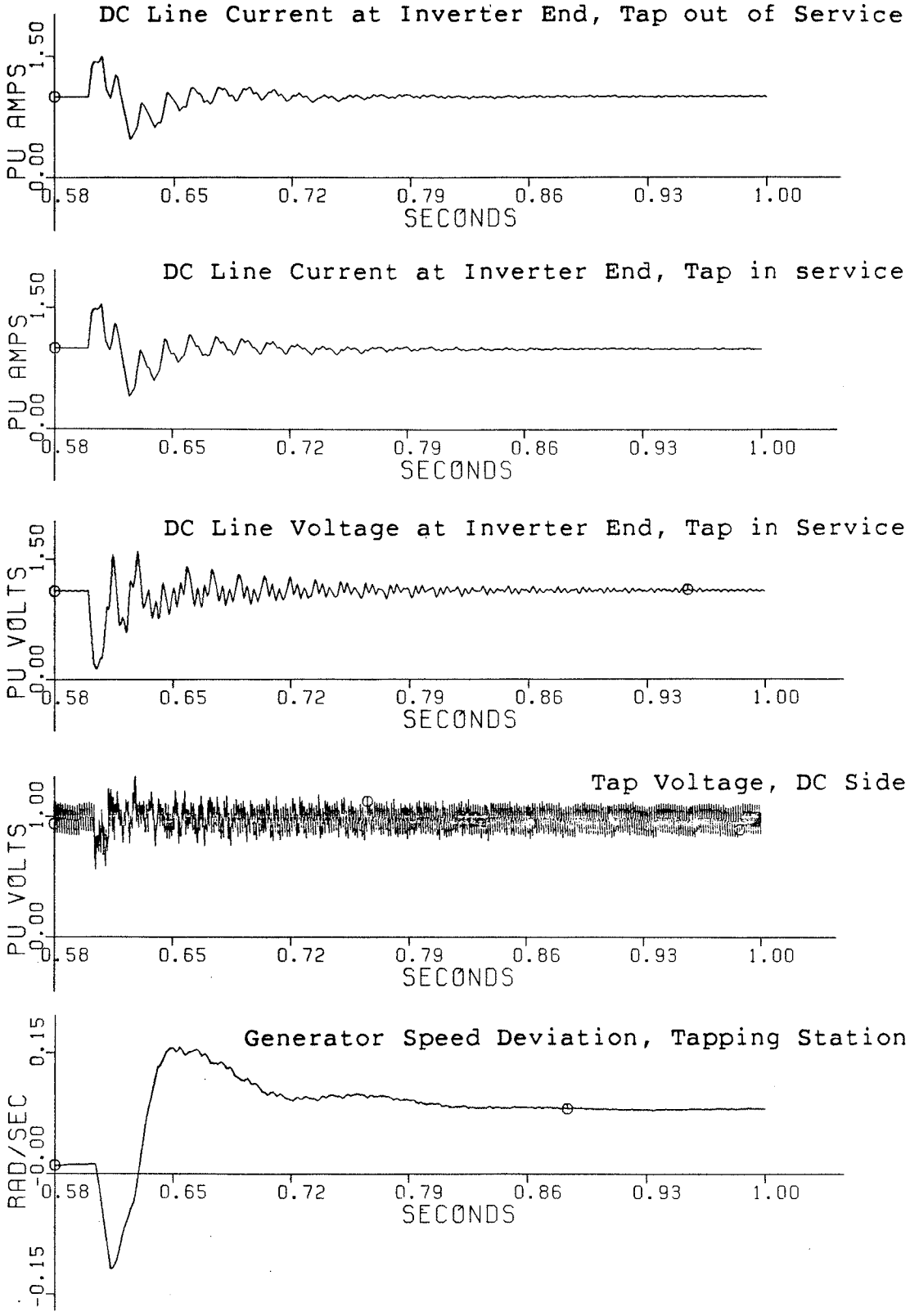

Figure 3.12: Single Commutation Failure at the Inverter.

Another rather large disturbance in the main system is partial blocking of the converters. The results of the blocking of one twelve-pulse bridge set at the main rectifier end (i.e., one half of the converter) at t = 0.65 s, which is followed by the blocking of one twelve-pulse bridge set at the inverter end after 20 ms, are presented in Figure 3.13. It may be noted that some extra voltage margin at the rectifier end would have been required if the tap had not existed, or the rectifier would not have been able to maintain the current (of course, after maintaing the current by the inverter, the rectifier voltage could have been increased by its transformer tap changers enabling it to control the current again). But, with the tap incorporated no extra voltage margin is required since, while the main converter voltages reduce to one half, the tap voltage remains the same and, thus, the total remaining rectifier voltage is able to maintain the current.

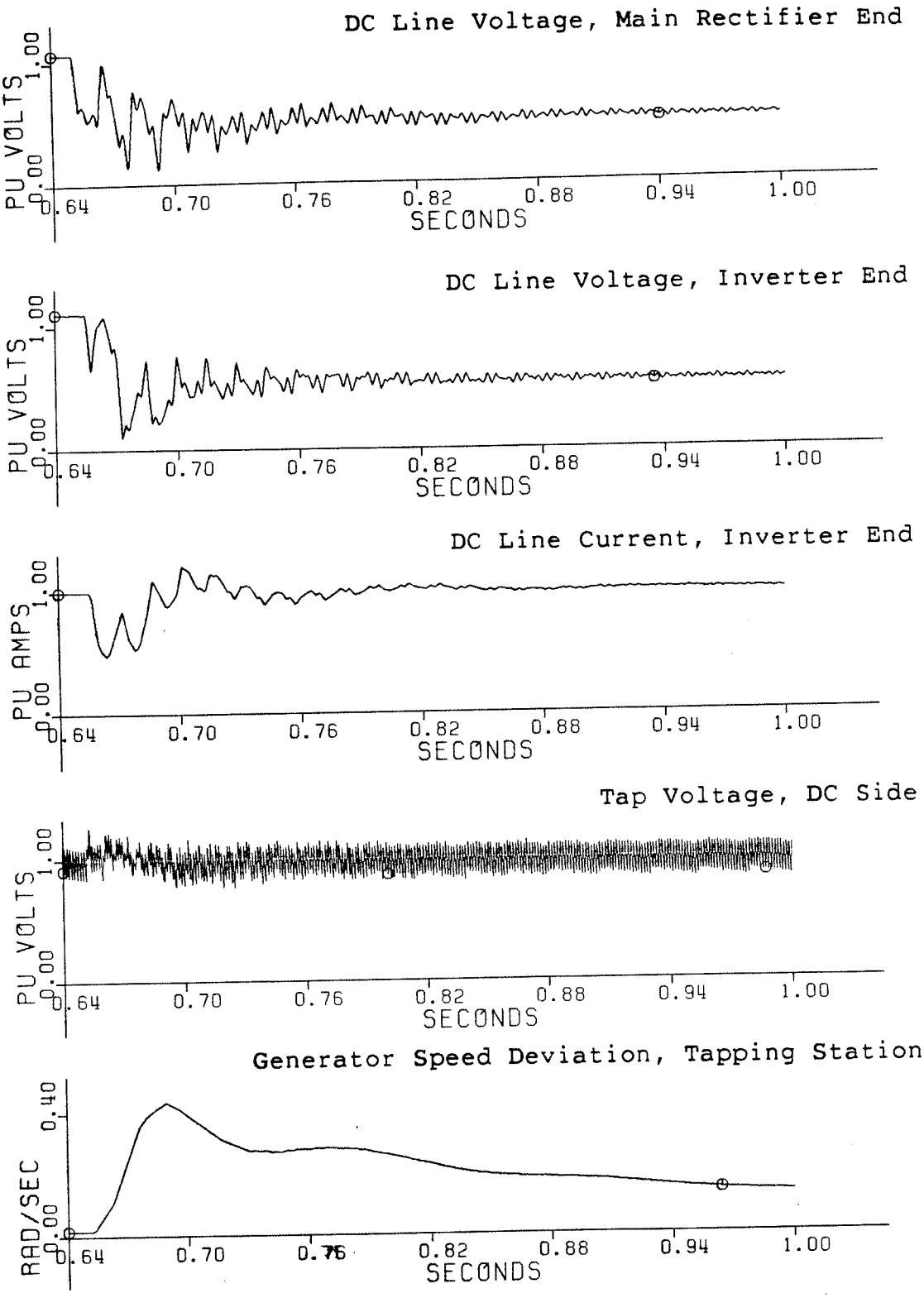

Figure 3.13: Partial Blocking in the Main System.

3.6 COMPARISON WITH OTHER SCHEMES

In a diode rectifier station, not only thyristors are replaced by simple diodes, but also, many other advantages may be obtained. Among them, elimination of ac filters, generator transformer and the corresponding bus work, controls, buldings and communication system, as well as easier operation and maintenance, higher reliability and possibly operation at higher frequencies for better efficiency may be mentioned. However, in a point-to-point (or a parallel multiterminal) HVDC system the employment of a diode rectifier station implies higher reactive power requirement and higher voltage rating of the valves at the inverter station (or at the inverter station that could have been operating at minimum margin angle). The requirement of a dc circuit breaker is implied as well. Usually, a considerable overall saving is possible (the system may also become more stable) [2,5,19].

In a diode rectifier series tapping station, all savings peculiar to a diode rectifier station can be achieved. For a small tap the dc harmonic filters can be eliminated as well. No extra costs at the inverter end is implied. No dc circuit breaker is required. A moderate increase in the voltage margin of the main rectifier may be required for comparable flexibility. However, this requirement is due to incorporation of a series tap rather than the application of diodes for controlled valves.

A comparitive overview of four different schemes is presented in Table 3.1. These schemes are as follows.

1. A point-to-point HVDC system (or a parallel arrangement) with controlled converters.
2. Similar to 1, except that the (main) rectifier is a diode rectifier.
3. An HVDC system with three controlled converters, namely, a main rectifier,, a small rectifier tap and an inverter, all in series.
4. Similar to 3, except that the tap is a diode rectifier station.

TABLE 3.1

Diode Rectifier Schemes Versus Controlled Rectifier Schemes

DESCRIPTION		(1) CONTROLLED CONVERTER AS A MAIN RECTIFIER	(2) DIODE RECTIFIER AS A MAIN RECTIFIER	(3) CONTROLLED CONVERTER AS A SERIES RECTIFIER TAP	(4) DIODE RECTIFIER AS A SERIES RECTIFIER TAP
Normal Steady-State Operation and Conditions	V_{dr}	$-V_{di} + I_d R_\ell$	1.0 pu (Constant)	$V_{drm}=-V_{di}+I_d R_\ell - V_{drt}$ V_{drt}=at Desired Value	$V_{drm}=-V_{di}+I_d R_\ell - V_{drt}$ $V_{drt}=V_0 - 3X_c I_d/\pi$
	V_{di}	1.0 pu (Constant)	$-V_{dr} + I_d R_\ell$	1.0 pu (Constant)	1.0 pu (Constant)
	I_d	Kept at I_{dO} by Rectifier α -Control	Kept at I_{dO} by Inverter β - Control	Kept at I_{dO} by Main Rectifier α-Control	Kept at I_{dO} by Main Rectifier α-Control
	α_{margin}	$\alpha_0=10^o$ to 15^o	Zero	$\geq \alpha_0$	$\geq \alpha_0$
When Total Rectifier Voltage Is Below Inverter Voltage	V_{dr}	$V_0 \cos\alpha_{min} - 3X_c I_d/\pi$	$V_0 - 3X_c I_d/\pi$	$V_{drm}=V_0\cos\alpha_{min}-3X_c I_d/\pi$ $V_{drt}=V_0\cos\alpha_{min}-3X_c I_d/\pi$	$V_{drm}=V_0\cos\alpha_{min}-3X_c I_d/\pi$ $V_{drt}=V_0 - 3X_c I_d/\pi$
	V_{di}	$- V_{dr} + I_d R_\ell$	$- V_{dr} + I_d R_\ell$	$-V_{drm}+I_d R_\ell - V_{drt}$	$-V_{drm}+I_d R_\ell - V_{drt}$
	I_d	Kept at $I_{dO}-I_{margin}$ by Inverter β-Control	Kept at $I_{dO}-I_{margin}$ by Inverter β-Control	Kept at $I_{dO}-I_{margin}$ by Inverter β-Control	Kept at $I_{dO}-I_{margin}$ by Inverter β-Control
Blocking or Deblocking of Rectifier Bridges Takes Place by Means of		By-Pass Valve Pair	Opening or Closing the AC Circuit Breaker	By-Pass Valve Pair	Main: By-Pass Valve Pair Tap: Opening or Closing the AC Circuit Breaker
Commutation Failure or Similar Faults May Be Handled by		Rectifier α-Control	Demanding Negative Ceiling of Exciter	Main Rectifier α-Control	Main Rectifier α-Control
To Clear DC Line Faults I_d is Forced to Zero by		Rectifier α- Control (Forced Retard)	Opening the D C C.B. (AC C.B. as Back-Up)	Main Rectifier α-Control and Tap α-Control	Main Rectifier α-Control

(Continued on the Next Page)

(Continued from Previous Page)

Reactive Power Requirement	at Rectifier	(Base)	Somewhat Lower	Main: A Little Higher Tap: Much Higher	Main: A Little Higher Tap: Lower
	at Inverter	(Base)	Much Higher	No Change	No Change
Transformer Tap Changer Is:	at Rectifier	To Reduce VAr Consumption	To Keep V_{dr} at 1.0 pu	Main: To Reduce VAr Tap: To Reduce VAr	Main: To Reduce VAr Tap: Not Essential
	at Inverter	To Keep V_{di} at 1.0 pu	To Reduce VAr	To Keep V_{di} at 1.0 pu	To Keep V_{di} at 1.0 pu
Harmonic Magnitudes (pu) in the Range of Operation	A C	(Base)	Lower	Main: Slightly Higher Tap: Higher	Main: Slightly Higher Tap: Lower
	D C	(Base)	Lower	Main: Slightly Higher Tap: Much Higher	Main: Slightly Higher Tap: Lower
Equipment at Rectifier Such as: Filters, Bus Work, Transformer, Buildings, etc.		(Base)	May Be Reduced Substantially	Main: The Same Tap: More or Less the Same	Main: The Same Tap: May Be Reduced Substantially
Operation & Maintenance		(Base)	Easier	Main System: The Same Tap: Similar to Main Rect.	Main System: The Same Tap: Easier
Communication System		Necessary	Not Needed	Normally Needed Between All Converters	Optional Between Tap & Main Converters
Reliability		(Base)	Higher	The Same	Main System: The Same Tap : Higher

3.7 CONCLUSIONS

In this chapter, diode rectifier series tapping has been described. The operation modes of the system do not need to be different from those of a conventional point-to-point HVDC system. The tapping station can operate without communication, harmonic filters and many other pieces of equipment normally used in an HVDC converter station. The tap can be blocked or deblocked smoothly. The system can satisfactorily recover from all major faults and transients without the need for any dc circuit breakers. The tap does not overly increase the complexity of the system and the flexibility of the main system remains more or less intact.

Diode rectifier series tapping is economically very attractive. Easier operation and maintenance (i.e., less personnel) as well as higher reliability of a diode rectifier tapping station are of special importance for an isolated remote generation site.

Chapter IV

DIFFERENTIAL FIRING IN SERIES TAPPING

4.1 GENERAL

In this chapter, the concept of differential firing is examined for two categories of objectives, namely, VAr control and harmonics control. The voltage regulation capability of the tap is calculated as a function of the number of bridge sets in series. Harmonics control is mainly discussed in the context of a quasi twenty four-pulse tap with an appropriate control method termed as "predetermined differential firing" method. A small disturbance analysis of a prototype tap is presented. The results of digital simulation studies of the prototype tap incorporated in an otherwise point-to-point HVDC system are presented and compared with the theoretical results. Economic aspects and other applications are discussed and some conclusions are drawn.

4.2 VAR CONTROL

In Chapter II, it was mentioned that with two bridge sets in series the voltage regulation on the tap's own ac bus are small at a large load. In fact, as can be seen from Figure 2.1, at P_d = -1.0 pu no controllable regulation exists, ir-

respective of the number of bridge sets. On the other hand, the voltage regulation can always be considerable at a light load (which is not needed much). Therefore, neither P_d = -1.0 pu, nor P_d = 0.0 can be used for assessment and comparison of different cases. A more reasonable point is the most probable load; P_d = -0.8 pu at I_d = 1.0 pu (equivalent to V_d = -0.8 pu at any I_d) will be used for calculation of the voltage regulation as a function of the number of bridge sets in series.

Assuming that the required reactive power is supplied by capacitor banks only, the voltage regulation of the tap can be calculated using the reasoning suggested in [16] for similar situations. If for some reason the voltage at the ac bus drops by ΔV_s, the VAr output of the capacitor banks drops by,

$$\Delta Q = Q_{cN}(1-V_s^2) \text{ pu}, \tag{4.1}$$

where, Q_{cN} is the per unit rated VAr output of the capacitor banks. A ΔQ VAr is needed to keep the voltage from further decreasing. Another ΔQ is needed to bring the voltage back to 1.0 pu. Similar reasoning can be made for a ΔV_s increase in the voltage. Therefore, in either case, $2\Delta Q$ should be compensated by the converter. Substituting V_o = 1.1146 V_s pu, P_d = -0.8 pu and I_d = 1.0 pu in Equation 2.3, the maximum and the minimum VAr consumptions of the converter are,

$$Q_{max} = [(1.1146\ V_{s\ max})^2 - 0.64]^{1/2} \text{ pu}, \tag{4.2}$$

$$Q_{min} = \{(NB-1)[(1.1146\ V_{s\ min})^2 - V_{d1}^2]^{1/2} + [(1.1146\ V_{s\ min})^2 - V_{d2}^2]^{1/2}\}/NB \text{ pu}, \tag{4.3}$$

where (using γ_{min} = 18 degrees, δV_N = 0.06 pu and ω = 1.0 pu),

$$V_{d1} = -1.06\ V_{s\ min} + 0.06, \tag{4.4}$$

$$V_{d2} = -0.8\ NB - (NB - 1)\ V_{d1}, \tag{4.5}$$

and NB = number of bridge sets = 1, 2, ..., 10. Now, let Q_{NB} be the VAr consumed by the converter with NB bridge sets at V_s = 1.0 pu. Q_{NB}'s are given by the points on constant power factor (i.e., 0.85 lagging) lines at P_d = -0.8 pu, in Figure 2.1. Then, using Equation 4.1,

$$Q_{max} - Q_{NB} = 2\Delta Q_{max} = 2Q_{cNB}(1 - V_{s\ max}^2), \tag{4.6}$$

$$Q_{min} - Q_{NB} = 2\Delta Q_{min} = 2Q_{cNB}(1 - V_{s\ min}^2), \tag{4.7}$$

where, Q_{cNB} is the per unit rated VAr output of the capacitor banks installed for the converter with NB bridge sets. Substituting for Q_{max} and Q_{min} from Equations 4.2 and 4.3 and then for V_{d1} and V_{d2} from Equations 4.4 and 4.5 in Equations 4.6 and 4.7 and after some simple manipulations, the following equations can be obtained:

$$4Q_{cNB}^2\ V_{s\ max}^4 - [1.1146^2 + 4Q_{cNB}(Q_{NB} + 2Q_{cNB})]$$
$$V_{s\ max}^2 + (Q_{NB} + 2Q_{cNB})^2 + 0.64 = 0, \tag{4.8}$$

and,

$$(NB - 1)[(1.1146\ V_{s\ min})^2 - (0.06 - 1.06\ V_{s\ min})^2]^{1/2}/NB +$$
$$\{(1.1146\ V_{s\ min})^2 - [(0.06 - 1.06\ V_{s\ min})(NB - 1) + 0.8\ NB]^2\}^{1/2}/NB$$
$$- Q_{NB} - 2Q_{cNB}(1 - V_{s\ min}^2) = 0. \tag{4.9}$$

Using Figure 2.1 to determine Q_{NB} and Q_{cNB}, one can calculate $V_{s\ max}$ and $V_{s\ min}$ from Equations 4.8 and 4.9, for any NB = 1, 2, ..., 10. They are plotted versus NB in Figure 4.1. Their limits as NB becomes very large are 1.05 pu and 0.97 pu respectively, and are shown in Figure 4.1 as well.

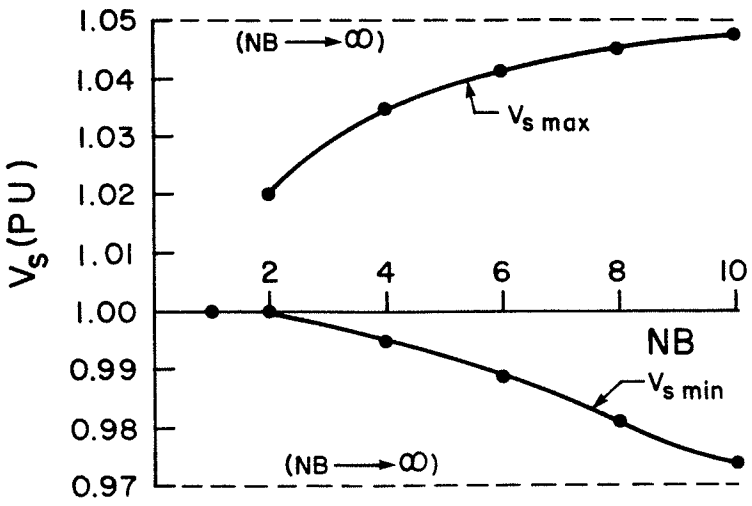

Figure 4.1: Voltage Regulation Versus Number of Bridge Sets at V_d = -0.8 pu.

According to Figure 4.1, for a considerable regulation a rather large number of bridges (say, $4 \leq NB \leq 10$) is required. This means a high degree of complexity in the tapping station. The frequency of commutation failures will increase, as well. Furthermore, the regulation capability drops drastically as one bridge set (or more) goes out of service. Thus, the cost increase (due to using smaller bridges) can hardly be attributed to higher flexibility. It may also be noted that operation on a minimum VAr characteristic results in somewhat lower overall magnitudes of harmonics, e.g., with two bridge sets 11th, 13th and 12th harmonics can theoretically reach as high as 7.55%, 5.92% and 7.85% respectively (as compared with 8.57%, 7.08% and 11.80% respectively). Nevertheless, such reductions will be undone in case of voltage regulation by the tap.

The above drawbacks indicate that the idea of voltage regulation by means of differential firing is rather unsuitable for small taps (for other series arrangements, however, some of these drawbacks may diminish and some can be improved by other means). On the other hand, as will be shown in subsequent sections of this chapter, a potentially advantageous alternative, namely, harmonic magnitude reduction, exists. Another possibility is the reduction of some of the transient overvoltages of the tap's ac bus by the tap itself, which is exploitable even under equal firing.

4.3 HARMONICS CONTROL

4.3.1 Control System Modifications

Basically the tap needs a power (or speed) regulator and a minimum margin angle controller to protect it against commutation failure [10,26,27]. Moreover, with two bridge sets in series, a proper difference should be effected between the firing angles of the bridge sets to cause a desired harmonic reduction. These controls are schematically shown in the block diagram of Figure 4.2. For any desired harmonics reduction, the difference angle is, at any instance, to be determined according to a predetermined function. Thus this control method will be referred to as "predetermined differential firing" method (it may be noted that this control method can be used for VAr control as well).

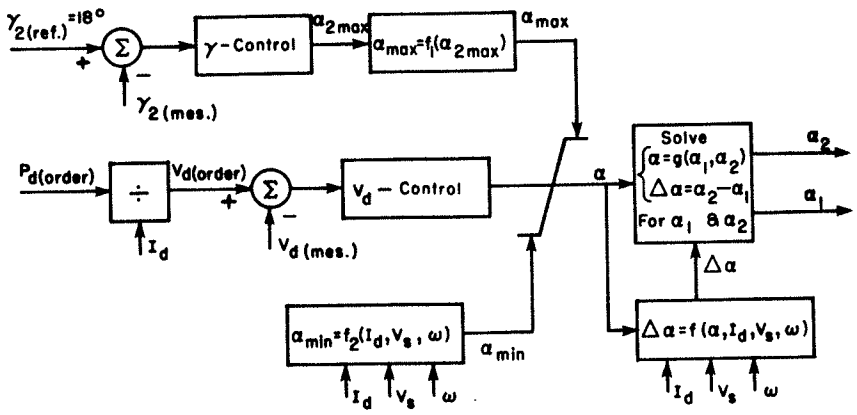

Figure 4.2: Control Block Diagram for Predetermined Differential Firing.

The output of the power regulator, α (after being checked with two limits, where, the minimum limit in rectification mode would be 2 to 5 degrees and the maximum limit would come from the minimum margin angle controller as well as forced retard signals), would normally be given to valve controls to effect the proper firing of individual valves within every valve group. However, in Figure 4.2, α is processed to two firing angles α_1 and α_2 according to a predetermined function, f. Also, the maximum and the minimum limits of α are modified according to two other predetermined functions, f_1 and f_2, respectively. Another function, g, is needed to properly relate α to α_1 and α_2. In fact, the first conceivable choice is either $\alpha = \alpha_1$ or $\alpha = \alpha_2$. But, in either case, V_d would be somewhat dependent on $\Delta\alpha$. With $\alpha = \alpha_e$, where,

$$\cos \alpha_e = (\cos \alpha_1 + \cos \alpha_2)/2, \qquad (4.10)$$

the dependence on $\Delta\alpha$ will be removed. This choice will have another advantage that will be mentioned at its own place. α_e is referred to as "effective firing angle", since it would produce the same dc power output as is produced by α_1 and α_2 together, if both bridge sets were fired by α_e. With $\alpha = \alpha_e$, the solution for α_1 and α_2 is,

$$\alpha_1 = \arccos [\cos \alpha_e / \cos (\Delta\alpha/2)] - \Delta\alpha/2 , \qquad (4.11)$$

$$\alpha_2 = \arccos [\cos \alpha_e / \cos (\Delta\alpha/2)] + \Delta\alpha/2 . \qquad (4.12)$$

Thus, the problem requires the determination of $f(\alpha_e, \omega I_d/V_s)$, $f_1(\alpha_{2max})$ and $f_2(\omega I_d/V_s)$. Note that, as was shown in Section 2.6, ω, I_d and V_s act as one independent variable, namely, $\omega I_d/V_s$.

4.3.2 Behavior of Overall Harmonic Magnitudes

In Chapter II, it was shown that to effect a quasi twenty four-pulse operation, $\Delta\alpha + 1/2\ \Delta\mu$ should be approximately 15 degrees. This approximation holds for small $\Delta\mu$; the larger the $\Delta\mu$, the higher the error. The largest $\Delta\mu$ occurs when one bridge set operates at its minimum margin angle limit (at highest $\omega I_d/V_s$). Using the exact relationships derived in Section 2.6, the 11th, the 13th and the 12th harmonics are plotted versus the difference angle, at synchronous frequency, rated ac voltage, rated dc line current and minimum margin angle for the second bridge set, in Figure 4.3.

In Figure 4.3, as the difference angle increases from zero, after a slight increase at the beginning, both the

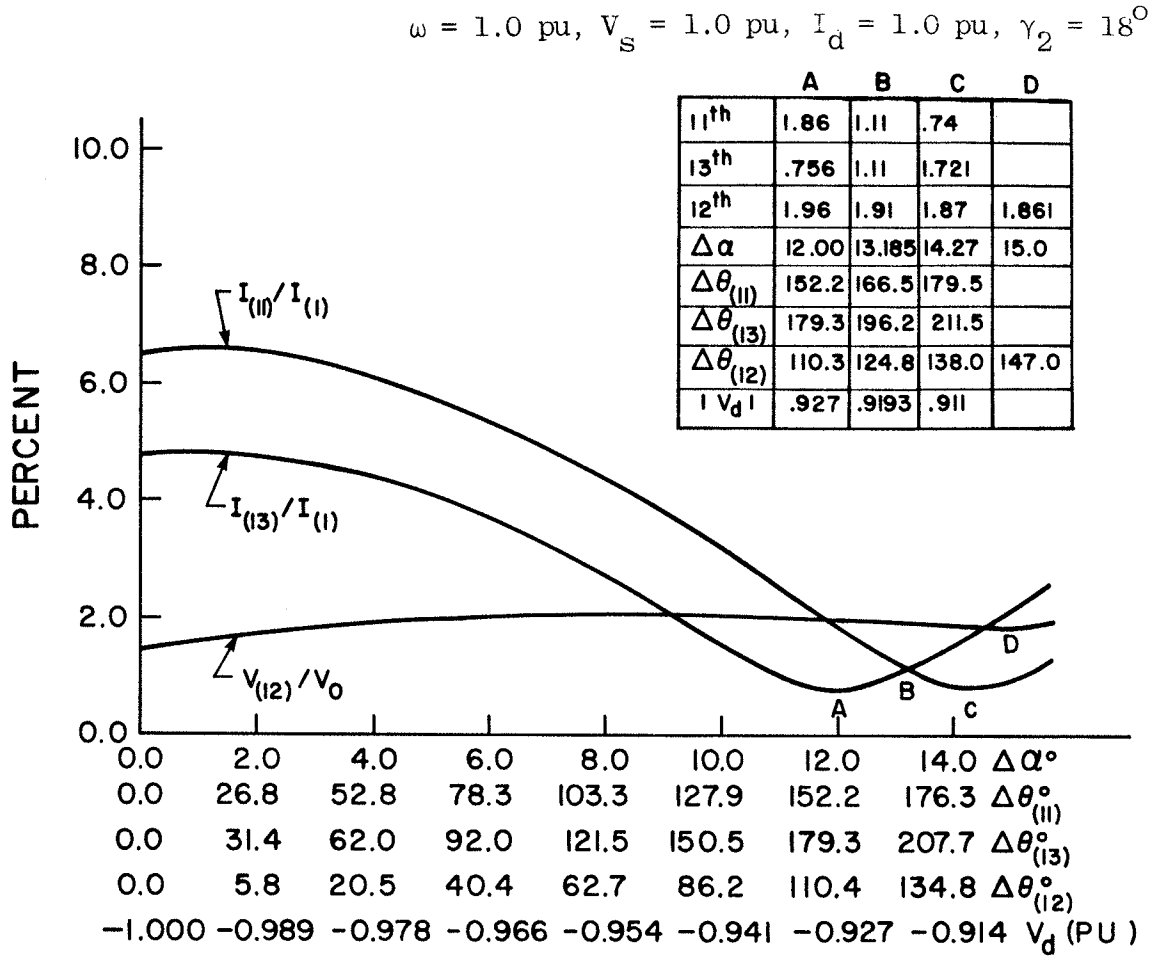

	A	B	C	D
11^{th}	1.86	1.11	.74	
13^{th}	.756	1.11	1.721	
12^{th}	1.96	1.91	1.87	1.861
Δα	12.00	13.185	14.27	15.0
$\Delta\theta_{(11)}$	152.2	166.5	179.5	
$\Delta\theta_{(13)}$	179.3	196.2	211.5	
$\Delta\theta_{(12)}$	110.3	124.8	138.0	147.0
$\lvert V_d \rvert$	.927	.9193	.911	

Figure 4.3: Overall Harmonics Versus Difference Angle.

11th and the 13th harmonics decrease drastically to their (first) minimums at points C and A, respectively. The change in the 12th harmonic is slight. The behaviors of the higher order harmonics (not shown) are similar, but their minimums occur at different locations. The 23rd and the 25th harmonics, in fact, almost reach their maximums at points C and A, respectively (after each having a minimum at about half of the difference angle corresponding to points C and A, respectively). The 35th and the 37th harmonics will have

their second minimums at the difference angles rather close to those of points C and A, respectively. The remaining magnitudes of the 35th, 37th and higher order harmonics are of little concern anyway (so are the dc harmonics). In other words, optimum difference angle virtually corresponds to a situation, where, the filtering requirement for 11th and 13th harmonics together is minimum.

It should be noted that the optimum difference angle alone is not sufficient to arrive at optimum level of filtering to be provided and other factors will have to be taken into account, as well. These factors are discussed in Section 4.6.

4.3.3 Typical Functions for a Quasi 24-Pulse Operation

It has been found that the optimum difference angle, as described above, typically occurs around that of point B in Figure 4.3, where, $I_{(11)} = I_{(13)}$. Theoretically it is limited between those of points A and C. According to this criterion, a typical $\Delta\alpha = f(\alpha_e, \omega I_d/V_s)$ has been found for the whole range of operation and is plotted in Figure 4.4. It is assumed that $\omega I_d/V_s$ can vary between 0.1 pu and 1.2 pu.

As can be seen from Figure 4.4, the difference angle has a virtually linear relationship with $\omega I_d/V_s$, which is another advantage of the introduction of the effective firing angle. In Figure 4.4, all lines of the bottom graph for

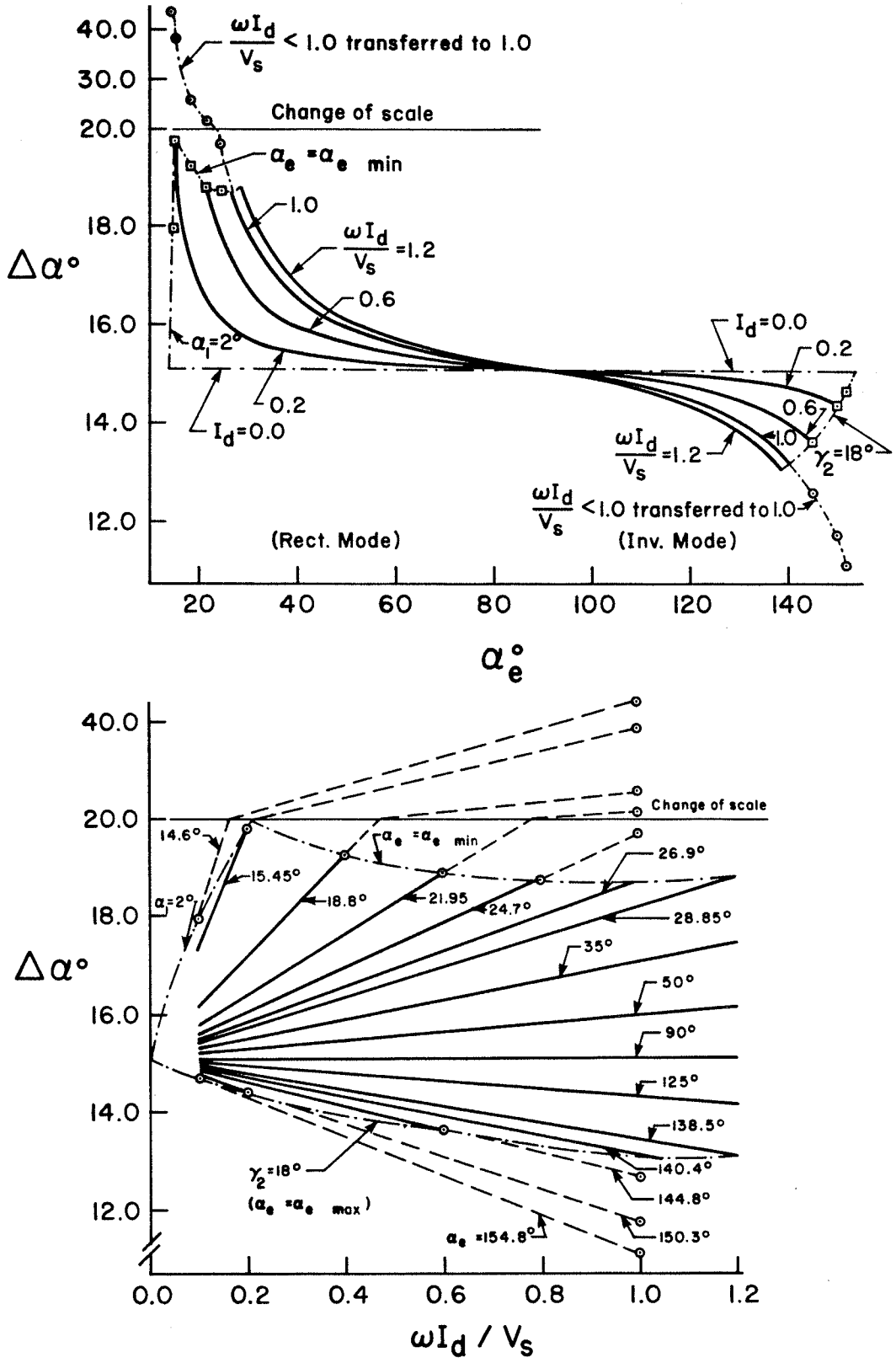

Figure 4.4: Typical Difference Angle for a Quasi 24-Pulse Operation.

which the effective firing angle reaches its limit at $\omega I_d/V_s < 1.0$ are extended to $\omega I_d/V_s = 1.0$. The corresponding points on the top graph are then transferred to $\omega I_d/V_s = 1.0$, which causes extentions on both ends of the curve for $\omega I_d/V_s = 1.0$. This curve (including its extentions) alone is sufficient to define the difference angle on the whole range of operation, namely,

$$\Delta\alpha \cong [f(\alpha_e, 1.0) - 15.1^\circ] \cdot \omega I_d/V_s + 15.1^\circ. \qquad (4.13)$$

The functions determining the maximum and the minimum limits of the firing angle (i.e., f_1 and f_2) are plotted in Figure 4.5. These functions correspond to the limits shown in Figure 4.4 and with different strategies of running the tap (see Section 4.6) they need to be modified accordingly. If the tap is to operate as an inverter only, then the minimum limit of the effective firing angle may simply be a constant (say, about 80 degrees). The maximum limit of the effective firing angle has a virtually linear relationship with the maximum firing angle of the second bridge set.

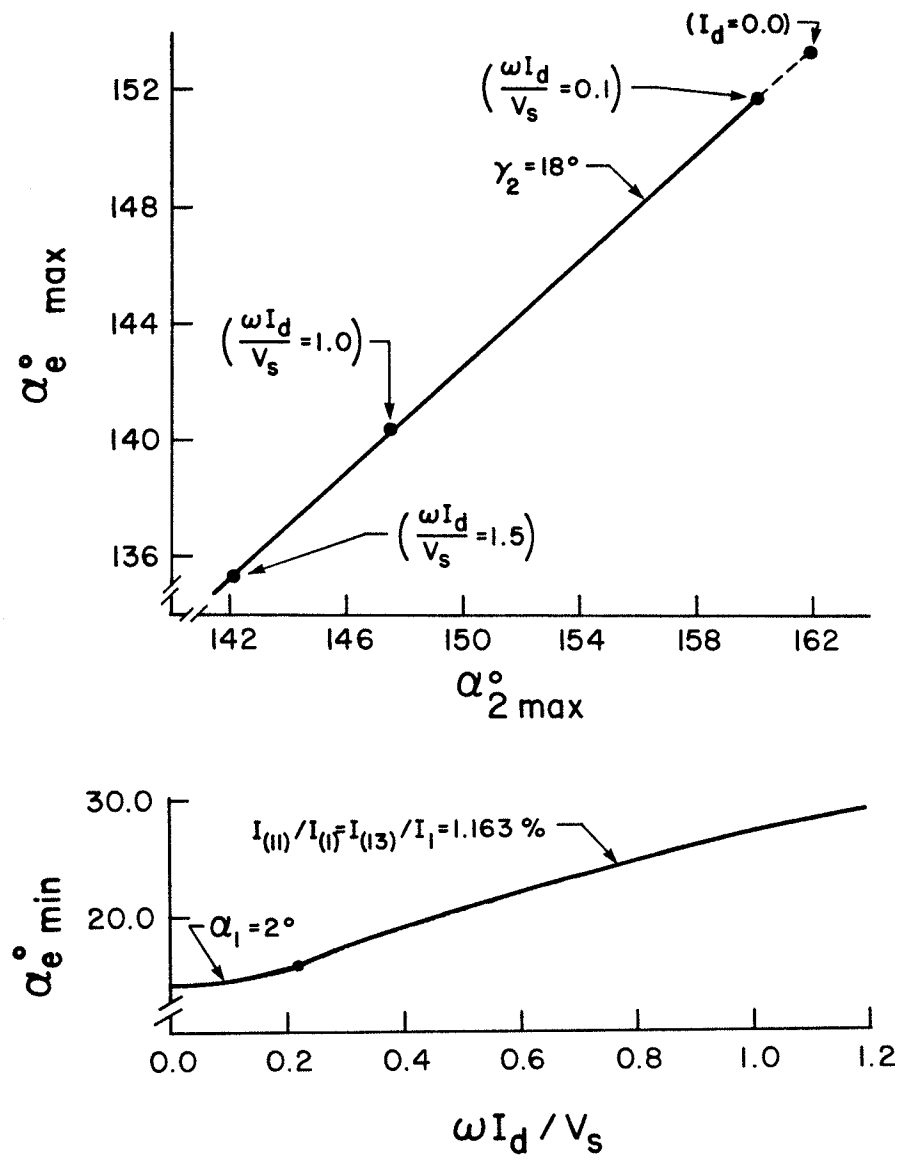

Figure 4.5: Maximum and Minimum Limits of the Effective Firing Angle.

4.3.4 Overall Harmonic Magnitudes and Other Effects

Using the functions established above, the overall magnitudes (in percentage) of 11th, 13th and 12th harmonics will theoretically be as shown in Figure 4.6.

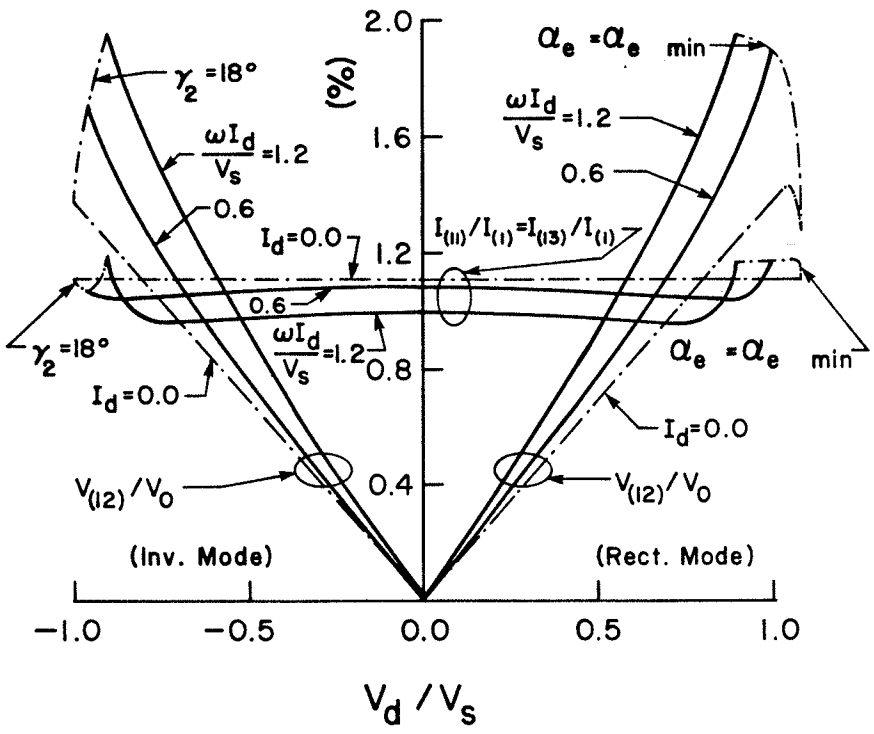

Figure 4.6: Overall 11th, 13th and 12th Harmonics (Theoretical).

Slight decreases in the overall magnitudes of 23rd, 25th and 24th harmonics are (theoretically) expected. Higher order characteristic harmonics have not been investigated in detail, but most of them are expected to be somewhat reduced; no characteristic harmonic magnitudes is expected to increase due to differential firing. So are non-characteristic harmonics.

Differential firing technique is not expected to increase the valve stresses. The overall reactive power demand of the tap will, in fact, decrease slightly, as is shown in Figure 2.1 for a difference angle of about 15 degrees.

4.4 SIMULATION NETWORK AND CONTROLS

For digital simulation studies the Bipole II (positive pole only) of Nelson River HVDC system is considered as the main system. A 10% series tap is inserted right at the middle of the dc transmission line. The network is schematically shown in Figure 4.7.

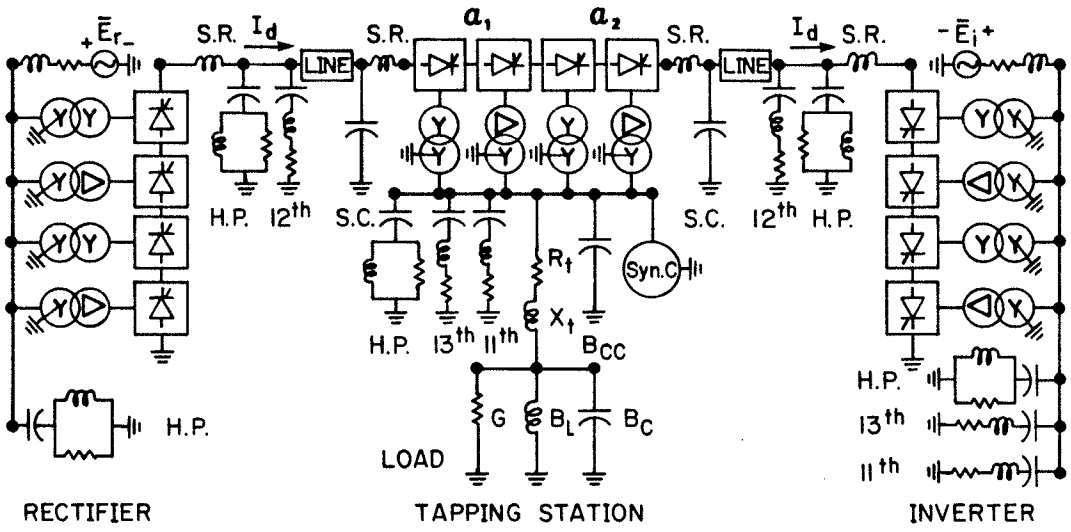

Figure 4.7: Simulation Network.

Each main converter station consists of four bridges in series, each two acting as one twelve-pulse bridge set. The ac systems of the main converters are represented by their Thevenin equivalents. The filters on the ac and the dc sides of these converters are as shown in Figure 4.7.

The tap also consists of four (controlled) bridges, each two acting as one twelve-pulse bridge set. However, the two

twelve-pulse bridge sets are to have different firing angles to effect a quasi twenty four-pulse operation. The arrangement of smoothing reactors and surge capacitors of the tap is shown in Figure 4.7, as well. The tap has no dc filters. The tap operates into an ac system which has no other source of power. Thus, obviously, the tap will operate as an inverter. The dc voltage of the tap is to be matched by increasing the transformer tap changers at the (main) rectifier. A synchronous condenser is used at the tap's ac bus to effect an effective short circuit ratio of 2.5 at full load which at light loads reduces to about 2.0. The rated reactive power supplied by the synchronous condenser is 70% of the rated real power of the tap. Part of the required reactive power (i.e., about 20% of the real power) is supplied by the 11th and the 13th tuned filters as well as the high-pass filter. For more details on tap's ac filters see Appendix B. The rest of the required reactive power is supplied by switchable capacitor banks at both tap's ac bus and load bus. The capacitors are assumed to be available in steps of 0.05 per unit MVAr. The load is represented by a resistance in parallel with an inductance. The tap's ac bus is connected to the load bus by a short ac line, which is represented by its series impedance. Any transformer in the path (e.g., isolation transformer) is also assumed as a series impedance included in the line impedance. The power factor of the circuit is assumed to be 0.85 lagging as seen from the tap's ac bus excluding the power factor correcting capacitors. The data of Figure 4.7 are given in Appendix C.

The simulation program is EMTDC [22]. All bridges are simulated using the subroutine B6P110 (it also includes the bridge transformer, valve dampers, firing arrangements, etc.). The distributed parameter line model of EMTDC program is used for simulation of the dc lines. The synchronous condenser is simulated by the subroutine MAC100, along with the subroutine SCRX19 for its excitation system. The main rectifier is equipped with a current controller which is simulated using the subroutine POL2C5 (i.e., pole controller). The main inverter is equipped with a similar current controller but with 10% lower ordered current. It is also equipped with a minimum margin angle controller, which is simulated by the subroutine VG1C16 (i.e., valve group controller). The controls of the tapping station are discussed in the following subsection.

4.4.1 Controls of the Tapping Station

The voltage at the tap's ac bus (i.e., the terminal voltage of the synchronous condenser) is to be regulated by the excitation control of the synchronous condenser along with the switching of the capacitor banks (the action of the transformer tap changers is neglected). A typical static exciter is assumed, namely, k_e = 100 and T_e = 0.05 s. The voltage regulator of the tap is as shown in Figure 4.8. The time constant of the voltage transducer, T_v, is assumed 0.01 s.

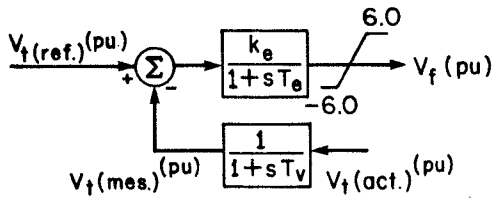

Figure 4.8: AC Voltage Regulator of the Tap.

The speed of the synchronous condenser will be regulated by controlling the effective firing angle of the tap (similar to Figure 4.2, but, with speed deviation as the error signal). The mechanical power applied to the shaft of the synchronous condenser, p_m, is constant and assumed zero. In a steady-state situation the electrical power of the synchronous condenser, p_e, as well as its power angle, δ, should be zero as well. The effective firing angle (as well as the individual firing angles) should have a specific value at any steady state situation. Suppose due to some small disturbance the speed has changed by $\Delta\omega$. The change in the effective firing angle, $\Delta\alpha_e$, should finally settle at a constant value (generally non-zero), while $\Delta\delta$ as well as $\Delta\omega$ should settle at zero. In other words, the effective firing angle is basically derived by integrating the speed deviation twice. Assuming a gain of k (or $2\pi f_s k$ with $\Delta\omega$ in per unit), the following equations can be written,

$$\dot{\Delta\alpha}_e = k\ \Delta\delta, \tag{4.14}$$

$$\dot{\Delta\delta} = -\ 2\pi f_s\ \Delta\omega, \tag{4.15}$$

where, ω is in per unit and δ and α_e are in radians (δ is as shown in Figure 4.9(b)). The dot means differentiation with respect to time. k will, then, have a dimension of s^{-1}. It may be noted that, for the moment, the measured value of ω is assumed to be equal to its actual value. Nevertheless, later on, at an appropriate place, a pole will be added to the system for the speed transducer. Furthermore, a proportional signal will be added to each integrator output, as well.

For the mechanical part of the machine the following equation can be written:

$$\dot{\Delta\omega} = \Delta p_e/M \quad (\text{Note that, } \Delta p_m = 0), \tag{4.16}$$

where, M is the moment of inertia and the self-dampingcoefficient, D, is neglected. The power is assumed positive when absorbed by the machine.

In Figure 4.8, the time constant of the voltage transducer is combined with the time constant of the exciter (i.e., for order reduction), resulting in,

$$\Delta v_f \cong - k_e \Delta v_t/\{1 + s(T_e+T_v)\}, \tag{4.17}$$

or,

$$\dot{\Delta v_f} = - \Delta v_f/(T_e+T_v) - k_e \Delta v_t/(T_e+T_v), \tag{4.18}$$

where, V_t and V_f are the terminal voltage and the field voltage of the machine (in per unit), respectively.

For the electrical part of the machine, neglecting the dampers and the armature resistance (i.e., using a basic ma-

chine model), the following equation can be written (in d-q axes) [28]:

$$\Delta e'_q = \{\Delta v_f + (x_d - x'_d)\ \Delta i_d\}/(1 + sT'_{do}), \tag{4.19}$$

or,

$$\Delta \dot{e}'_q = \{-\ \Delta e'_q + \Delta v_f + (x_d - x'_d)\ \Delta i_d\}/T'_{do}, \tag{4.20}$$

where, e'_q, x_d, x'_d, i_d and T'_{do} are the internal quadrature axis voltage, the direct axis synchronous reactance, the direct axis transient reactance, the direct axis current and the open-circuit field time constant of the machine, respectively. The following equations of the machine [28] will also be needed:

$$p_e = i_d v_d + i_q v_q, \tag{4.21}$$

$$v_d = -\ x_q i_q, \tag{4.22}$$

$$v_q = e'_q + x'_d i_d, \tag{4.23}$$

$$v_t^2 = v_d^2 + v_q^2, \tag{4.24}$$

where, v_d, v_q, i_q and x_q are the direct axis voltage, the quadrature axis voltage, the quadrature axis current and the quadrature axis synchronous reactance of the machine, respectively. Note that the direction of the machine current is assumed from the terminal bus into the machine (see Figure 4.9).

At any operating point the following initial conditions (denoted by the additional subscript 0) may be assumed for the synchronous condenser:

$$v_{t0} = 1.0 \text{ pu},$$

$$v_{d0} = 0.0,$$

$$v_{q0} = 1.0 \text{ pu},$$

$v_{f0} = 1.0$ pu,

$i_{q0} = 0.0$,

$\omega_0 = 1.0$ pu,

and $\delta_0 = 0.0$.

Using these initial conditions, Equations 4.21 through 4.24 can be linearized about any operating point for a small disturbance as,

$$\Delta p_e = i_{d0}\,\Delta v_d + \Delta i_q, \tag{4.25}$$

$$\Delta v_d = - x_q\,\Delta i_q, \tag{4.26}$$

$$\Delta v_q = \Delta e'_q + x'_d\,\Delta i_d, \tag{4.27}$$

$$\Delta v_t = \Delta v_q\ . \tag{4.28}$$

Substituting for Δp_e in Equation 4.16 from Equation 4.25 and then substituting for Δv_d from Equation 4.26 result in:

$$\Delta\dot{\omega} = (1 - i_{d0}x_q)\Delta i_q / M. \tag{4.29}$$

Substituting for Δv_t in Equation 4.18 from Equation 4.28 and then substituting for Δv_q from Equation 4.27 result in:

$$\Delta\dot{v}_f = (-\Delta v_f + k_e\Delta e'_q + k_e x'_d\Delta i_d)/(T_e + T_v). \tag{4.30}$$

The relationship of the machine current, i, with the tapping inverter current, i_i, and the load current, i_ℓ, can be found using Figure 4.9. In Figure 4.9(a), a simplified representation of the tapping station is shown, where it is assumed that all harmonic currents produced by the tap are perfectly absorbed by the filters and, therefore, the currents and the voltages are represented by their fundamental components and the filters are represented by their capacitance at fundamental frequency only. In Figure 4.9(b), the situation in d-q axes after a small disturbance is shown.

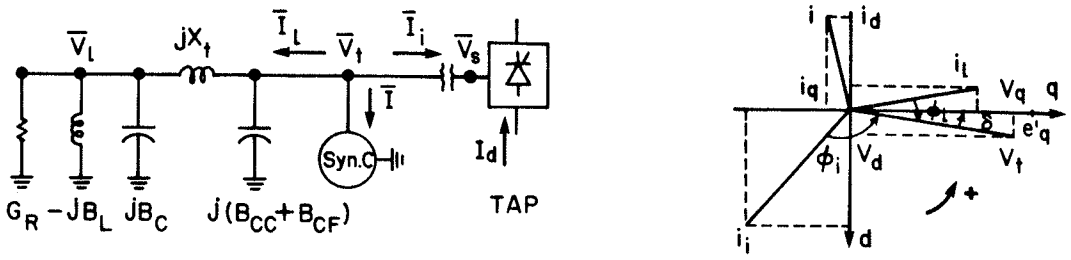

(a) Simplified Representation (b) Geometrical Relationships

Figure 4.9: Simplified Tap and dc (d-q) Quantities.

From Figure 4.9(b), the following equations can be written:

$$i_d + i_i \sin(\phi_i+\delta) + i_\ell \sin(\phi_\ell+\delta) = 0, \tag{4.31}$$

$$i_q + i_i \cos(\phi_i+\delta) + i_\ell \cos(\phi_\ell+\delta) = 0, \tag{4.32}$$

where, ϕ_i and ϕ_ℓ are the power factor angles of the tap and the load, respectively. After expanding the sine and cosine terms, Equations 4.31 and 4.32 can be rewritten as:

$$i_d = I_{iQ} \cos\delta - I_{iP} \sin\delta + I_{\ell Q} \cos\delta - I_{\ell P} \sin\delta, \tag{4.33}$$

$$i_q = - I_{iP} \cos\delta - I_{iQ} \sin\delta - I_{\ell P} \cos\delta - I_{\ell Q} \sin\delta, \tag{4.34}$$

where,

$$I_{\ell P} = I_\ell \cos\phi_\ell = V_t\, G(\omega), \tag{4.35}$$

$$I_{\ell Q} = - I_\ell \sin\phi_\ell = V_t\, B(\omega), \tag{4.36}$$

$$I_{iP} = I_i \cos\phi_i = I_d(V_{ON}V_t\cos\alpha_e - \omega I_d \delta V_N)/V_t, \tag{4.37}$$

$$I_{iQ} = - I_i \sin\phi_i = - V_{ON}^2\, V_t \{2\mu_1+2\mu_2+\sin 2\alpha_1+\sin 2\alpha_2 - \sin(2\alpha_1+2\mu_1)-\sin(2\alpha_2+2\mu_2)\}/(16\ V_N). \tag{4.38}$$

Note that $V_s = V_t$ in per unit (i.e., the converter transformer tap changer ratio is 1.0) and the magnitudes of the phasor quantities in per unit are equal to their correspond-

ing dc values in dq axes. Moreover, it is assumed that the converter causes no delay, i.e., a transfer function of unity is assumed for the tapping converter. G + jB is the equivalent impedance of the load, the capacitors and the line in Figure 4.9(a), as seen from the tap's bus. Thus:

$$G(\omega) = (G_R B_t^2/\omega^2)/\{(B_C\omega - B_L/\omega - B_t/\omega)^2 + G_R^2\} , \quad (4.39)$$

$$B(\omega) = (B_{CC}+B_{CF})\omega - B_t/\omega - (B_C\omega - B_t/ - B_L/\omega)B_t^2/\omega^2\}/ \{(B_C\omega - B_t/\omega - B_L/\omega)^2 + G_R^2\} . \quad (4.40)$$

The operating point about which Equations 4.33 through 4.38 will be linearized for a small disturbance is assumed to be P_d = -0.83 pu at I_d = 1.0 pu. This load is assumed to be the maximum steady-state load that can be normally supplied by the tap with about 10% voltage margin reserved for dynamic variations; from Figure 4.3, it can be seen that at point B the load is 0.92 pu (at I_d = 1.0 pu) and to have a quasi twenty four-pulse operation, the remaining 0.08 pu capacity of the tap is blocked (it will be shown later that the blocked portion can usually be reduced to about 0.064 pu). Moreover, it has been found that the system response is worst at maximum load. Thus the analysis will be presented for the above-mentioned operating point only. This operating point leads to the following initial conditions (in addition to the initial conditions of the synchronous condenser stated before):

$$I_{d0} = 1.0 \text{ pu},$$

$$G_0 = 0.83 \text{ pu},$$

$$B_{CF0} = 0.2 \text{ pu},$$

$B_{CC0} = 0.05$ pu,

$X_{t0} = 0.3$ pu,

$B_{C0} = 0.4$ pu,

$B_{L0} = 0.283$ pu,

$G_{R0} = 0.824$ pu,

$B_0 = 0.159$ pu,

$G'_0 = dG(\omega)/d\omega|_0 = 0.285$ pu,

$B'_0 = dB(\omega)/d\omega|_0 = 0.648$ pu,

$\alpha_{e0} = 2.333$ rad (133.7 degrees),

$\Delta\alpha_0 = 0.241$ rad (13.80 degrees),

$\alpha_{10} = 2.220$ rad (127.2 degrees),

$\alpha_{20} = 2.461$ rad (141.0 degrees),

$\mu_{10} = 0.143$ rad (8.220 degrees),

$\mu_{20} = 0.196$ rad (11.23 degrees),

$\Delta\alpha'_0 = d(\Delta\alpha)/d(\alpha_e)|_0 = -0.0784$,

$I_{\ell P0} = 0.83$ pu,

$I_{iP0} = -0.83$ pu,

$I_{\ell Q0} = 0.159$ pu,

$I_{iQ0} = -0.727$ pu,

and $i_{d0} = -0.57$ pu.

Now, from Equations 4.33 through 4.38 the following equations can be derived:

$$\Delta i_d = \Delta I_{iQ} + \Delta I_{\ell Q}, \tag{4.41}$$

$$\Delta i_q = - \Delta I_{iP} - \Delta I_{\ell P} - i_{d0} \Delta\delta, \tag{4.42}$$

$$\Delta I_{\ell P} = G'_0 \Delta\omega + G_0 \Delta e'_q + G_0 x'_d \Delta i_d, \tag{4.43}$$

$$\Delta I_{\ell Q} = B'_0 \Delta\omega + B_0 \Delta e'_q + B_0 x'_d \Delta i_d, \tag{4.44}$$

$$\Delta I_{iP} = - \delta V_N I_{d0}^2 \Delta\omega + \delta V_N I_{d0_2}^2 \Delta e'_q - I_{d0} V_{0N} \sin\alpha_{e0} \Delta\alpha_e + \delta V_N I_{d0}^2 x'_d \Delta i_d, \tag{4.45}$$

$$\Delta I_{iQ} = a_1 \Delta\omega + a_2 \Delta e'_q + a_3 \Delta\alpha_e + a_4 \Delta i_d , \qquad (4.46)$$

where, the main system is treated as a constant direct current source. The synchronous condenser used for simulation studies has the following data (for full data see Appendix C):

$$x_d = 1.56 \ (2.33) \text{ pu},$$
$$x_q = 1.10 \ (1.57) \text{ pu},$$
$$x'_d = 0.30 \ (0.43) \text{ pu},$$
$$T'_{do} = 11.0 \text{ s},$$
$$M = 2.0 \ H = 3.0 \ (2.1) \text{ pu},$$

where, H is the inertia constant of the machine. The values in paranteses are based on the same MVA base (i.e., 100 MVA) as used for the tapping converter. Using the above value for x'_d, a_1 through a_4 have been evaluated as 0.745, -0.745, 0.932 and -1.660, respectively. Substituting Equations 4.43 through 4.46 in Equations 4.41 and 4.42 and solving for Δi_d and Δi_q, and then sustituting for Δi_d and Δi_q in Equations 4.20, 4.29 and 4.30 result in three differential equations in terms of the space variables δ, ω, e'_q, v_f and α_e. These three differential Equations along with Equations 4.14 and 4.15 are one set of the state space equations of the system, which can be written in matrix form as:

$$\dot{\underline{X}} = \underline{A}\,\underline{X} , \qquad (4.47)$$

where,

$$\underline{X} = \begin{bmatrix} \delta \\ \omega \\ e'_q \\ v_f \\ \alpha_e \end{bmatrix}, \quad \dot{\underline{X}} = \begin{bmatrix} \dot{\delta} \\ \dot{\omega} \\ \dot{e}'_q \\ \dot{v}_f \\ \dot{\alpha}_e \end{bmatrix},$$

and,

$$\underline{A} = \begin{bmatrix} -0.461 & 0.509 & -0.833 & 0 & 0.389 \\ -377.0 & 0 & 0 & 0 & 0 \\ 0.123 & 0 & -0.077 & -0.077 & 0.158 \\ -534.8 & 0 & -1728. & -16.67 & -689.8 \\ 0 & 377\,k & 0 & 0 & 0 \end{bmatrix}.$$

From matrix $\underline{A}$ the characteristic equation of the system can be derived as:

$$s(s+0.245+j13.76)(s+0.245-j13.76)(s+8.357+j9.511)(s+8.357 -j9.511)+146.5k(s+8.303+j14.22)(s+8.303-j14.22) = 0. \qquad (4.48)$$

As k increases (from zero) one complex conjugate pair of the roots of Equation 4.48 enter the right half of the s-plane. Adding two zeros to the open loop transfer function (i.e., for the proportional signals in parallel with the integrators) may cause a stable situation. To make the poles closest to the $j\omega$ axis have as little contribution to the system response as possible, these zeros should be rather close to the $j\omega$ axis [29]. They have been set (after several iterations) at s = -2.0, which result in $T_1 = T_2 = 0.5$ s. A pole at s = -50.0 is also added to the open loop transfer function for the speed transducer (i.e., $T_\omega = 0.02$ s). Therefore, the poles of the closed loop transfer function (i.e., the eigenvalues of the system) are the roots of the following equation:

$$1 + GH = 1+1831.25k(s+8.303+j14.22)(s+8.303-j14.22)(s+2)^2/$$
$$\{s(s+50)(s+0.245+j13.76)(s+0.245-j13.76)$$
$$(s+8.357+j9.511)(s+8.357-j9.511)\} = 0. \qquad (4.49)$$

The root locus plot of Equation 4.49 is presented in Figure 4.10, for $k \geq 0$ [29].

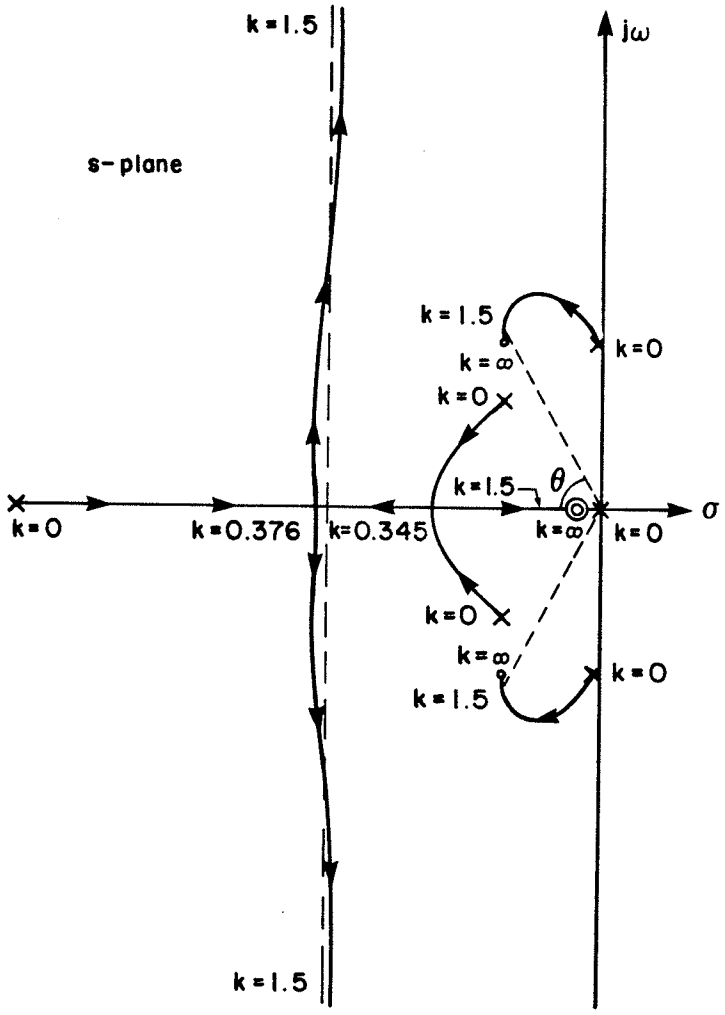

Figure 4.10: Root Locus Plot of the Closed Loop System for $k \geq 0$.

Requiring $\rho = \cos\theta \geq 0.5$ for the dominant complex conjugate roots, the loop sensitivity turns out to be $k \geq 1.5$. For $k = 1.5$, the settling time constant of these oscillatory roots is 0.12 s with an oscillation frequency of 2.3 Hz. Increasing k beyond this value is not necessary, as a very large k may cause, in some cases, commutation failures. $k = 1.5\ s^{-1}$ is used for all simulation studies. The speed regulator of the tapping station is shown in Figure 4.11. $\alpha_{e\ min} = 80$ degrees is assumed. $\alpha_{e\ max}$ is determined from $\alpha_{2\ max}$ according to the top graph of Figure 4.5. $\alpha_{2\ max}$ is determined by the minimum margin angle controller of the tap. This controller is used for the second twelve-pulse bridge set (i.e., the one having the larger firing angle α_2) only, and is simulated using the subroutine VG1C16 of EMTDC program. All data of the controls of the tap are given in Appendix C, as well.

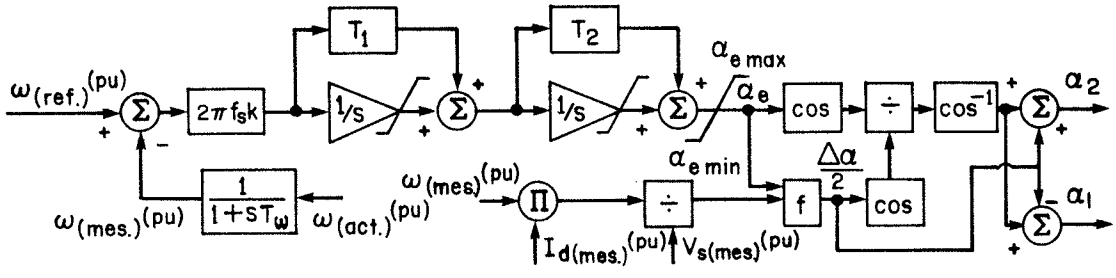

Figure 4.11: Speed Regulator of the Tap.

4.5 SIMULATION RESULTS

A time step of 0.000025 s has been used for all simulation studies. For steady-state studies the synchronous condenser is set at constant speed, namely, 376.991 rad/s. Note that for ac waveforms the maximum (rather than the r.m.s.) rated values are used as the per unit bases.

4.5.1 Steady-State Studies

The current and the voltage waveforms of the tap at two different load conditions, namely, full load and no load, are presented in Figure 4.12. For comparison, the corresponding waveforms for (conventional) twelve-pulse operation of the same tapping station are presented in Figure 4.13. Note that for a twelve-pulse operation of the same tap, the 11th and the 13th tuned filters have to be modified as the 11th and the 13th harmonic magnitudes are much higher than those of the quasi twenty four-pulse operation. For the details of these filters see Appendix B.

The harmonic magnitudes of the waveforms of Figures 4.12 and 4.13 are presented in Table 4.1. They are in agreement with the theoretical results of Figures 4.6, 2.3, 2.4 and 2.6, taking into account the effect of the system impedance. Non-characteristic harmonics are more or less the same for both kinds of operation.

I_d = 1.0 pu, ω = 1.0 pu, V_s = 1.0 pu

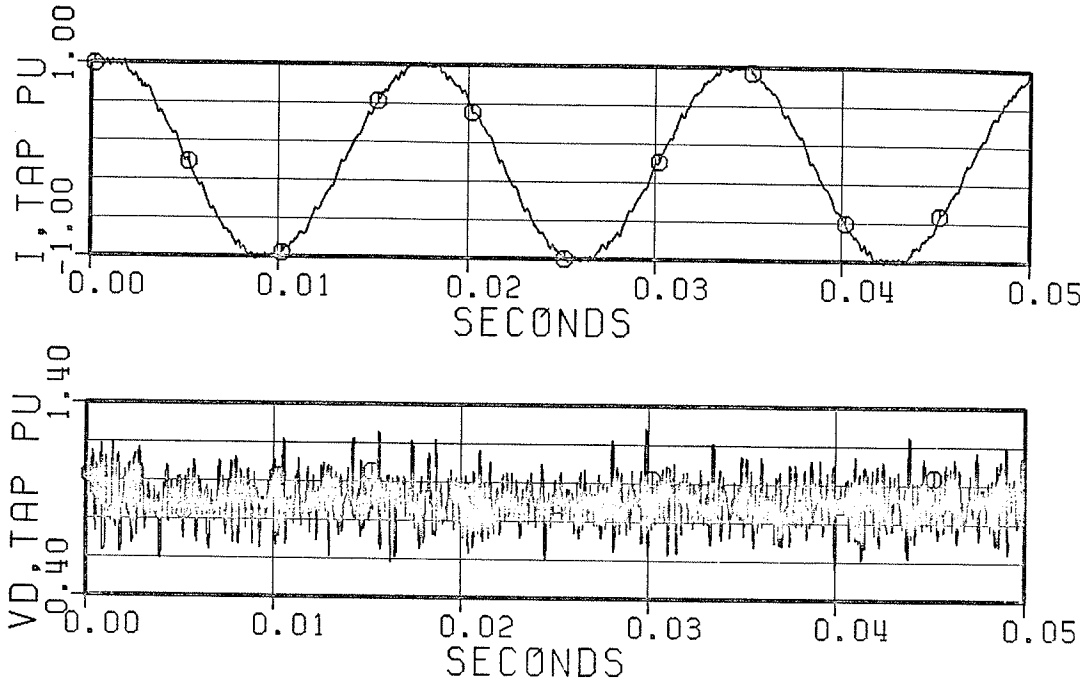

(a) Full Load (0.92 pu)

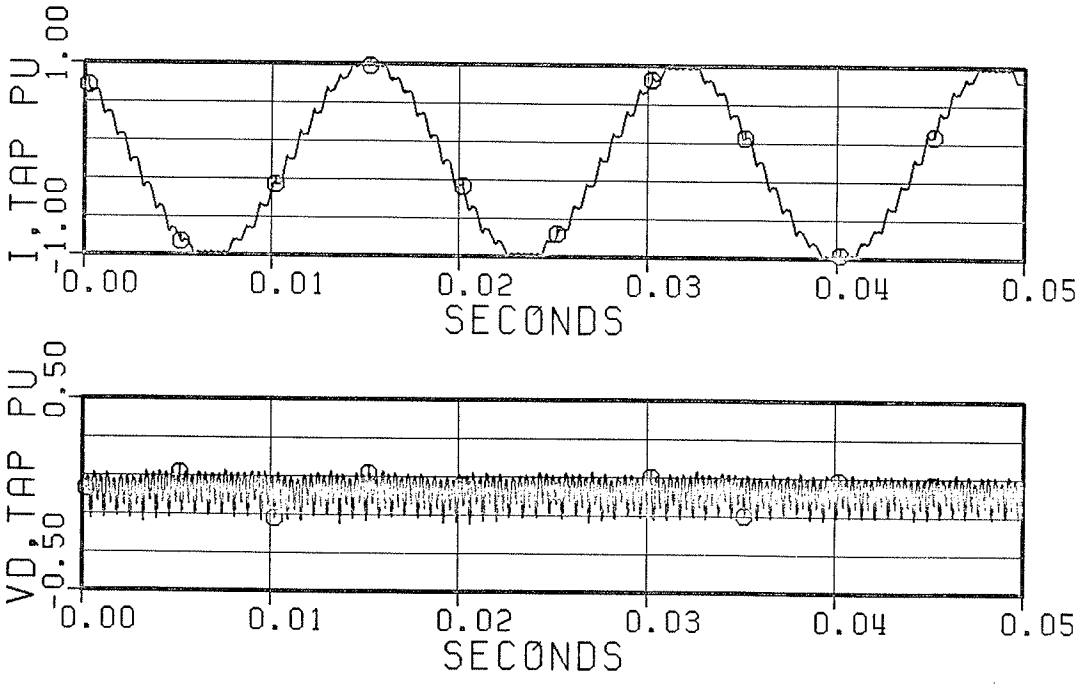

(b) No Load (< 0.02 pu)

Figure 4.12: Current and Voltage Waveforms of a Quasi 24-Pulse Tap.

I_d = 1.0 pu, ω = 1.0 pu, V_s = 1.0 pu

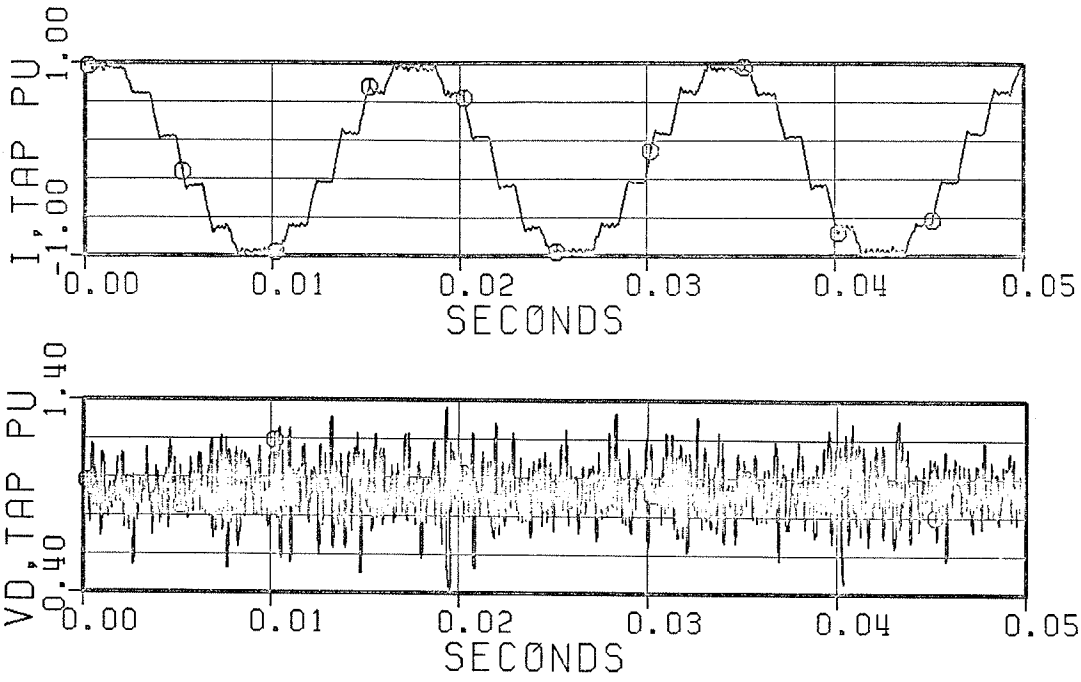

(a) 0.92 pu Load

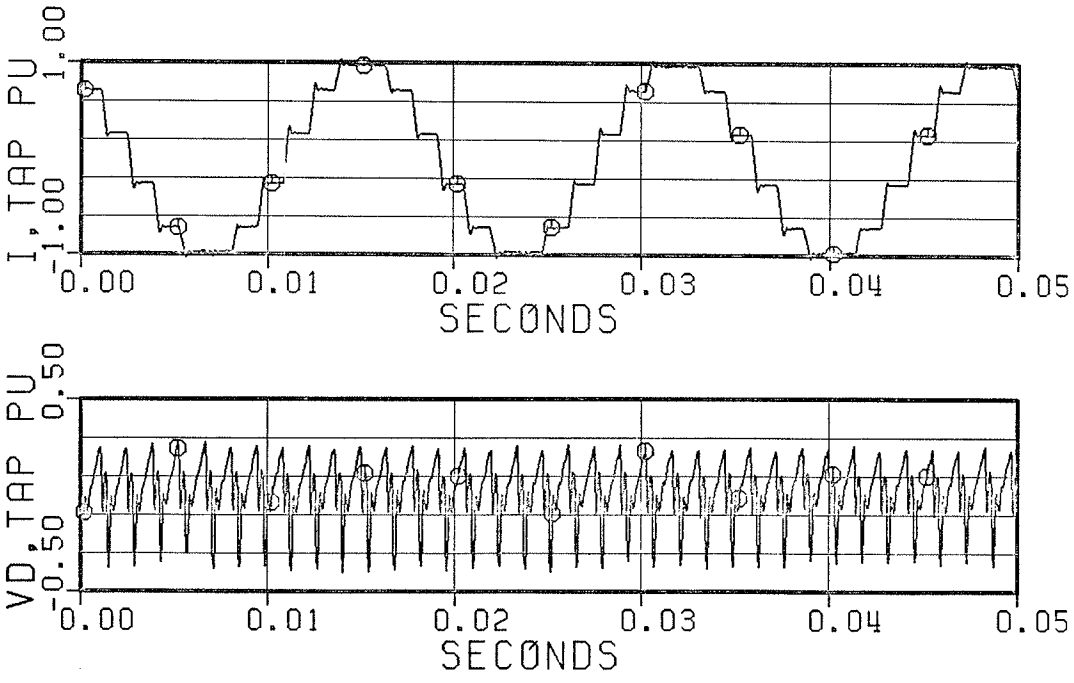

(b) No Load (< 0.02 pu)

Figure 4.13: Current and Voltage Waveforms of a 12-Pulse Tap.

TABLE 4.1

Overall Harmonic Magnitudes (Simulation)

		$I_{(n)}/I_{(1)}\%$ or $V_{(n)}/V_0\%$			
		Quasi 24-Pulse Operation		Twelve-Pulse Operation	
	n	0.92 pu Load 4.12(a)	No Load 4.12(b)	0.92 pu Load 4.13(a)	No Load 4.13(b)
ac side	5	0.24	0.10	0.07	0.23
	7	0.21	0.24	0.02	0.22
	11	1.05	1.34	8.02	9.07
	13	1.24	1.16	6.19	7.32
	17	0.17	0.21	0.18	0.27
	19	0.23	0.23	0.19	0.17
	23	1.65	3.77	1.86	3.87
	25	1.10	3.28	0.88	3.18
dc side	6	0.70	0.04	0.65	0.29
	12	2.17	0.33	3.26	10.28
	18	0.02	0.02	0.20	0.14
	24	2.45	1.94	2.69	1.97

From each twelve-pulse bridge set one valve of the same position is studied. The simulation results of the voltages and currents (their derivatives are not shown) of these valves, at two load conditions, namely, full load and no load, are presented in Figures 4.14 and 4.15, respectively. For comparison, the corresponding waveforms for twelve-pulse operation are presented in Figure 4.16 (in this case both valves have the same waveforms). The results indicate that the valve stresses are basically the same for both kinds of operation.

$|V_d|$ = 0.92 pu, I_d = 1.0 pu, ω = 1.0 pu, V_s = 1.0 pu

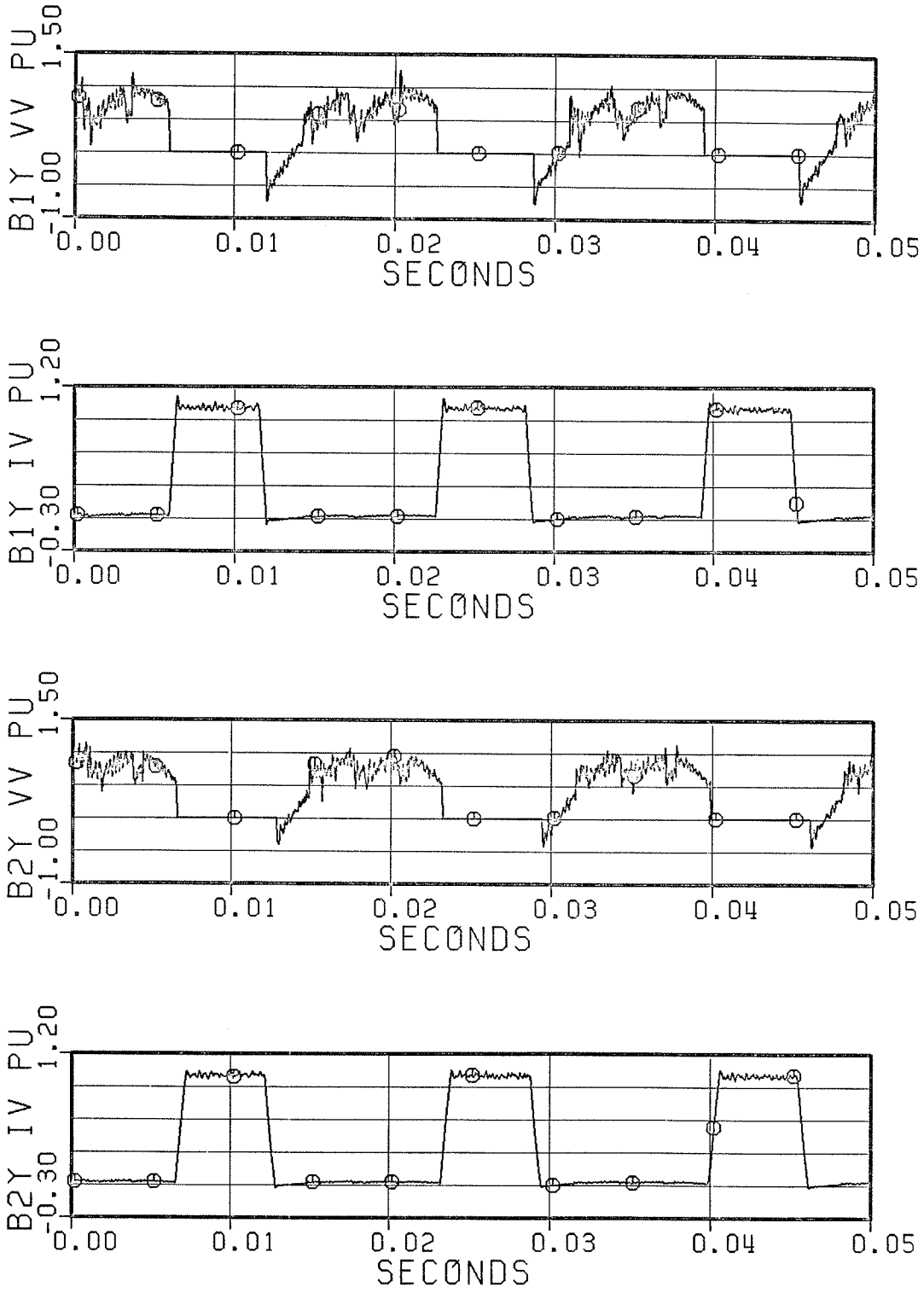

Figure 4.14: Valve Voltages and Currents of a Quasi 24-Pulse Tap (FL).

$|V_d| \cong 0.0$, $I_d = 1.0$ pu, $\omega = 1.0$ pu, $V_s = 1.0$ pu

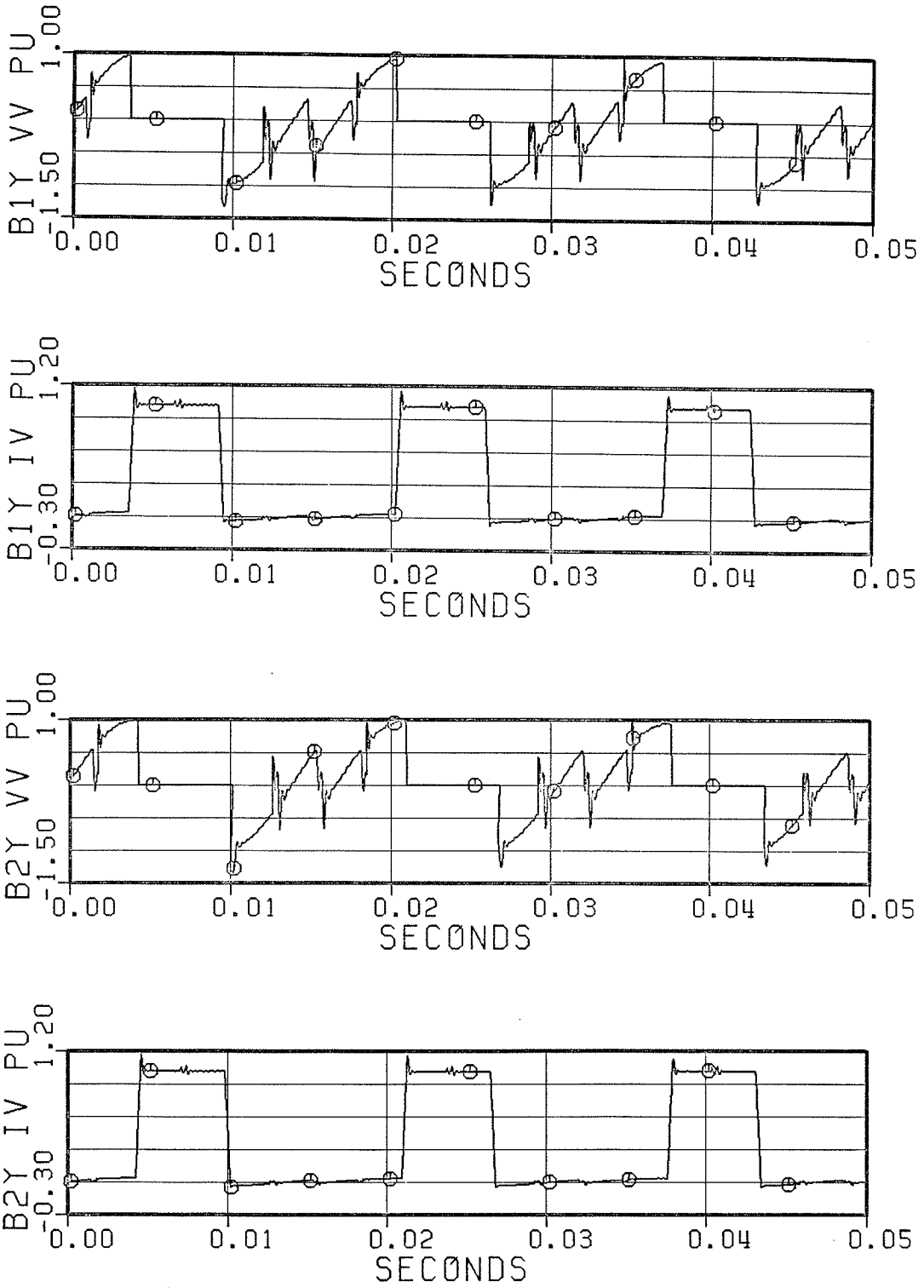

Figure 4.15: Valve Voltages and Currents of a Quasi 24-Pulse Tap (NL).

I_d = 1.0 pu, ω = 1.0 pu, V_s = 1.0 pu

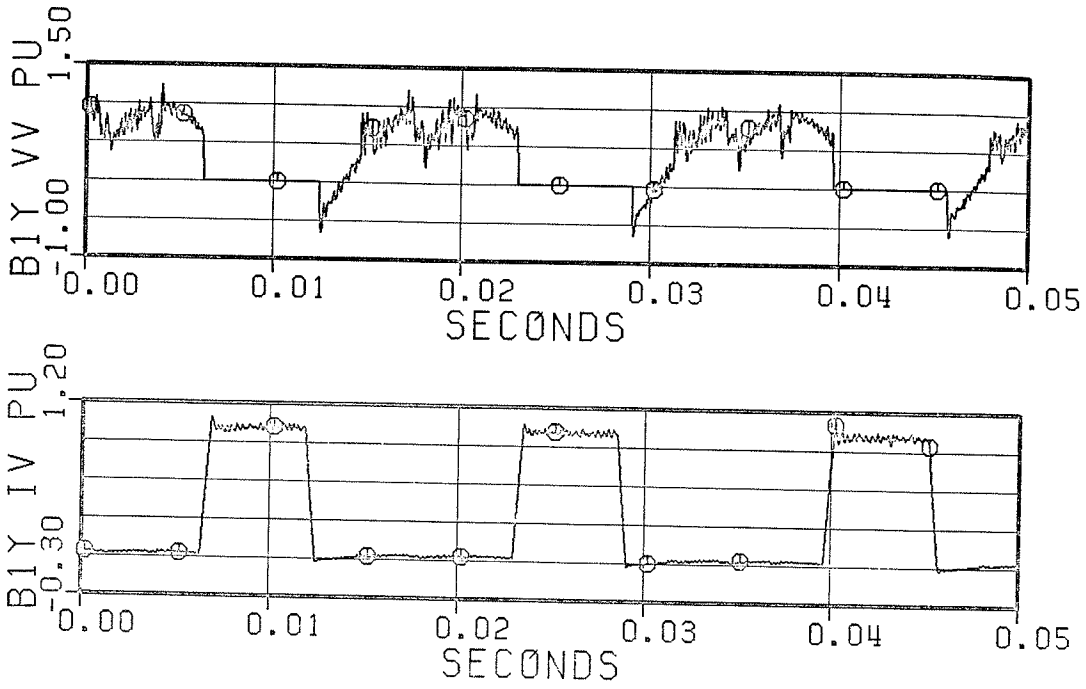

(a) 0.92 pu Load

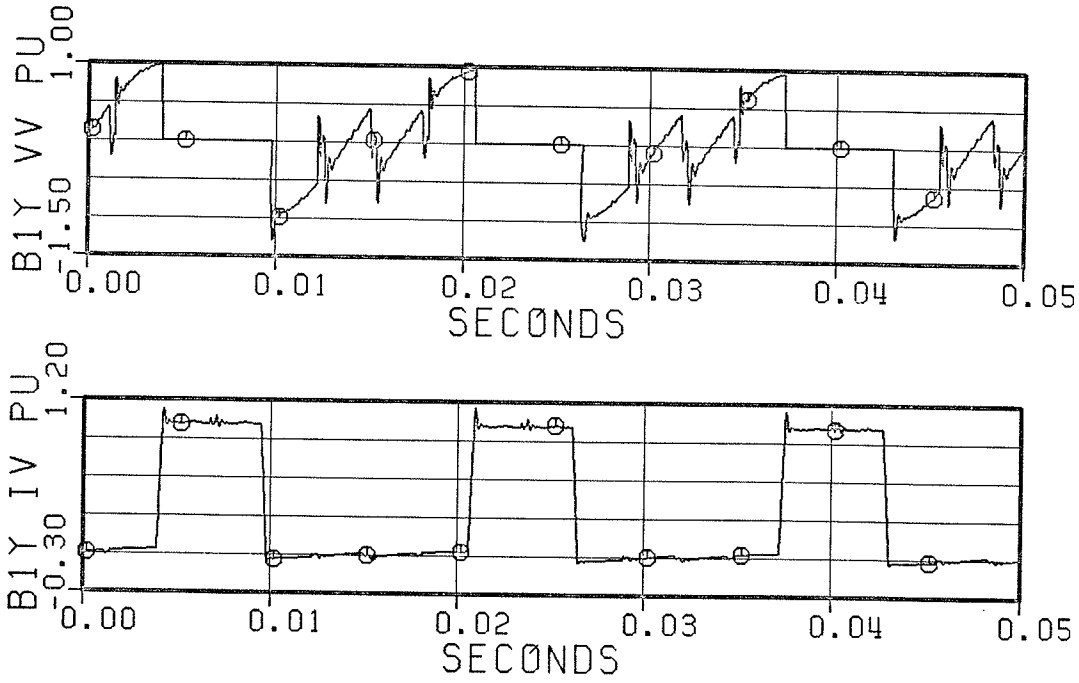

(b) No Load (< 0.02 pu)

Figure 4.16: Valve Voltages and Currents of a 12-Pulse Tap.

4.5.2 Disturbances in the Tapping Station

The results of a 10% load change are presented in Figure 4.17. The initial load is 0.83 pu and is reduced by 10% at t = 0.05 s. At the same time, the reactive component of the load, B_L, is also reduced so that the power factor remains the same (i.e., 0.85). At t = 0.2 s (i.e., 9 cycles after the load change) the capacitors are switched (i.e., B_C reduced from 0.40 pu to 0.35 pu and B_{CC} increased from 0.05 pu to 0.10 pu) to keep the voltages within acceptable limits. From the speed deviation curve in Figure 4.17, it can be seen that the dominant oscillation has a frequency of about 1.92 Hz (i.e., the period of the first cycle after t = 0.2 s is about 0.52 s). The magnitude of the oscillation reduces by a factor of 0.03 at the end of the first cycle, which means a decaying time constant of about 0.148 s. Similar results can be derived from the firing angle curves in Figure 4.17. These results are in close agreement with the theoretical results, considering the simplifications used in the theoretical model.

The results of a 50% load reduction are presented in Figure 4.18. The conditions are the same as those of Figure 4.17 (but, B_C is reduced to 0.25 pu and B_{CC} is increased to 0.2 pu).

Using the differential firing technique for harmonic control does not preclude the possibility of reducing some of

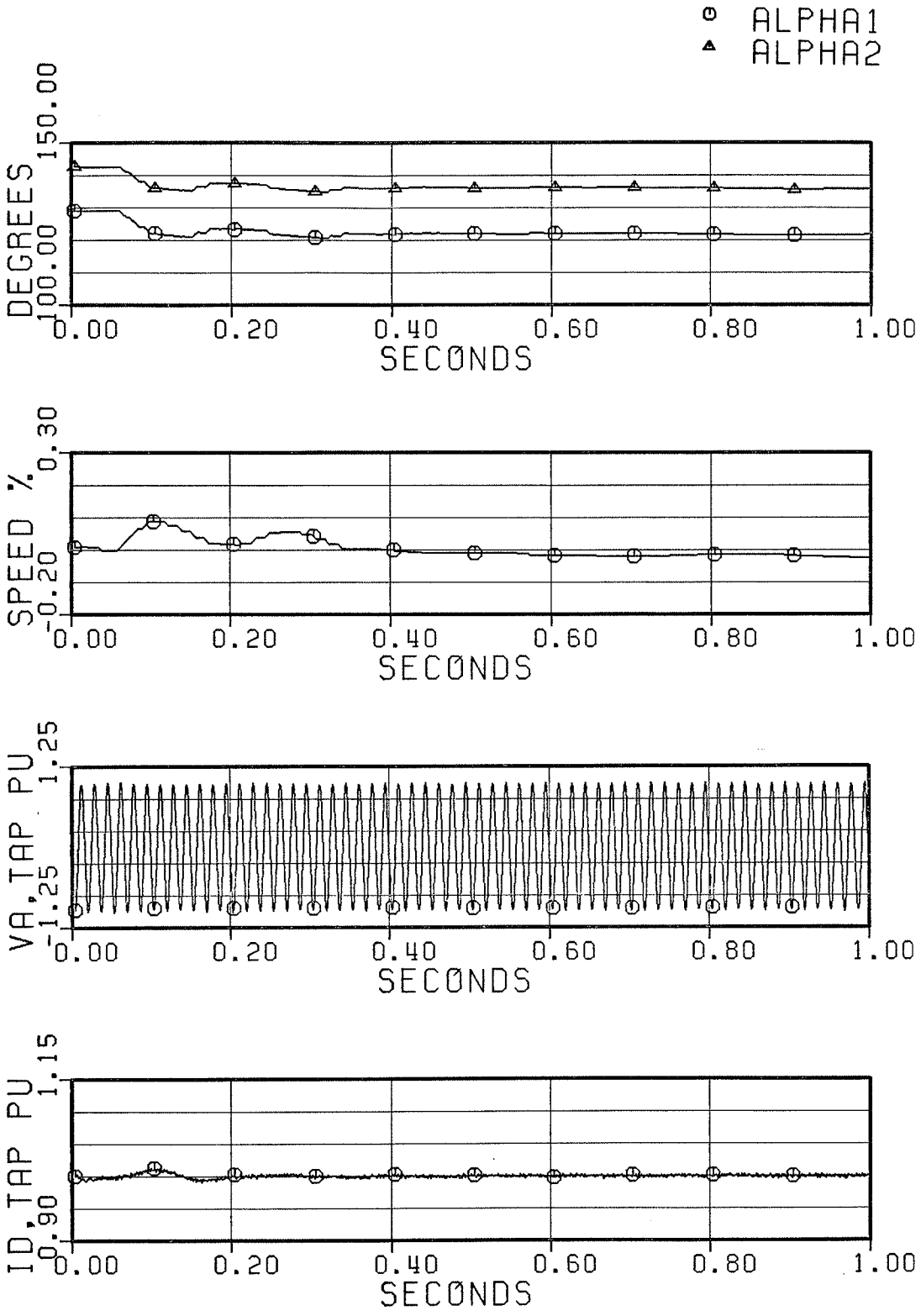

Figure 4.17: 10% Load Reduction (Initial Load 0.83 pu).

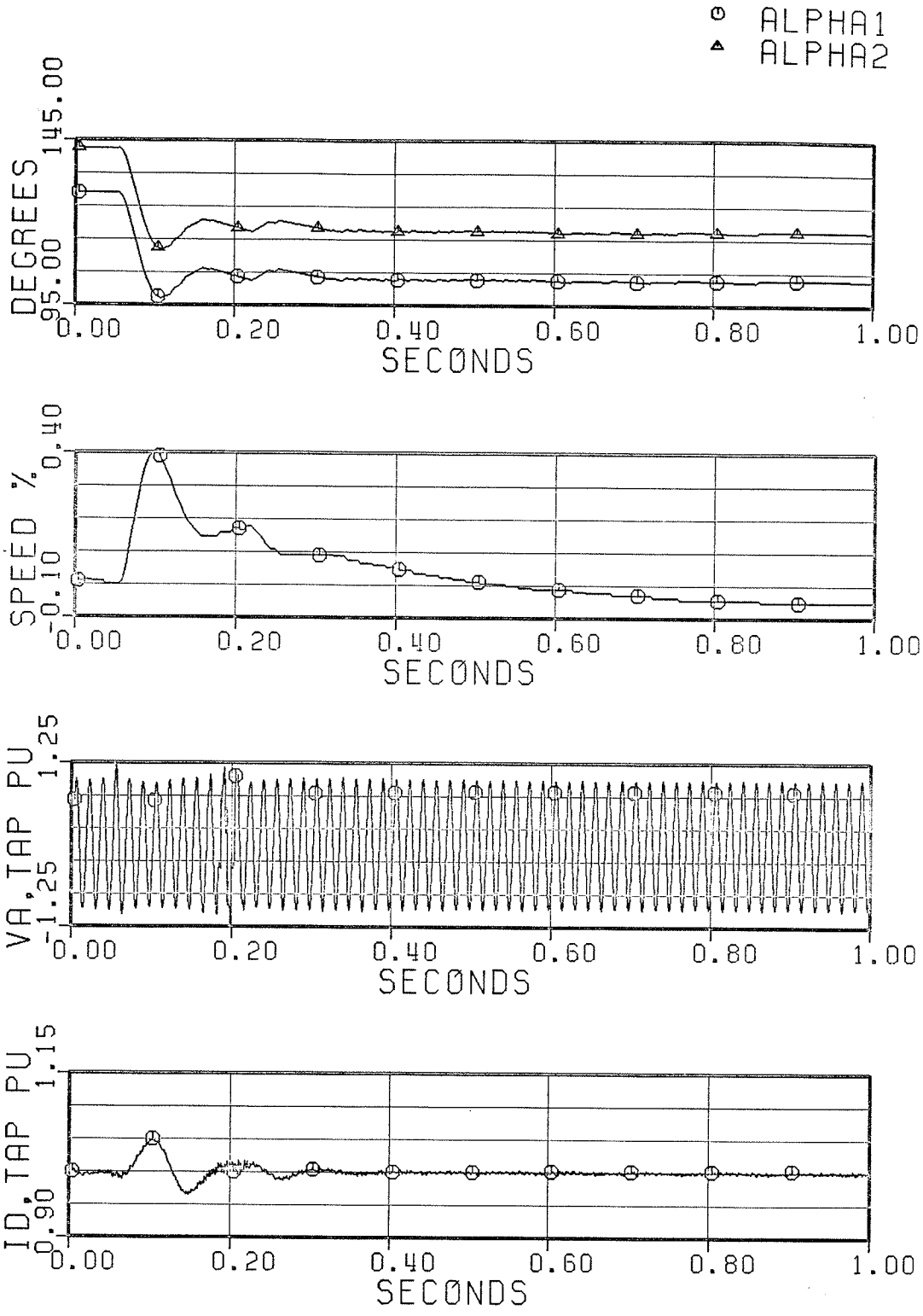

Figure 4.18: 50% Load Reduction (Initial Load 0.83 pu).

the transient overvoltages of the tap's ac bus by the tap itself. In fact, with two bridge sets in series, operation on the minimum VAr characteristics offers rather small VAr absorption capabilities at large loads (see Figure 2.1), if the real power is to remain unchanged. If the real power is allowed to be changed (e.g., for a short duration during a transient overvoltage), then the VAr absorption capability of the tap substantially increases at large loads (where it is needed most), regardless of the (steady-state) operation characteristic; in any case, the VAr consumption of the tap can be increased to as high as $1.1146V_sI_d$ pu, as can be seen from Equation 2.3. This capability of the tap (under the quasi twenty four-pulse operation) can be seen by comparison of Figures 4.19 and 4.20. Figure 4.19 is the result of a complete load disconnection at t = 0.05 s, without any over-voltage control by the tap (B_C is reduced to 0.0 and B_{CC} is increased to 0.3 pu at t = 0.2 s). The initial load is o.83 pu. It can be seen that the overvoltage at the tap's ac bus is very large; it has (momentarily) reached as high as 2.2 pu. Figure 4.20 is the result of the same disturbance, but this time, 5 ms after the load disconnection the effective firing angle is reduced to about 95 degrees and then released according to a ramp with a slope of 20 rad/s. In Figure 4.20, the tap's ac bus voltage has reached as high as 1.73 pu.

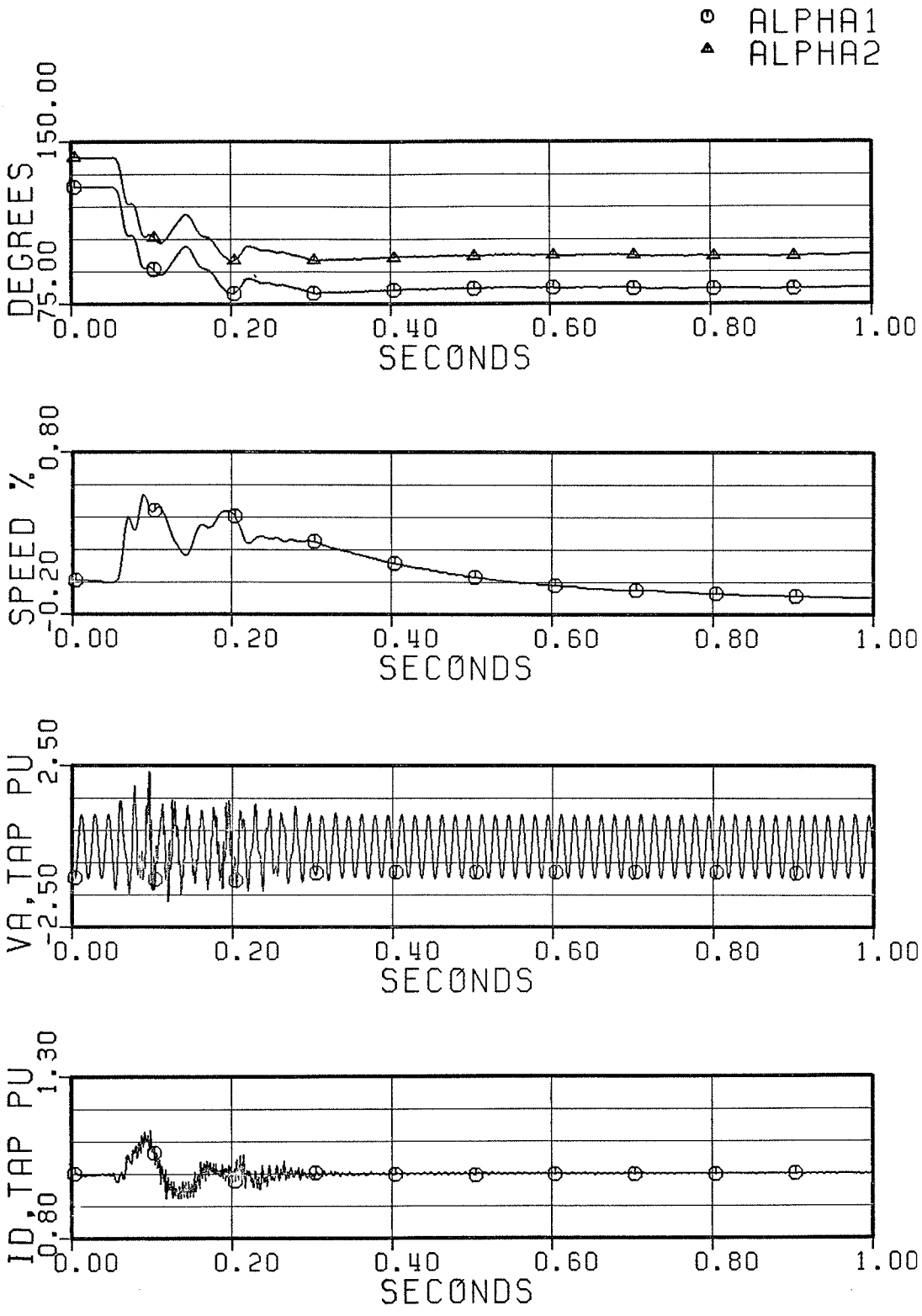

Figure 4.19: Load Disconnection with No Overvoltage Reduction by the Tap.

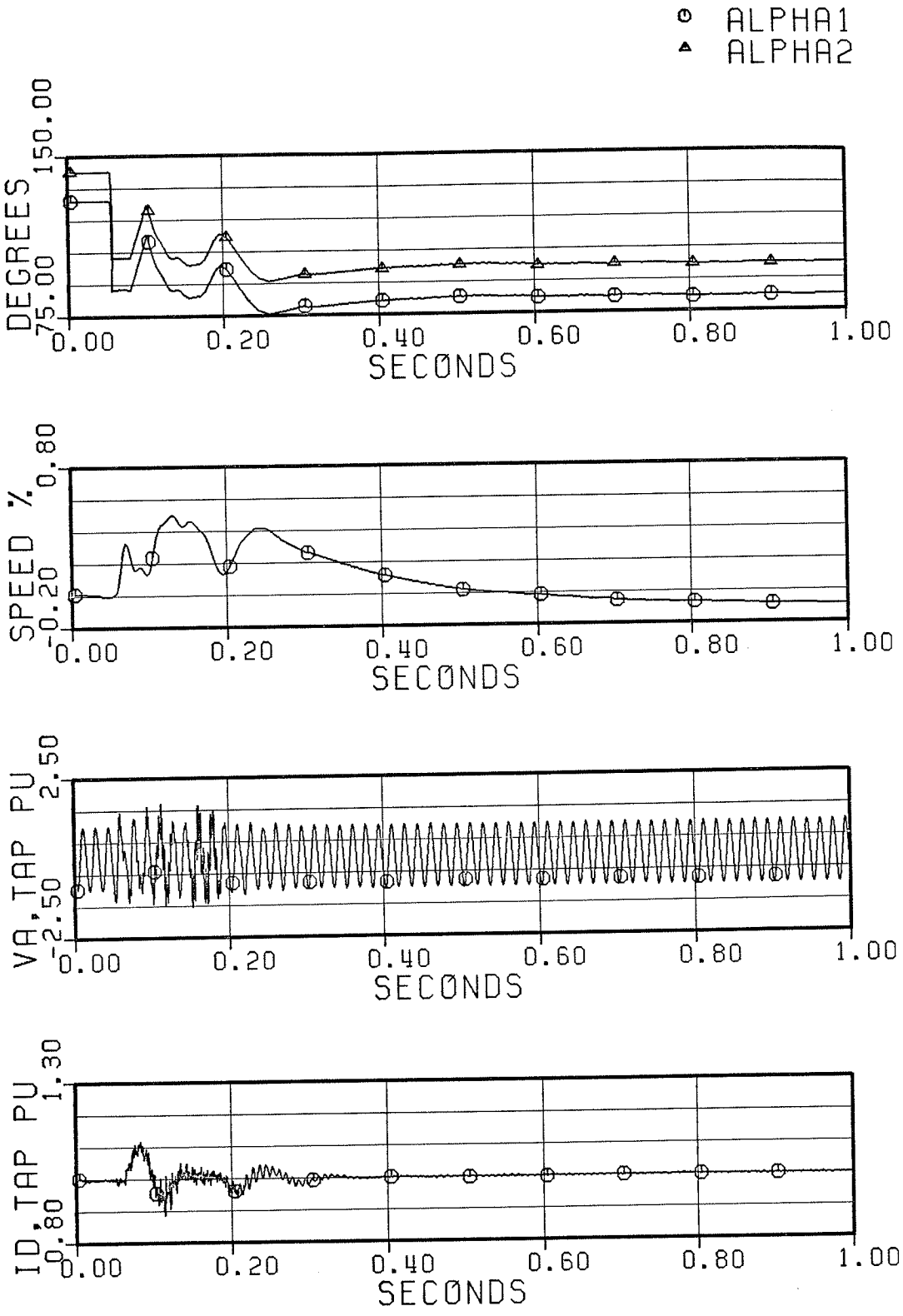

Figure 4.20: Load Disconnection with Some Overvoltage Reduction by the Tap.

The results of a three-phase (to ground) fault at the tap's ac bus are presented in Figure 4.21. The fault occurs at t = 0.05 s and lasts for 6 cycles. The load is 0.83 pu. Before removing the fault, the effective firing angle is reduced to about 90 degrees and after removing the fault, it is released according to a ramp with a slope of 20 rad/s. Figure 4.22 is the result of a single phase-to-ground fault at the tap's ac bus with similar conditions as those of Figure 4.21.

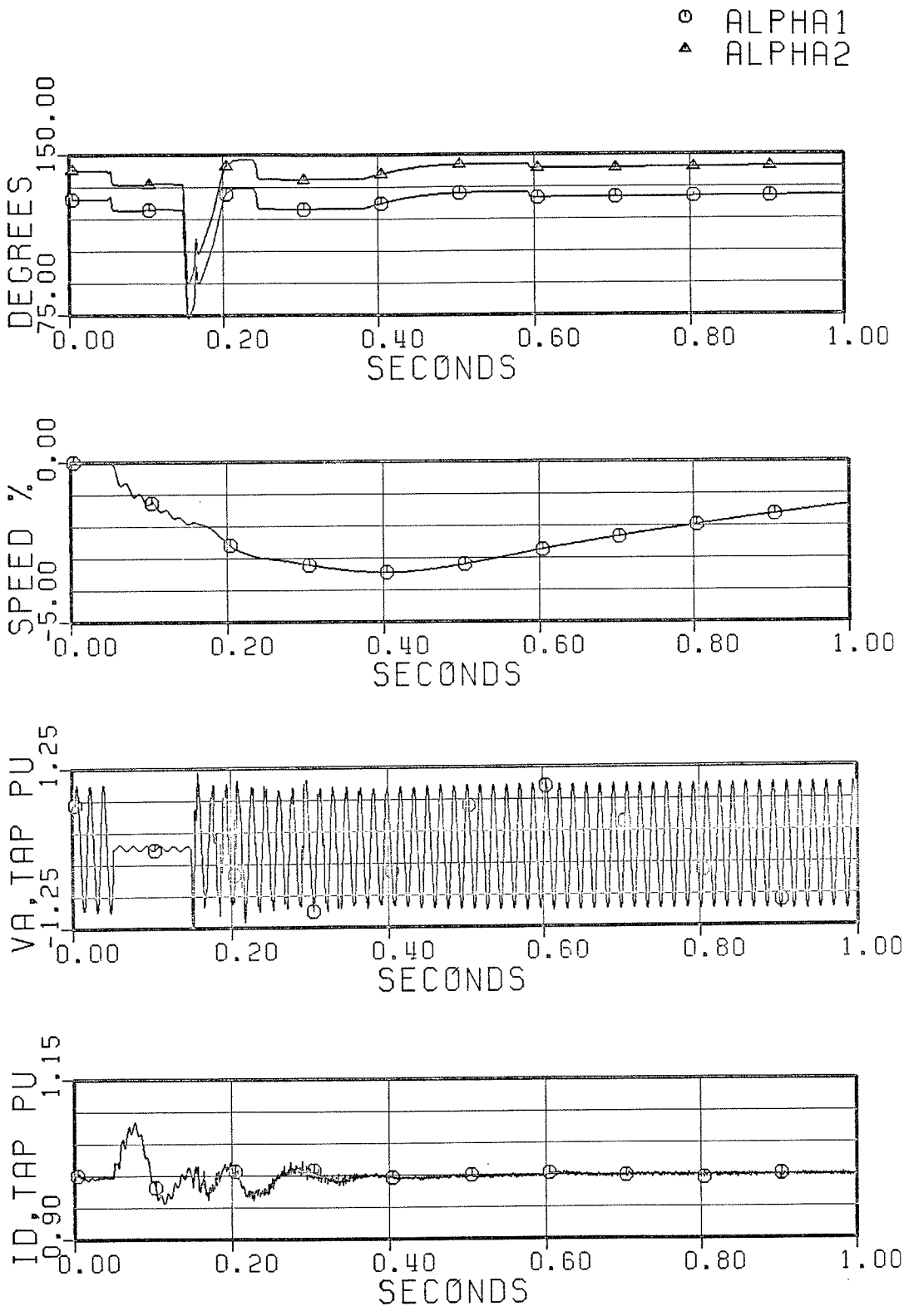

Figure 4.21: 6-Cycle 3-Phase Fault at the Tap's Bus.

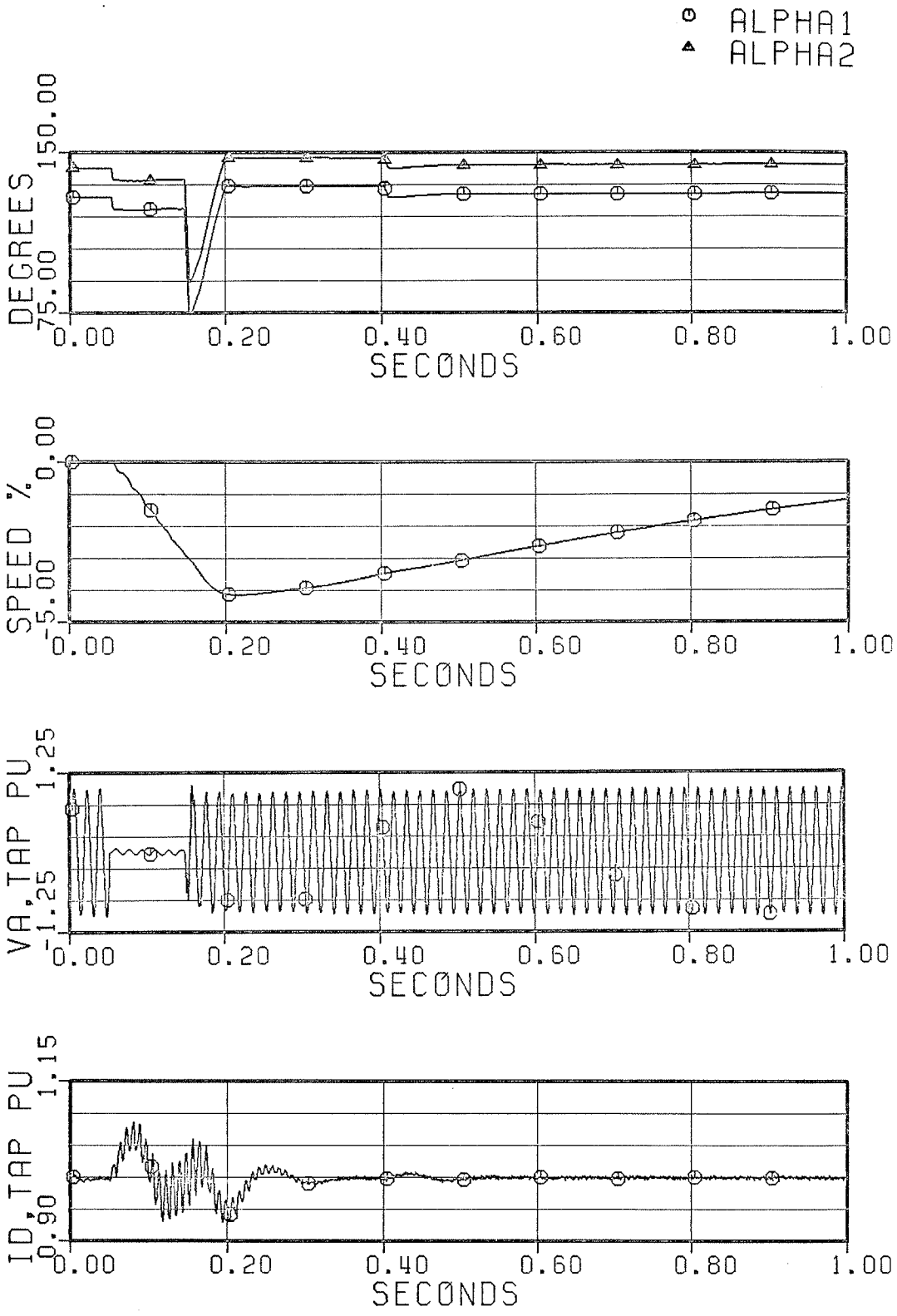

Figure 4.22: 6-Cycle Single Phase-to-Ground Fault at the Tap's Bus.

4.5.3 Disturbances of the Main DC System

The results of a 20% change in the ordered current of the system are presented in Figure 4.23. The initial dc line current is 1.0 pu. The ordered current of the system is reduced to 0.8 pu at t = 0.05 s. The load at the tapping station is 0.41 pu. At t = 0.2 s, B_{CC} is reduced to 0.0 (from 0.20 pu). B_C remains the same (i.e., 0.25 pu).

The results of a dc line (to ground) fault at the main inverter end (right before its smoothing reactor) are presented in Figure 4.24. The load at the tapping station is 0.83 pu. The fault is initiated at t = 0.05 s. After 6.5 ms, a forced retard is applied at the main rectifier end by simply changing the ordered current from 1.0 pu to zero. When the dc line current drops to zero, the tap is blocked. The fault is removed at t = 0.25 s (i.e., 200 ms after the conception of the fault, to allow for deionization). At the same time the ordered current is changed to 1.0 pu. Prior to deblocking of the tap at t = 0.26 s, the effective firing angle is reduced to about 90 degrees. After deblocking, it is released according to a ramp with a slope of 20 rad/s.

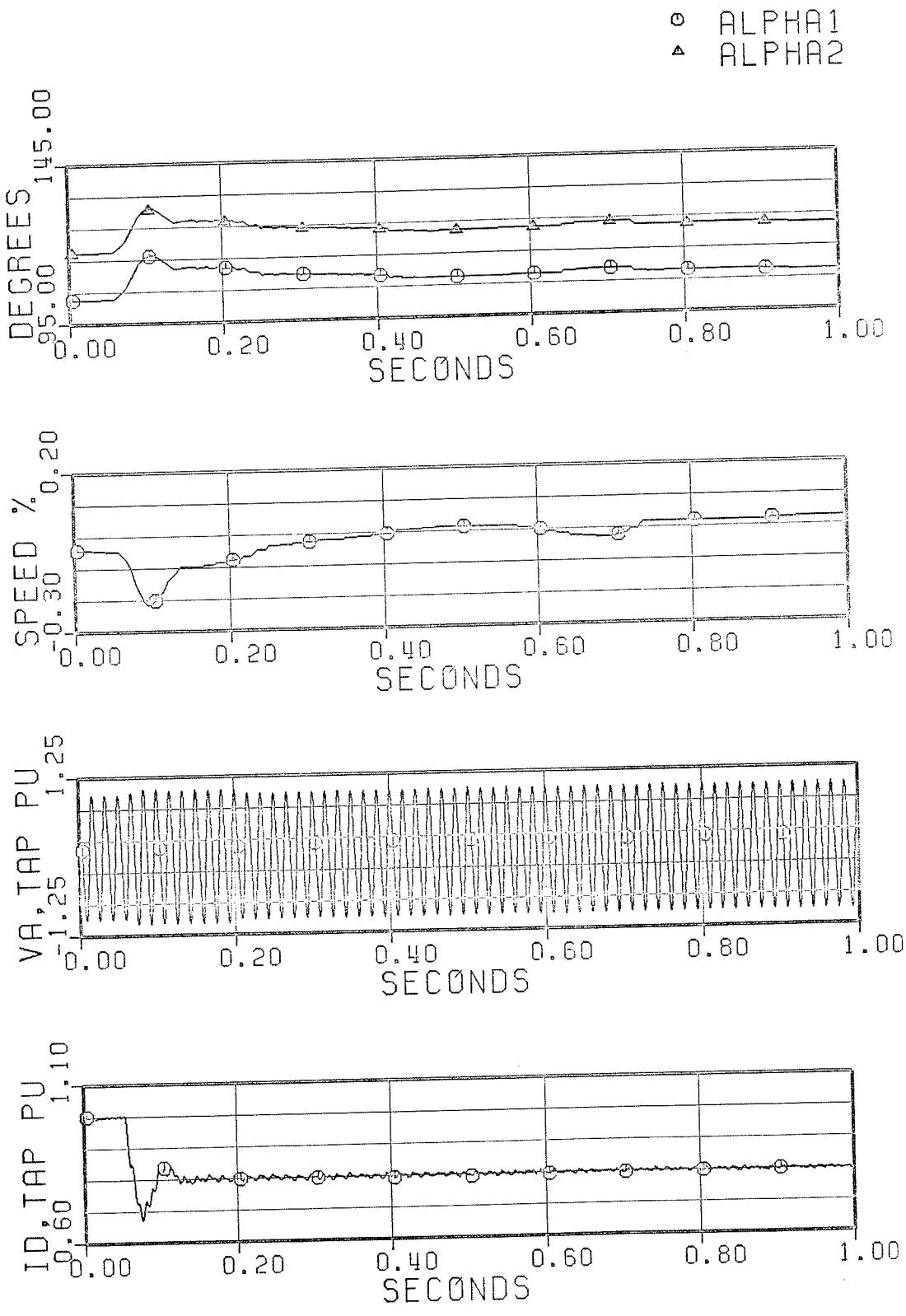

Figure 4.23: 20% Reduction in the Ordered Current.

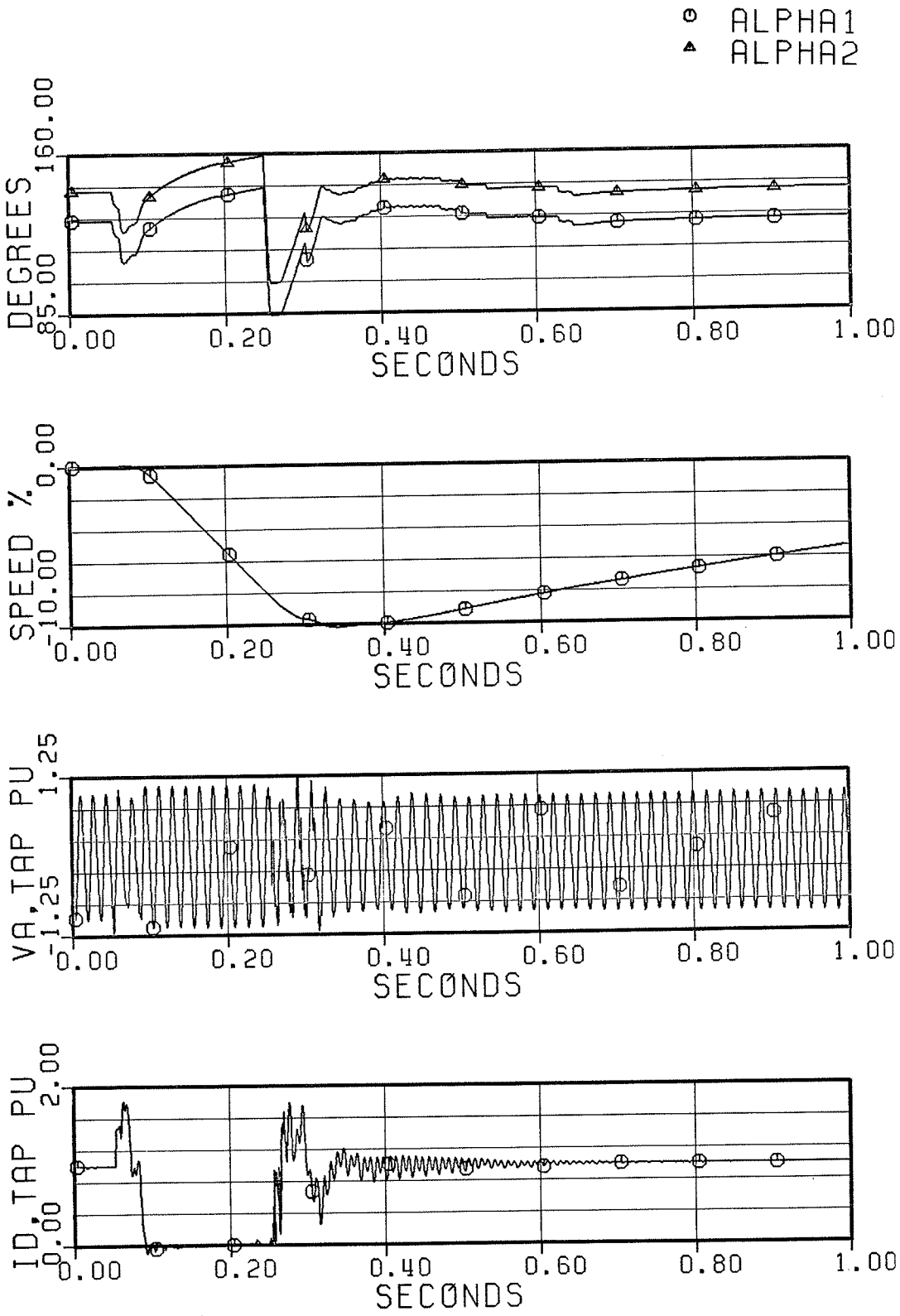

Figure 4.24: DC Line Fault at the Inverter End.

4.6 ECONOMIC ASPECTS AND OTHER APPLICATIONS

Doubling the number of bridge sets will usually somewhat increase the cost (per kW) of a converter station. But it is assumed to be offset by the higher flexibility that is gained, provided that the converter is capable of operating with one bridge set out of service. A quasi twenty four-pulse series tap will be able to operate with one bridge set out of service, if the filters are still capable of performing adequate filtering. In this case, in a bipolar configuration, 11th and 13th current harmonic magnitudes can reach slightly higher than one quarter of their corresponding values at normal (i.e., with all bridges in service) twelve-pulse operation of the tap (see Appendix B). A similar situation exists in case of using phase-shifting transformers, which usually makes the case uneconomical [12,13]. In case of ac voltage regulation by the tap, the extra cost due to increasing the number of bridge sets can not be attributed to higher flexibility, as the regulation capability drops drastically when one bridge set is taken out of service. Operation on the minimum VAr characteristic, however, will have the flexibility of performing under the condition of one bridge set out of service.

4.6.1 Cost Comparison

To get some idea about the economic advantages of differential firing technique and provide a basis for recognizing other advantageous (or disadvantageous) applications, a comparative cost evaluation will be attempted for the three following cases, based on the tapping station that has been used for the digital simulation studies presented earlier in this chapter.

1. Twelve-pulse operation with equal firing angles.
2. Quasi twenty four-pulse operation.
3. Minimum VAr operation.

It may be noted that in every case the tap consists of two twelve-pulse bridge sets in each pole and each twelve-pulse bridge set is rated at 50 MW.

The following unit costs in 1985 Canadian dollar [30] will be used:

cost of turnkey terminal (100 MW) = $130.00/kW,

additional cost of series tapping = $10.00/kW,

cost of synchronous condenser = $55.00/kVA,

cost of capacitor banks = $6.50/kVAr,

cost of energy = $0.02/kWh,

cost of capacity loss = $2000.00/kW-installed.

In a conventional converter terminal, the cost of smoothing reactors and the cost of filters are about 5.3% and 8.3% [30], respectively. The cost of ac tuned filters are esti-

mated to be one half of the cost of all (ac and dc) filters, i.e., 4.15%. The 11th and the 13th harmonic magnitudes of a series tap are higher than those of a conventional converter by factors of 1.314 and 1.478, respectively. thus on the average,

cost of ac tuned filters = 130.00 X 0.0415 (1.314 + 1.478) / 2 = $7.53/kW.

And,

cost of smoothing reactors = 130.00 X 0.053 = $6.89/kW.

The loss of the ac tuned filters of the equal firing operation at fundamental frequency is 27.771 kW, as calculated in Appendix B. Assuming that the tap will be in service 95% of the time,

c = cost of energy loss per year
= 27.771 X 8760 X 0.95 X 0.02
= $4622.21/year.

Assuming,

r = annual fixed charged rate = 0.15,

and,

i = annual interest rate = 0.06,

the present day worth of the lost energy is,

$$cr/(1+i) + 2cr/(1+i)^2 + 3cr/(1+i)^3 + \ldots = cr(1+i)/i^2$$
$$= \$204147.61$$
$$= \$2.042/kW.$$

Adding the cost of capacity loss to the cost of energy loss,

cost of the losses of ac tuned filters = 2.042 + 2000.00 X 27.771 / 100000 = $2.60/kW.

The savings on the costs of the ac tuned filters of the quasi twenty four-pulse operation and the minimum VAr operation have been found to be 33.65% and 6.17% (see Appendix B), respectively, as compared with the equal firing operation. The savings on their losses have also been found to be 68.11% and 13.66%, respectively. The savings on smoothing reactors are 48% and 24%, respectively, which have been calculated using Equation 2.39 (for the data see Appendix C). The rating of the synchronous condenser for the quasi twenty four-pulse tap is 70 MVA, which effects an effective short circuit ratio (ESCR) of 2.5 at 0.92 pu load (at 1.0 pu dc line current). To have the same effective short circuit ratio for either of the other cases, a 74 MVA synchronous condenser is needed. The total capacitance used for reactive power compensation in each case is calculated based on keeping both the voltage at the tap's ac bus and the voltage at the load bus within the same limits in all three cases. In case of the quasi twenty four-pulse tap the provided filtering level allows $|V_d|$ (in inversion mode) to be increased upto 0.936 pu at I_d = 1.0 pu, i.e., 6.4% of the capacity of the tap has to be blocked (see Figure 4.3). However, as the dc line current decreases, it is possible to run the tap in a way that the blocked portion tapers off; for $I_d \leq 0.31$ pu no portion has to be blocked. This way of runing the tap is advantageous in reducing the transmission losses. The average of the conversion capacity loss is estimated to be 3.4%.

The results of the above considerations are presented in Table 4.2. The savings for the quasi twenty four-pulse operation and the minimum VAr operation are in excess of 2.0% and 1.7%, respectively.

TABLE 4.2

Cost Comparison of Equal and Differential Firing Operations

	Coefficient (pu)			$/kW-Capacity		
Description	12-P	Q 24-P	Min VAr	12-P	Q 24-P	Min VAr
Cost of Terminal	1.0	1.0	1.0	130.00	130.00	130.00
Additional Cost for a Series Tap	1.0	1.0	1.0	10.00	10.00	10.00
Cost of Synchronous Condenser at $55.00/kVA	0.74	0.70	0.74	40.70	38.50	40.70
Cost of Capacitor Banks at $6.50/kVAr	0.65	0.628	0.536	4.23	4.08	3.48
Saving on Smoothing Reactors at $6.89/kW	0.0	0.48	0.24	0.00	-3.31	-1.65
Saving on AC Tuned Filters at $7.53/kW	0.0	0.3365	0.0617	0.00	-2.53	-0.46
Saving on the Losses of AC Tuned Filters at $2.60/kW	0.0	0.6811	0.1366	0.00	-1.77	-0.36
Total Unit Cost Including the Capacity Loss of the Q 24-P Tap	1.0	1.0352	1.0	184.93 (100%)	181.13 (98.%)	181.71 (98.3%)

4.6.2 Other Applications

It is possible to reduce the conversion capacity loss of the quasi twenty four-pulse tap, even to the point that it vanishes altogether, by increasing the level of filtering. The required level of filtering will, in any case, be considerably lower than that of the normal twelve-pulse operation of the tap, as the magnitudes of 11th and 13th harmonics will be at most equal to those of the same converter operating around $V_d = -1.0$ pu. In this case there is no need to decrease the 11th and the 13th harmonic magnitudes to the values of the quasi twenty four-pulse operation. Instead, while the magnitudes of 11th and 13th harmonics are kept around the values corresponding to the operation at minimum margin angle, the magnitudes of other harmonics such as 23rd and 25th can be reduced as well.

One possibility is to look for minimum commutation failures, namely, minimum difference angle. In this case, the difference angle can be approximated by,

$$\Delta\alpha = - 1.31 \, (\omega I_d / V_s)^2 + 10.04 \quad \text{degrees.} \qquad (4.50)$$

It may be noted that when one bridge set reaches its minimum margin angle limit, the difference angle can be reduced down to zero to meet larger loads and, therefore, no capacity will be lost (i.e., no blocked portion).

Another possibility is to maximize the reactive power reduction (i.e., to maximize the difference angle), while the

11th and the 13th harmonic magnitudes are kept at or below the same levels. The required difference angle will be about 20 degrees.

A third possibility is to obtain the maximum possible reduction on the installed reactive power (i.e., 8.0% as shown in Figure 2.1) and reduce the harmonic magnitudes as much as possible, as well. This case will require a difference angle of about 42 degrees.

The maximum (theoretical) magnitudes of the harmonics and the amount of the reactive power reduction of the above possibilities are presented in Table 4.3. For comparison, the corresponding values of the equal firing operation are provided, as well.

TABLE 4.3

Comparison of Various Possibitities

Case Description	Maximum Harmonic Magnitudes (%)						VAr Reduction (%)
	AC Side				DC Side		
	n=11	n=13	n=23	n=25	n=12	n=24	
Equal Firing	8.57	7.08	3.33	2.91	11.84	5.86	0.0
$\Delta\alpha \cong -1.31\ I_d^2 + 10.04$ degrees	6.57	4.83	1.35	1.15	5.98	2.93	0.3
$\Delta\alpha \cong 20$ degrees	6.57	4.83	1.69	1.40	5.94	2.90	2.5
$\Delta\alpha \cong 42$ degrees	7.46	5.77	1.86	1.54	6.51	3.10	8.0

Another application that has been mentioned before is a quasi twelve-pulse operation which is not economical as compared with the twelve-pulse operation using wye- and delta-connected transformer windings, as the remaining magnitudes of the 5th and the 7th harmonics are rather large and, at 1.0 pu dc line current, about 18% of the capacity of the converter will have to be blocked.

It should be noted that the application of differential firing technique is not restricted to series tapping and can be applied to the converters of a point-to-point system, as well. However, in this case, the required installed reactive power will increase. To have a quasi twenty four-pulse inverter, the increase in the required installed reactive power will be 0.061 pu (in case of a series tap it, in fact, decreases by about 0.01 pu). Moreover, the original magnitudes of the characteristic harmonics of the converter are considerably lower than those of a series tap and, therefore, the savings on the unit cost of filters (and their losses) will be considerably less. A cost analysis similar to that of Table 4.2 reveals that this case is unlikely to result in any savings. Nevertheless, the idea of harmonics reduction using differential firing can be implemented, at virtually no cost, in converters with two (or two sets of) bridges in series, to be in effect in case of filter outages; the converter will be able to operate at somewhat decreased dc voltage and possibly at somewhat decreased dc

line current. Several predetermined functions for the difference angle can be considered to take care of different harmonic filters and, thereby, considerably increase the continuity of service and improve the reliability of the system as a whole.

4.7 CONCLUSIONS

In this chapter, the concept of differential firing has been investigated for two groups of potentially advantageous possibilities, namely, VAr control and harmonic control. At large loads, the voltage regulations are small for two bridge sets and improve considerably as the number of bridge sets increases. However, as the number of bridge sets increases, so does the complexity of the tapping station and technical as well as economic problems may arise.

In case of harmonic control several advantageous possibilities exist, of which a classical application, namely, a quasi twenty four-pulse operation, has been investigated in detail. An appropriate control method, namely, the predetermined differential firing method, has been developed. The introduction of the effective firing angle has made the case more practical. Theoretical as well as digital simulation studies have been performed and their results have been compared. The technical feasibility of the idea has been shown by both theoretical and simulation results and, even with a weak ac system at the tapping station, no side effect has

been detected. The tap's capability to reduce some of the transient overvoltages of its own ac bus may still be exploited. The economic advantages of the idea have been shown, as well. Harmonic magnitude reduction using differential firing may have advantageous applications in converters other than series taps, as well.

Chapter V

CONCLUSIONS AND SUGGESTIONS FOR FURTHER STUDIES

The main objective of this thesis has been to increase the viability of series tapping of HVDC transmission. In persuit of this objective, two techniques, namely,

1. diode rectifier series tapping and
2. differential firing in series tapping,

have been investigated.

5.1 CONCLUSIONS

Based on the results of the analytical studies, the digital simulation studies and the economic comparisons presented in this thesis, the following major conclusions are derived:

1. Diode rectifier series tapping is technically feasible and economically very attractive. There is no need for dc circuit breakers and the tap can satisfactorily operate without many components such as filters, communication system, etc., normally used in an HVDC converter station. The tap does not overly increase the complexity of the system and the flexibility of the main system remains more or less intact.

2. Two inherent drawbacks of HVDC converters, namely, the consumption of reactive power and the production of characteristic harmonics, are more apparent and more intense in a (conventionally controlled) converter operating as a series tap. The concept of differential firing is, to some extent, capable of mitigating these problems.
3. Some voltage regulation on the tap's own ac bus can be exercised by using differential firing. At a large load the voltage regulation that can be obtained with two bridge sets in series is relatively small, but improves considerably as the number of bridge sets increases. However, as the number of bridge sets increases, so does the complexity of the tapping station, and technical as well as economic problems may arise.
4. Harmonic magnitude reduction using differential firing is technically feasible and can result in overall economic gains. A viable application is the so-called quasi twenty four-pulse operation.
5. The quasi twenty four-pulse operation of a series tap does not preclude the reduction of some of the transient overvoltages of the tap's ac bus by the tap itself.
6. The option of combining the harmonic magnitude reduction and the VAr reduction exists, which may result in even more economic gains.

7. Harmonic magnitude reduction using differential firing may have valuable applications in converter stations other than series taps, as well.

5.2 MAJOR CONTRIBUTIONS

The major contributions of this thesis are as follows:

1. Comprehensive analyses of the reactive power requirements and the characteristic harmonics of a series tap and their comparison with those of other (primarily conventional) converter operations.
2. Analysis of the effect of the location of a series tap on the characteristic harmonics entering the dc transmission line from the tap.
3. Proposal and analysis of a diode rectifier series tap on an HVDC line and its comparison with other schemes.
4. Digital simulation studies of an HVDC system incorporating a prototype diode rectifier series tap and development of a method for smooth deblocking (or blocking) of the tap.
5. Analysis of the ac voltage regulation capability of a series tap as a result of differential firing.
6. Development of the firing algorithm for a quasi twenty four-pulse series tap.
7. Proposal of the appropriate modifications in the control system of the tapping station, as required for

harmonic magnitude reduction using differential firing, and the small signal analysis of a prototype system.

8. Digital simulation studies of an HVDC system incorporating a prototype quasi twenty four-pulse series tap.
9. Examination of the economic implications of various applications of differential firing.

5.3 SUGGESTIONS FOR FURTHER STUDIES

1. From the results of the digital simulation studies of the 10% diode rectifier series tap presented in this thesis, it appears that the tap can, in fact, be larger than 10%. Thus, further digital simulation (or simulator) studies as to the relative magnitude of the tap is suggested. Moreover, the configuration of the diode rectifier tapping station (Figure 3.1(b)) suggests that unit connection schemes can be used in further investigations of the diode rectifier series tapping technique. Operation at higher frequencies (for better efficiency) may be investigated as well.
2. An inverter series tap requires the maintenance of a corresponding rectifier voltage in the dc system. It appears to be more logical, as well as more economical, to provide the required rectifier voltage by a diode rectifier series tap. In this case, the reduc-

tion of dc harmonics of the inverter tap by using differential firing will be more valuable.

3. When an actual series tapping project is available, a comprehensive cost analysis of various possibilies of differential firing, in order to arrive at the optimum case, is recommended (the optimum case, if available, can be used for the inverter tap of the configuration suggested in (2) above).

4. Finally, the application of harmonic magnitude reduction using differential firing as a contingency plan (i.e., in case of filter outages) in a conventional HVDC converter, is another area for further studies.

REFERENCES

1. J. Reeve, "Multiterminal HVDC Power Systems", IEEE Transactions on Power Apparatus and Systems, Vol. PAS-99, No. 2, pp. 729-737, March/April 1980.

2. J. P. Bowles, L. Vaughan and N. G. Hingorani, "Specification of HVDC Circuit Breakers for Different System Applications", CIGRE, 13-06, August 1976.

3. U. Lamm, E. Uhlmann and P. Danfors, "Some Aspects of Tapping HVDC Transmission Systems", Direct Current, Vol. 8, No. 5, pp. 124-129, May 1963.

4. J. Reeve and J. Arrillaga, "Series Connection of Converter Stations in an HVDC Transmission System", Direct Current, Vol. 10, No. 2, pp. 72-78, May 1965.

5. J. P. Bowles, "Multiterminal HVDC Transmission Systems Incorporating Diode Rectifier Stations", IEEE Transactions on Power Apparatus and Systems, Vol. PAS-100, No. 4, pp. 1674-1678, April 1981.

6. A. M. Gole and R. W. Menzies, "Analysis of a Small Series Tap on an HVDC System Using Forced Commutation", IEE International Conference on Thyristors and Variable State Equipment for AC and DC Transmission, London, IEE Conf. Record 205, pp. 137-140, November 30/1981.

7. John McNichol, S. T. Ranade, H. Ring and D. Meyl, "Parallel Operation of Nelson River HVDC Bipoles 1 and 2, Control System Simulator Studies", IEEE Transactions on Power Apparatus and Systems, Vol. PAS-101, No. 3, pp. 653-661, March 1982.

8. J. P. Bowles, H. L. Nakra and A. B. Turner, "A Small Series Tap on an HVDC Line", IEEE Transactions on Power Apparatus and Systems, Vol. PAS-100, No. 2, pp. 857-862, February 1981.

9. K. W. Kanngiesser and W. Kuehn, "Tapping of an HVDC Point-To-Point Transmission as Feed-In to a Relatively Weak AC System", CIGRE, Study Committee 14, July 1/1981.

10. H. B. Gels, K. W. Kanngiesser, H. Ring and T. Wess, "Transient Behaviour of a Series-Connected HVDC Tapping Substation", CIGRE, Study Committee 14, Meeting in Vienna/Austria, 1983.

11. R. L. Vaughan, J. P. Bowles and J. Dalzell, "The Control and Performance of a Series Connected Multiterminal HVDC Transmission System", IEEE Transactions on Power Apparatus and Systems, Vol. PAS-94, No. 5, pp. 1868-1877, September/October 1975.

12. E. W. Kimbark, Ed. Direct Current Transmission, Volume 1. New York: John Wiley and sons, 1971.

13. C. Adamson, and N. G. Hingorani, Ed. High Voltage Direct Current Power Transmission. London: Garraway Limited, 1960.

14. Brown, Boveri and Company (BBC), "Static VAR Compensators for HV Power Systems, Basic Design and Application", Publication No. CH-N22.001.0E, by E. Wirth, B. Roesle, K. Sadek, M. Franzl and M. Hausler.

15. H. M. Turanli, R. W. Menzies and D. A. Woodford, "Feasibility of DC Transmission with Forced Commutation to Remote Loads", IEEE Transactions on Power Apparatus and Systems, Vol. PAS-103, No. 6, pp. 1256-1262, June 1984.

16. K. W. Kanngiesser and H. P. Lips, "Control Methods for Improving the Reactive Power Characteristic of HVDC Links", IEEE Transactions on Power Apparatus and Systems, Vol. PAS-89, No. 6, pp. 1120-1125, July/August 1970.

17. J. P. Bowles, "Alternative Techniques and Optimization of Voltage and Reactive Power Control at HVDC Converter Stations", Proceedings of IEEE International Conference on Over Voltages and Compensation of Integrated AC-DC Systems, Winnipeg, Canada, July 8-12, 1980.

18. M. Z. Tarnawecky, "Tapping of an HVDC Transmission", A Preliminary Internal Report for BBC, Mannhein, 3/4/1974.

19. J. P. Bowles, "HVDC System Developments and Concepts - The Diode Rectifier", Submitted to CIGRE Study Committee No. 14, Winnipeg, June 1977.

20. C. V. Thio, "Nelson River HVDC Bipole-Two", Part I - System Aspects, IEEE Transactions on Power Apparatus and Systems, Vol. PAS-98, No. 1, pp. 165-173, January/February 1979.

21. "Electromagnetic Transients Program (EMTP) of Bonneville Power Administration (BPA), Mode 28, User's Manual, September 1980.

22. "Electromagnetic Transients-Direct Current (EMTDC) Program" of Manitoba Hydro, the Incomplete Book by D. A. Woodford, September 1983.

23. R. Foerst, G. Heyner, K. W. Kanngiesser and H. Waldmann, "Multiterminal Operation of HVDC Converter Stations", IEEE Transactions on Power Apparatus and Systems, Vol. PAS-88, No. 7, pp. 1042-1052, July 1969.

24. J. Arrillaga, Ed. High Voltage Direct Current Transmission. London: Peter Peregrinus Ltd., 1983.

25. S. Arabi and M. Z. Tarnawecky, "A Diode Rectifier Series Tap on an HVDC Line", 85 WM 217-5, Presented at the IEEE/PES Winter Meeting, New York, New York, February 3-8, 1985.

26. E. Rumpf and S. Ranade, "Comparison of Suitable Control Systems for HVDC Stations Connected to Weak AC Systems", Part I: New Control Systems, IEEE Transactions on Power Apparatus and Systems, Vol. PAS-91, pp. 549-555, 1972.

27. E. Rumpf and S. Ranade, "Comparison of Suitable Control Systems for HVDC Stations Connected to Weak AC Systems", Part II: Operational Behavior of the HVDC Transmission, IEEE Transactions on Power Apparatus and Systems, Vol. PAS-91, pp. 555-564, 1972.

28. Yao-nan Yu, Ed. Electric Power System Dynamics. Academic Press, Inc., 1983.

29. John J. D'azzo and Constantine H. Houpis, Ed. Linear Control System Analysis and Design: Conventional and Modern. McGraw-Hill, Inc., 1975.

30. HVDC Course Notes, by M. Z. Tarnawecky, University of Manitoba, 1985.

Appendix A

SIMULATION DATA OF DIODE RECTIFIER SERIES TAPPING

A.1 THE MAIN RECTIFIER

Ratings: 529 kV/pole = 1.058 pu,

2000 A = 1.0 pu,

1058 MW/pole.

$R_{eq} = 3\omega L_c/\pi = 26.46$ ohms.

$\alpha_{margin} = 13$ degrees.

$\alpha_{min} = 2$ degrees.

$\alpha_{max} = 135$ degrees.

Smoothing Reactors = 750 mH.

DC High-Pass Filter: 0.6 μF , 20.36 mH, 1000 ohms.

DC 12th Tuned Filter: 0.4 μF , 122.2 mH, 7.94 ohms.

KR1 = -5.882 degrees/A.s.

KR2 = 0.0136 s.

$T_i = 0.006$ s.

A.2 THE INVERTER

Ratings: 1.1 X 500 kV/pole = 1.1 X 1.0 pu,

2000 A = 1.0,

1.1 X 1000 MW/pole.

$R_{eq} = 3\omega L_c/\pi = 25$ ohms.

$\alpha_{min} = 110$ degrees.

$\gamma_{min} = 18$ degrees.

I_{margin} = 10% of the Rated DC Line Current.

Smoothing Reactor = 750 mH.

DC High-Pass Filter: 0.6 μF, 20.36 mH, 1000 ohms.

DC 12th Tuned Filter: 0.4 μF, 122.2 mH, 7.94 ohms.

KI1 = -5.882 degrees/A.s.

KI2 = 0.0136 s.

$T_i = 0.006$ s.

A.3 DC TRANSMISSION LINES

Rectifier Side: 193.7 mi,
0.025 ohms/mi,
2.528 mH/mi,
0.01442 μF /mi.

Inverter Side: 387.3 mi,
0.025 ohms/mi,
2.528 mH/mi,
0.01442 μF /mi.

A.4 TAPPING STATION

Ratings: 50 kV/pole = 1.0 pu,

2000 A = 1.0 pu,

100 MW/pole.

Each Smoothing Reactor = 75 mH.

Each Surge Capacitor = 1.0 μF.

Each Snubber Circuit = 0.5 μF, 182.5 ohms.

Converter Transformer: AC Side Three-Phase MVA = 111.0,

AC Side kV = 13.8 (L-L),

DC Side kV = 19.63/winding (L-L),

Leakage Reactance = 11.32%,

Series Resistance = 0.5%,

Parallel Resistance = 1.0 MΩ,

Knee of Saturation Curve = 1.2 pu.

Generator: MVA= 120, kV = 13.8, f_s = 60 Hz,

r_a = 0.0033 pu, x_ℓ = 0.165 pu, x_0 = 0.165 pu,

x_d = 1.106 pu, x'_d = 0.301 pu, x''_d = 0.233 pu,

x_q = 0.640 pu, x'_q = ... , x''_q = 0.242 pu,

T'_{do} = 4.10 s, T''_{do} = 0.019 s, T''_{qo} = 0.048 s,

H = 3.42 MW.s/MVA, D = 2.0 pu.

Appendix B

AC FILTERS WITH DIFFERENTIAL FIRING

B.1 QUASI TWENTY FOUR-PULSE OPERATION

The cost of a filter tuned for a particular harmonic varies with the size of the filter [12] as,

$$K = A.S + B.S^{-1} , \qquad (B-1)$$

where,

K = cost ($),

S = size (MVAr),

A = constant ($/MVAr),

and B = constant ($.MVAr).

Assuming,

U_C = unit cost of capacitor ($/MVAr),

and U_L = unit cost of inductor ($/MVAr) = 1.8 U_C ,

the above constants can be described as,

$$A = U_C + U_L/n^2 = (1 + 1.8/n^2)\, U_C , \qquad (B-2)$$

and,

$$B = V_{(1)}^2\, I_{(n)F}^2\, (U_C + U_L)/n = 2.8\, V_{(1)}^2\, I_{(n)F}^2\, U_C/n , \qquad (B-3)$$

where,

$V_{(1)}$ = fundamental voltage (kV/phase),

and $I_{(n)F}$ = nth harmonic current through the filter (kA).

The size for minimum cost, S_{min} , is found by equating the derivative of Equation B-1 to zero. Thus,

$$S_{min} = (B/A)^{\frac{1}{2}} , \qquad (B-4)$$

and,

$$K_{min} = 2(A.B)^{\frac{1}{2}} \quad . \qquad (B\text{-}5)$$

Assuming,

ϕ_m = maximum network impedance angle = 75 degrees,

and δ_m = maximum per unit deviation of frequency from tuned frequency = 0.02,

the optimum quality factor of the filter [12] is,

$$Q_o = 0.65 \; / \; \delta_m = 32.5,$$

and the nth (ac) harmonic voltage in per unit of fundamental voltage is,

$$V_{(n)} = 3.17 \; \delta_m (n^2+2)^{\frac{1}{2}} \cos(\phi_m/2)/(3n^3)^{\frac{1}{2}} \quad . \qquad (B\text{-}6)$$

Thus,

$$V_{(11)} = 0.883\% < 1.0\%,$$

$$V_{(13)} = 0.810\% < 1.0\%,$$

and there is no need to increase the size of the tuned filters beyond S_{min}.

For the quasi twenty four-pulse series tap in digital simulation studies,

$$V_{(1)} = 9.815 \text{ kV},$$

$$I_{(1)} = 3.79 \text{ kA},$$

$$I_{(11)F} = 0.027 \; I_{(1)} \sec(\phi_m/2) = 0.129 \text{ kA},$$

$$I_{(13)F} = 0.023 \; I_{(1)} \sec(\phi_m/2) = 0.110 \text{ kA}.$$

Note that the values 0.027 and 0.023 are the maximum per unit 11th and 13th harmonic currents of the bipolar tap when one twelve-pulse bridge set is out of service. Then,

$$S_{(11)} = 0.634 \text{ MVAr/phase } (= 1.9\%),$$

$$K_{(11)} = \$1.287 \; U_C \text{ per phase},$$

$C_{(11)} = S_{(11)}/(\omega V_{(1)}^2)$ = 17.46 xF,

$L_{(11)} = 1/(C_{(11)}\omega^2 n^2)$ = 3.33 mH,

$R_{(11)} = (L_{(11)}/C_{(11)})^{\frac{1}{2}}/Q_o$ = 0.425 ohm,

$Loss_{(11)} = (\omega C_{(11)} V_{(1)})^2 R_{(11)}$ = 1.774 kW/phase,

$S_{(13)}$ = 0.498 MVAr/phase (= 1.5%),

$K_{(13)}$ = \$1.007 Ux per phase,

$C_{(13)}$ = 13.71 xF,

$L_{(13)}$ = 3.04 mH,

$R_{(13)}$ = 0.458 ohm,

$Loss_{(13)}$ = 1.178 kW/phase.

To decrease the arithmatic sum of the voltage harmonics up to 25th inclusive to 2.5% [12], the arithmatic sum of 23rd and 25th should be,

$2.5 - (0.883 + 0.810) = 0.807\%$.

The arithmatic sum of the 23rd and the 25th harmonic currents through the high-pass filter is,

$$I_{(H.P.)F} = (0.0333 + 0.0291)\, I_{(1)}\, \sec(\phi_m/2) = 0.298 \text{ kA}.$$

The magnitude of the impedance of the high-pass filter at the resonance frequency (i.e., at n = 24) is,

$$|Z| = R_{(H.P.)}/\{Q(1 + Q)^{\frac{1}{2}}\}, \qquad \text{(B-7)}$$

$$= 0.00807\, V_{(1)}/I_{(H.P.)F} = 0.266 \text{ ohm},$$

where,

$$Q = \omega\, n\, R_{(H.P.)}\, C_{(H.F.)}. \qquad \text{(B-8)}$$

Assuming that the total reactive power supplied by the filters should be 20% of the real power of the tap,

$S_{(H.P.)}$ = 20 - (1.9 + 1.5) = 16.6% = 5.533 MVAr/phase,

and,

$C_{(H.P.)}$ = 152.36 xF,

$L_{(H.P.)}$ = 0.08 mH,

$R_{(H.P.)}$ = 1.84 ohms.

B.2 COMPARISON WITH TWELVE-PULSE OPERATION

For the same tapping station but with equal firing angles, the same high-pass filter can be used. But the 11th and the 13th tuned filters have to have much larger sizes, namely,

$S_{(11)}$ = 0.634 X 8.57 / 2.7 = 2.012 MVAr/phase (= 6.04%),

and $S_{(13)}$ = 0.498 X 7.08 / 2.3 = 1.533 MVAr/phase (= 4.60%).

The corresponding costs and losses are,

$K_{(11)}$ = 1.287 U_C X 8.57 / 2.7 = \$4.085 U_C per phase,

$K_{(13)}$ = 1.007 U_C X 7.08 / 2.3 = \$3.010 U_C per phase,

$Loss_{(11)}$ = 1.774 X 8.57 / 2.7 = 5.631 kW/phase,

and $Loss_{(13)}$ = 1.178 X 7.08 / 2.3 = 3.626 kW/phase.

Thus, the total (three-phase) VAr, the total cost and the total loss of both 11th and 13th tuned filters are,

total VAr = 6.04 + 4.60 = 10.64%,

total cost = 3 (4.085 + 3.010) U_C = \$21.285 U_C,

total loss = 3 (5.631 + 3.626) = 27.771 kW.

In comparison, the tuned filters of the quasi twenty four-pulse tap supply a total VAr of 3.4%. Assuming that the difference, namely,

10.64 - 3.40 = 7.24%,

is supplied by capacitor banks, the total cost will then be,

3 (1.287 + 1.007) U_C + 7.24 U_C = \$14.122 U_C,

which means 33.65% saving. The saving on the filter losses is,

$$100\ [27.771 - 3\ (1.774 + 1.178)]\ /\ 27.771 = 68.11\%.$$

B.3 MINIMUM VAR OPERATION

If the tap operates on minimum VAr characteristics, the 11th and the 13th harmonic currents of the tap will reduce to 7.55% and 5.92%, respectively. Thus,

total VAr = 9.24%,

total cost = $18.572\ U_C + (10.64 - 9.24)\ U_C$

$= \$19.972\ U_C$ (6.17% saving),

and,

total loss = 23.978 kW (13.66% saving).

Appendix C

SIMULATION DATA OF DIFFERENTIAL FIRING

C.1 THE RECTIFIER

Ratings: 1.1 X 529 kV/pole,

2000 A,

1.1 X 1058 MW/pole.

α_{margin} = 13 degrees.

α_{min} = 5 degrees.

α_{max} = 135 degrees.

Smoothing Reactor = 750 mH.

Each Snubber Circuit: 3000 ohms, 0.018 μF.

DC High-Pass Filter: 0.6 μF, 20.36 mH, 1000 ohms.

DC 12th Tuned Filter: 0.4 μF, 122.2 mH, 7.94 ohms.

AC High-Pass Filter: 10.0 μF, 4.9 mH, 134.0 ohms.

Thevenin Equivalent of the AC System: 136.5 kV (L-G),

0.8 + j 6.92 ohms.

Converter Transformers: Three-Phase MVA = 316.78,

AC Side kV = 230.0 (L-L),

DC Side kV = 112.0 (L-L),

Leakage Reactance = 20%,

Knee of Saturation Curve = 1.2 pu.

KR1 = - 5.294 degrees/A.s.

KR2 = 0.0136 s.

T_i = 0.006 s.

C.2 THE MAIN INVERTER

Ratings: 500 kV/pole,
2000 A,
1000 MW/pole.

γ_{min} = 18 degrees.

α_{min} = 110 degrees.

α_{max} = 180 degrees.

Smoothing Reactor = 750 mH.

Each Snubber Circuit: 3000 ohms, 0.018 μF.

DC High-Pass Filter: 0.6 μF, 20.36 mH, 1000 ohms.

DC 12th Tuned Filter: 0.4 μF, 122.2 mH, 7.94 ohms.

AC High-Pass Filter: 6.0 μF, 2.21 mH, 158.0 ohms.

AC 11th Tuned Filter: 4.1 μF, 14.3 mH, 1.08 ohms.

AC 13th Tuned Filter: 2.9 μF, 14.3 mH, 1.27 ohms.

Thevenin Equivalent of the AC System: 134.6 kV (L-G),
0.85 + j 7.14 Ohms.

Converter Transfomers: Three-Phase MVA = 308.3,
AC Side kV = 230.0 (L-L),
DC Side kV = 109.0 (L-L),
Leakage Reactance = 20%,
Knee of Saturation Curve = 1.2 pu.

KI1 = - 5.294 degrees/A.s.

KI2 = 0.0136 s.

T_i = 0.006 s.

I_{margin} = 10%.

C.3 DC TRANSMISSION LINES

Rectifier Side: 290.5 mi,

0.02494 (Lower Frequency) ohm/mi,

0.02977 (Higher Frequency) ohm/mi,

2.528 mH/mi,

0.01442 μF/mi.

Inverter Side : 290.5 mi,

0.02494 (Lower Frequency) ohm/mi,

0.02977 (Higher Frequency) ohm/mi,

2.528 mH/mi,

0.01442 μF/mi.

C.4 TAPPING STATION

Ratings: 50 kV/pole = 1.0 pu,

2000 A = 1.0 pu,

100 MW/pole = 1.0 pu.

$\gamma_{2\ min}$ = 18 degrees.

$\alpha_{e\ min}$ = 80 degrees.

$\alpha_{e\ max} = 0.92\ \alpha_{2\ max} + 0.0824$ rad.

$\Delta\alpha = (-\ 0.092374\ \alpha_e^3 + 0.511267\ \alpha_e^2 - 0.955492\ \alpha_e + 0.597138)(\omega I_d/V_s) + 0.263632$ rad.

Each Smoothing Reactor = 75.0 mH.

Each Surge Capacitor = 0.5 μF.

Each Snubber Circuit: 0.4 μF, 200.0 ohms.

Capacitor across each Bridge = 0.6 μF.

AC High-Pass Filter: 152.36 μF, 0.08 mH, 1.84 ohms.

Ac 11th Tuned Filter for Quasi Twenty Four-Pulse Operation:

17.46 μF, 3.33 mH, 0.425 ohm.

AC 13th Tuned Filter for Quasi Twenty Four-Pulse Operation:

13.71 μF, 3.04 mH, 0.458 ohm.

AC 11th Tuned Filter for Twelve-Pulse Operation:

55.42 μF, 1.05 mH, 0.134 ohm.

AC 13th Tuned Filter for Twelve-Pulse Operation:

42.2 μF, 0.988 mH, 0.149 ohm.

Converter Transformers: Three-Phase MVA = 29.18,

AC Side kV = 17.0 (L-L) = 1.0 pu,

DC Side kV = 10.316 (L-L),

Leakage Reactance = 10.77%,

Knee of Saturation Curve = 1.2 pu.

Synchronous Condenser: MVA = 70, kV= 17.0, f_s = 60 Hz,

r_a = 0.00232 pu, x_ℓ = 0.17 pu,

x_0 = 0.13 pu, x_d = 1.56 pu,

x'_d = 0.3 pu, x''_d = 0.19 pu,

x_q = 1.10 pu, x''_q = 0.23 pu,

T'_{do} = 11.0 s, T''_{do} = 0.17 s,

T''_{qo} = 0.32 s, H = 1.5 MW.s/MVA,

D = 1.0 pu, Saturation Included.

Speed Regulator: k = 1.5 s^{-1}, $T_1 = T_2$ = 0.5 s, T_ω = 0.02 s.

Voltage Regulator: k_e = 100, T_e = 0.05 s, T_v = 0.01 s,

$v_{f\ max}$ = 6.0 pu, $v_{f\ min}$ = - 6.0 pu.

Switchable Capacitors: C = 8 X 45.9 μF, C_C = 6 X 45.9 μF.

Short AC Line: R_t = 0.1 ohm, L_t = 2.3 mH.